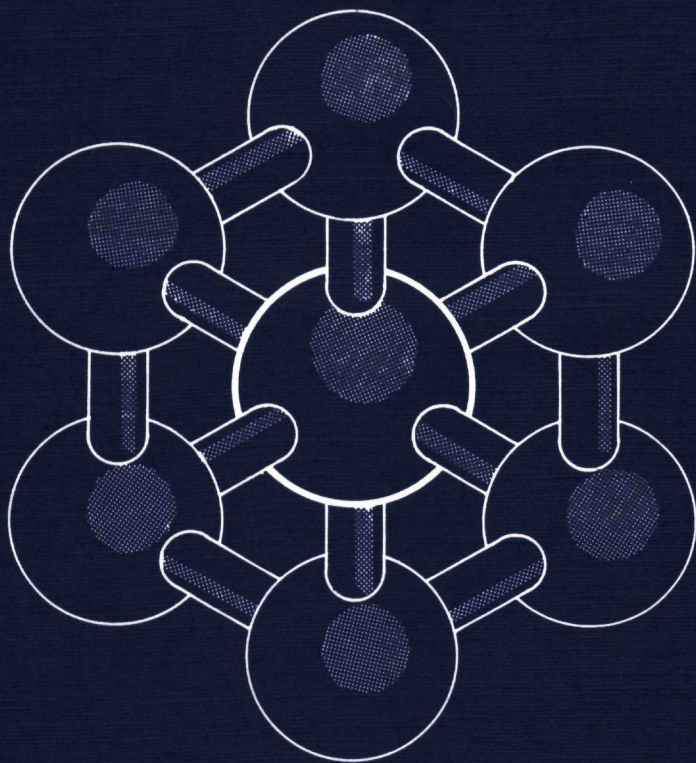


4519

**HIGH RESOLUTION MEASUREMENTS OF
MULTIPHOTON
MULTI LASER EXCITATION OF SF₆**



SACCO TE LINTEL HEKKERT

**HIGH RESOLUTION MEASUREMENTS OF
MULTIPHOTON
MULTI LASER EXCITATION OF SF₆**

HIGH RESOLUTION MEASUREMENTS OF MULTIPHOTON MULTI LASER EXCITATION OF SF₆

EEN WETENSCHAPPELIJKE PROEVE OP HET GEBIED VAN
DE NATUURWETENSCHAPPEN

PROEFSCHRIFT

TER VERKRIJGING VAN DE GRAAD VAN DOCTOR
AAN DE KATHOLIEKE UNIVERSITEIT NIJMEGEN,
VOLGENS BESLUIT VAN HET COLLEGE VAN DECANEN
IN HET OPENBAAR TE VERDEDIGEN
OP DONDERDAG 4 FEBRUARI 1993,
DES NAMIDDAGS TE 3.30 UUR PRECIES

door

SACCO TE LINTEL HEKKERT

geboren op 11 maart 1963
te Deventer

Promotor : Prof. Dr. J. Reuss

Een woord van dank

De laatste zes jaar heb ik een groot deel van mijn tijd op de afdeling Molecuul- en laserfysica doorgebracht, met veel genoegen kijk ik terug op deze periode. Van deze gelegenheid wil ik dan ook gebruik maken om iedereen te bedanken die op enigerlei wijze een bijdrage heeft geleverd aan het totstandkomen van dit proefschrift. Enkelen van hen wil ik met naam noemen.

- Arjen, ondanks dat wij de laatste drie jaar gemeten hebben aan dezelfde opstelling, heb ik toen ik tijdelijk dakloos was van zijn huis gebruik mogen maken. Hiervoor nog bedankt en veel succes met je promotie.
- Mijn altijd enthousiaste begeleider J. Reuss, die gedurende de hele periode grote interesse heeft getoond voor het onderzoek. Hiermee wil ik hem bedanken voor de mogelijkheden die hij mij in de afgelopen vier jaar heeft geboden om onderzoek te kunnen doen in het buitenland: een half jaar in Frascati, een onvergetelijke ervaring, vooral als je in Rome woont, bovendien een maand in Gottingen en een weekje Dijon.
- Steven, die mij op zijn eigen onnavolgbare wijze begeleid heeft tijdens mijn afstudeerstage. Sorry dat ik maar een (zeer klein) deel van al je ideeën verwezenlijken kon, 24 uur in een etmaal is ook veel te weinig.
- Coen, die mijn eerste stappen met de CO₂ lasers begeleidde en me de geheimen van de bolometer onthuld heeft.
Jose, Sandra, Hidde en Iwan, de studenten die tijdens hun afstudeerstage mijn cynische opmerkingen hebben moeten verdragen.
- Voglio ringraziare G. Sanna, M. Nardi, L. Martinis e M. Giorgi per il piacevole e istruttivo periodo trascorso nel laboratorio ENEA di Frascati.
- H.-J. Waldapfel, R. Hasse, S. Mohr, M. Knepper und R. Duren für die gute Zeit in Gottingen. Viel Erfolg mit euren schonen Experimenten.
- Boris, spasibo za sotroednitsjestwo i interesnee obsoerjdenija. Ja nadejoesw snowa wskore oewidetsja s Wami w Moskwe.
- Gerard Pierre, mes remerciements sinceres pour l'appui théorique il nous donnait et pour l'hospitalité pendant mes visites a Dijon.
- Alle overige vaste medewerkers en AIO's die gedurende mijn promotie de sfeer op de afdeling bepaald hebben. Met name degenen die tijdens de lunchpauzes van de studentenkamer een echte koffiekamer maakten: Lukas, Ger, Mark, Huug, Frans, Fransje, Richard, Freek, Nico, Jos en Daniëlla.
- Annet en Wilke, hun bijdrage tot het goed functioneren van de afdeling wordt nog te vaak onderschat.
- Cor, John, Frans en Eugene, de technische staf zonder wiens hulp het onmogelijk is een opstelling draaiende te houden. Cor nog bedankt voor de mooie tijden die we dankzij jou met de medewerkers van de afdeling in Friesland hebben doorgebracht.

-
- Computer goeroe Leo, voor het ontwikkelen van het computerprogramma waarmee de meeste spectra, gepresenteerd in dit proefschrift, gemeten zijn.
 - De medewerkers van de grote werkplaats, quick-service, glasblazerij, illustratie en fotografie, en uiteraard Ferry van de zelfservice. In de loop van de tijd heb ik toch heel wat op het eerste gezicht onmogelijke klussen verzonnen, Ferry wist er altijd raad mee.
 - En natuurlijk het F.O.M. (stichting fundamenteel onderzoek der materie) zonder wiens geldelijke ondersteuning dit onderzoek niet gedaan had kunnen worden.

Contents

1	General introduction	9
2	One and two photon spectra of SF₆, molecular beam measurements	15
2.1	Introduction	16
2.2	Experimental set-up	17
2.3	Experimental results	19
2.4	The P(4) one-photon transitions	25
2.5	Two photon transitions with $J \leq 14$	26
2.6	Inversion vs saturation, illustrated by double resonance experiments	30
2.7	Outlook	31
2.8	Table	33
2.9	Appendix	44
2.10	Acknowledgement	45
3	Calculation of two photon transitions in SF₆, fit to measured frequencies	49
3.1	Introduction	50
3.2	Calculation of two photon transitions	50
3.3	Fitting procedure	53
3.4	Results of the fitting procedure	54
3.5	Tables	57
4	Multiphoton experiments on SF₆, molecular quantum electronics with infrared radiation	63
4.1	Introduction	64
4.2	Experimental set-up	65
4.3	Depletion measurements	66
4.4	Two level systems, $N=2$	68
4.5	Three level system, $N=3$	70
4.6	$N > 3$ level systems	73
4.7	Acknowledgement	75
5	Multiphoton multi laser excitation of the ν_3 mode of SF₆ in a molecular beam	77
5.1	Introduction	78

5 2	Experimental set-up	79
5 3	Multiphoton depletion measurements	82
5 4	Absence of power broadening and background signals	84
5 5	Dynamic Stark effects	85
5 6	Two colour, two photon transitions	88
5 7	Three and four photon transitions	89
5 8	Outlook	91
5 9	Tables	92
6	Outlook	101
	Samenvatting	107
	Curriculum Vitae	109

Chapter 1

General introduction

The research on SF₆ started in 1934 when the first measured Raman and infrared spectra were published [1]. At the same time theoretical considerations of the normal modes in SF₆ were published [2]. The discovery of infrared Multiphoton excitation (MPE) and multiphoton dissociation (MPD) in 1973 [3, 4] created much interest and projects were initiated where laser induced processes and new concepts like the quasicontinuum of states and the leakage of energy to dark bath-states played an important role. In many studies detailed aspects of these phenomena were elucidated, for review see [5]. MPD was observed in a molecular beam in 1979 by Yuan Lee and coworkers demonstrating above any doubt the collisionless character of MPE and MPD [6]. The somewhat deluding conclusion was forced upon the scientists that in dissociation always the weakest bond was ruptured and that a steering of the process by appropriate laser wave lengths and intensities was more difficult than expected [7].

To investigate the first steps in the MPE process, McDowell et al [8] and Patterson et al [9] refined the theory of one, two and three photon transitions. Overtone measurements of $3\nu_3$ transitions in SF₆ were published in [10] where a spectral resolution of 30 MHz is achieved.

SF₆ measurements with resolutions in the kHz region for the one photon transitions are performed by the group of Bordé in Paris [11, 12, 13, 14]. 200 kHz resolution in measurements on two photon transitions is achieved by Herlemont et al [15, 16]. In both measurements saturation spectroscopy is performed in an absorption cell at room temperature.

The onset of the quasicontinuum/stochastisation was investigated by Letokhov et al [4] and Alimpiev et al [17]. Letokhov and coworkers utilized spontaneous Raman probing of the molecules excited by a pulsed CO₂ laser. In the quasicontinuum the density of vibrational states is assumed to become sufficiently high so that within the experimental resolution levels overlap and interact so that the laser frequency does not have to fit a specific level to produce absorption. In [4] the quasicontinuum is predicted to begin for energies exceeding 5000 cm⁻¹, for SF₆.

Problems exist concerning the life time properties and energy distribution of the intermediate states excited during the MPE-process. Energy transfer among those states by

collisions turns out to form an obstacle for dissociation. In 1981 Bloembergen et al [18] utilized two independent 0.5 ns pulsed CO₂ lasers in a classic pump-probe experiment and observed a fast collisional scrambling rate for excited SF₆ molecules ($P\tau=2$ nsTorr). Thus studies of the states excited by the MPE process require highly rarefied conditions such as those present in a molecular beam environment.

Molecular beam measurements were performed in the same years by A. Giardini and coworkers [19]. They observed spectral features resulting from MPE, MPD also was often found to possess spectral structure. Continuously tunable infrared radiation produced with a high pressure pulsed CO₂ laser was used by Alimpiev et al [20] to measure the completely resolved frequency dependence of the MPE probability for bulk SF₆ at $T=140$ K and $P=0.3$ Torr. A surprisingly structured spectrum was recorded and found to be very different from the smooth spectral envelopes resulting from measurements produced utilizing line tunable CO₂ lasers. The spectrum of [20] contains several sharp peaks (0.15 cm⁻¹ FWHM), which have been assigned as Q-branches belonging to two and three photon resonances of the infrared active ν_3 vibrational mode [9, 10].

Employing a sensitive bolometer as a detector [21] Boschetti et al [22] investigated the MPE probability of SF₆ as a function of the laser frequency of a line tunable TEA CO₂ laser. At constant fluence of 1 J/cm², excitation spectra were measured for several stagnation conditions and shown to depend slightly on the rotational and strongly on the vibrational temperature of the SF₆ molecules. At their most elevated stagnation temperature ($T_0=398$ K) and at a laser frequency of 944.2 cm⁻¹ (10P20) the maximum absorption of an average of $n=15$ photons per molecule was observed. At lower stagnation temperatures this maximum turned out to be lower (for $T_0=198$ K, $n=7$) and to occur at slightly less red shifted laser transitions (shifts up to 1 cm⁻¹). The envelope of these line tuned spectra shows resemblance with those collected by Schulz et al [23], measuring at a fluence of 5 J/cm² the MPD probability of SF₆ in a molecular beam. Both series of spectra [22, 23] appear to be blue shifted in comparison with the spectra obtained in bulk experiments by Tsay et al [24].

C. Liedenbaum et al [25, 26, 27] started to investigate MPE by cw lasers, in our laboratory. Bolometric detection was employed to measure the energy deposited into the molecules by the laser interaction. Up to five photons of about 1000 cm⁻¹ each, could be absorbed by the beam molecules before saturation occurred at about 1 J/cm². This saturation behaviour contrasted MPD observed with pulsed lasers and pointed to a different character of the laser-molecule interaction. This difference was evidenced by the observation of multiphoton rapid adiabatic passage (RAP) processes due to the curved wave fronts of the tightly focussed cw CO₂ laser [27]. Double resonance experiments demonstrated that RAP-MPE was an extremely narrow band phenomenon although the one-laser spectra appeared to be broad due to congestion [25].

The experiments in this thesis are restricted to the region below the quasicontinuum

One photon transitions are measured with very high accuracy by the group of Bordé [28] and recently by Herlemont et al [29] We cannot compete with their accuracies and accordingly no spectroscopy is performed on these transitions For the two photon transitions the group of Herlemont [15, 16] achieved a resolution of 200 kHz This is better than our resolution (2 MHz), however, we perform our measurements in a molecular beam in which low J-values are favoured [30, 31] Another difference between the measurements of [15, 16] and the measurements presented in this thesis are the spectral regions which are covered With the measurements utilizing two counterpropagating lasers interacting simultaneously with the SF₆ molecules (as presented in chapter 4 of this thesis) new spectral regions are covered in this way 95 new two photon transitions have been assigned

With the new method it is also possible to measure n-photon transitions with $n \geq 3$ with much higher accuracy than earlier measurements have achieved (for three photon transitions our resolution is 2 MHz, the measurements in [10] were performed with 30 MHz resolution) Due to selection rules it is possible to measure many more transitions utilizing multiphoton processes instead of overtone spectroscopy For overtone transitions leading to the third energy level, $\Delta J = -1, 0$ or 1 and the vibrational symmetry is restricted to F_{1u} , while for a three photon transition ΔJ can be $-3, -2, -1, 0, 1, 2$ or 3 and the vibrational symmetry of the final level can be either A_{2u} , F_{1u} or F_{2u} With the same configuration with which the three photon transitions are measured it is also possible to measure transitions going to energetic levels exceeding 3000 cm^{-1} without losing resolution

In this thesis the emphasis will be on the multiphoton spectroscopy of SF₆, in chapter 2 the measured frequencies obtained by measurements utilizing a CO₂ waveguide laser in combination with an Acousto Optic Modulator are presented The fitting procedure and results of this fit are presented in chapter 3 The experimental set-up utilized to investigate two colour, two photon transitions is described in section 4, the resulting transitions are presented and discussed in chapter 5 In chapter 6 an outlook is given on the experiments which can be done utilizing the new information presented in this thesis

Not only spectroscopy on SF₆ has been performed, some interesting general features are investigated and discussed through the thesis In chapter 2, RAP effects [27] are investigated in double resonance experiments Nearly 100% population inversion is observed for one and two photon transitions For the first time a two photon Rabi frequency is measured To investigate which energy levels participate in the multiphoton process double resonance experiments are performed utilizing either an intra-cavity laser or a 150 Watt Apollo laser as a pump and a waveguide laser as a probe laser It seems that mainly transitions starting from already thermally excited SF₆ molecules contribute to the multiphoton signal while molecules in the ground state barely participate

References

- [1] Yost, Steffenson and Gross, *J. Chem. Phys.* 2 (1934) 311
- [2] A. Eucken and F. Sauter, *Z. Physikal. Chem. Abt. B. Bd* 26, 6 (1934) 463
- [3] N.R. Isenor, V. Merchant, R.S. Hallsworth and M. Richardson, *Can. J. Phys.* 51 (1973) 1281
- [4] V.S. Letokhov and A.A. Makarov, *Opt. Comm.* 17 (1976) 250
- [5] D.W. Lupo and M. Quack, *Chem. Rev.* 87 (1987) 181
- [6] P.A. Schulz, A.S. Sudbo, D.J. Krajnovich, H.S. Kwok, Y.R. Shen and Y.T. Lee, *Ann. Rev. Phys. Chem.* 30 (1979) 379
- [7] E.R. Grant, P.A. Schulz, A.S. Sudbo, Y.R. Shen and Y.T. Lee, *Phys. Rev. Lett.* 40 (1978) 115
- [8] R.S. McDowell, H.W. Galbraith, B.J. Krohn and C.D. Cantrell, *Optics Comm.* 17 (1976) 178
- [9] C.W. Patterson, R.S. McDowell, P. Moulton and A. Mooradian, *Opt. Lett.* 6 (1981) 39
- [10] C.W. Patterson, B.J. Krohn and A.S. Pine, *J. Mol. Spec.* 88 (1981) 133
- [11] B. Bobin, C.J. Bordé, J. Bordé and C. Bréant, *J. Mol. Spec.* 121 (1987) 91
- [12] J. Bordé and C.J. Bordé, *Chem. Phys.* 71 (1982) 417
- [13] J. Bordé, C.J. Bordé, C. Salomon, A. van Lerberghe, M. Ouhayoun and C.D. Cantrell, *Phys. Rev. Lett.* 45 (1980) 14
- [14] C. Salomon, C. Bréant, A. van Lerberghe, G. Camy and C.J. Bordé, *Appl. Phys. B* 29 (1982) 3
- [15] C.W. Patterson, F. Herlemont, M. Azizi and J. Lemaire, *J. Mol. Spec.* 108 (1984) 31
- [16] F. Herlemont, M. Lyszyk and J. Lemaire, *Appl. Phys.* 24 (1981) 369
- [17] V.M. Akulin, S.S. Alimpiev, N.V. Karlov, A.M. Prokhorov, B.G. Sartakov and E.M. Khokhlov, *JETP Lett.* 25 (1977) 401
- [18] R.C. Sharp, E. Yablonovich and N. Bloembergen, *J. Chem. Phys.* 74 (1981) 5357

- [19] E Borsella, R Fantoni, A Giardini-Guidoni, D Masci, A Palucci and J Reuss, *Chem Phys Lett* 93 (1982) 523
- [20] S S Alimpiev, N V Karlov, S M Nikiforov, A M Prokhorov, B G Sartakov, E M khokhlov and A L Shtarkov, *Opt Comm* 31 (1979) 309
- [21] T E Gough, R E Miller and G Scoles, *Appl Phys Lett* 30 (1977) 338
- [22] A Boschetti, M Zen, D Bassi and M Scotoni, *Chem Phys* 87 (1984) 131
- [23] P A Schulz, A S Sudbo, E R Grant, Y R Shen and Y T Lee, *J Chem Phys* 72 (1980) 4985
- [24] W Tsay and C Riley, *J Chem Phys* 70 (1979) 3558
- [25] C Liedenbaum, S Stolte and J Reuss, *Chem Phys* 122 (1988) 443
- [26] C Liedenbaum, S Stolte and J Reuss, *infrared Phys* 29 (1989) 397
- [27] C Liedenbaum, S Stolte and J Reuss, *Phys Rep* 178 (1989) 1
- [28] C J Bordé, M Ouhayoun, A van Lerberghe, C Salomon, S Avrillier, C D Cantrell and J Bordé, *Laser Spectroscopy 4* (Edited by H Walther and K W Rothe), Springer, New York (1979) 142
- [29] M Azizi, J Legrand and F Herlemont, measurements presented on the Twelfth colloquium on high resolution molecular spectroscopy, Dijon-France (1991)
- [30] P K Chakraborti, V B Kartha, R K Talukdar, P N Bajaj and A Joshi, *Chem Phys Lett* 101 (1983) 397
- [31] B J C Wu, P P Wegener and G D Stein, *J Chem Phys* 68 (1978) 308

Chapter 2

One and two photon spectra of SF₆, molecular beam measurements

A.F. Linskens, S. te Lintel Hekkert and J. Reuss

Department of Molecular and Laser Physics, University of Nijmegen
Toernooiveld, 6525 ED Nijmegen, The Netherlands

Abstract

Experiments on the saturation behaviour of one and two photon transitions have been performed on a molecular beam of SF₆-molecules, using single mode cw CO₂-lasers. Application of an Acousto Optic Modulator allowed a total tuning range of 0.6 GHz around each CO₂ laser line. Numerous, partially new absorptions have been observed and are catalogued. From the assigned transitions on the 10P16 laser line a rotational Boltzmann plot was derived showing strong deviation from a thermal distribution. Transitions from the RAP regime, with inversion, to the Rabi regime, with power broadening, have been observed, utilizing opto-thermal detection. A clear two photon Rabi frequency has been observed.

2.1 Introduction

The ν_3 -excitation of SF_6 has been widely studied by IR-spectroscopy it possesses a large transition strength and near coincidences with strong CO_2 laser lines [1-7] Theoretical effort has led to a good understanding of its spectral features including two and three photon transitions [8, 9, 10] Recently, multi-photon excitation spectra have been published showing featureless broadband absorption together with Rapid Adiabatic Passage (RAP) phenomena [11, 12, 13] Up to five ν_3 -photons were deposited into SF_6 by crossing a molecular beam with a cw CO_2 laser Opto thermal detection [14, 15] was applied to provide sensitive detection of the photons absorbed by the molecules The present study forms a continuation of the work of Liedenbaum et al [13]

Due to a number of refinements and extensions of the experimental set up (section 2), numerous one and two photon transitions became measurable with respect to recently published measurements [13, 16] The CO_2 wave guide laser was tuned over a range of 0.6 GHz around the CO_2 laser transitions utilizing an Acousto Optic Modulator as frequency shifter, with single and double passage of the laser beam Secondly, the laser intensity was amplified (by about a factor two) in a conventional 14 mm diameter discharge tube Third, the laser has been locked to a transmission peak of a Fabry Perot interferometer and has been scanned by changing the length of the Fabry-Perot cavity, the laser frequency was hereby stabilised to better than 1 MHz Fourth, the bolometer detector was cooled down to 1.7 K yielding a five fold improved signal to noise ratio as compared to its 4.2 K performance Spectra were taken around the 10P12 to 10P24 laser transitions

The P(4)-quadruplet one photon transition of SF_6 was predicted but observed before, for technical reasons, as a triplet only [1, 2] We succeeded in observing its fourth component at the expected spectral position confirming the predicted intensity ratio with respect to the other lines of the quadruplet Other very strong absorption signals were found due to two photon transitions, most of them could be assigned (see table 1^a-1^g, section 3)

From all the assigned one and two photon transitions it is possible to derive a Boltzmann plot It indicates that the rotational cooling of molecules with high J-values ($J \geq 40$) is very poor ($T_{\text{ROT}} \approx 300$ K), this in contrast with the lowest observed J-values ($3 \leq J \leq 9$) for which a temperature of 5 K is obtained (section 3)

In section 4 we show that the transition from the RAP to the conventional Rabi regime can be made just by increasing the laser power, at maximum laser power the saturation regime is entered This is demonstrated with the help of the strong P(4) one photon transition which can easily be saturated, utilizing the double resonance technique When the fluence is low enough not to saturate the P(4) transition the FWHM is approximately 2 MHz Increasing the fluence by a factor 500 leads to considerable, but still limited line broadening A second effect is the decrease of the intensity by almost a factor 2, indicating that the transition from the RAP regime (with 100% population inversion) to the saturation

regime (in which eventually only 50% of the molecules are excited) occur

For two photon processes with a well defined initial and final state in a single mode/ single frequency field we found a quadratic power dependence. This contrasts earlier studies of multi-photon transitions in SF₆ (e.g. [11]), where no sharp spectral features were observed and the linear power dependence observed for non saturating fields has been explained by the high density of excited states, many pathways are available up to the fifth level, e.g. the bottleneck level [17]

The P(4) two photon transition, observed at +174 MHz from the line centre of the 10P16 CO₂ laser line, was used to investigate two photon Rabi oscillations. The effect of having both RAP and Rabi processes in the same measurement, in variable proportions, is discussed. For the first time a clear two photon Rabi oscillation was measured (section 5)

In section 6, the double resonance technique is applied to demonstrate the different degrees of saturation, for one and two photon processes

2.2 Experimental set-up

The molecular beam apparatus has been described before [11, 16]. New are a Fabry-Perot Interferometer (FPI), an Acousto Optic Modulator (AOM), a CO₂ amplifier and the cooling of the bolometer temperature below 4.2 K. The experimental set up is schematically drawn in figure 1

By modulating the length of the FPI with a piezo, using a split-off beam with about 10% of the laser power, the waveguide CO₂ laser could be locked to a well determined frequency. The temperature controlled FPI consists of two spherical mirrors, $f = 25$ cm, reflectivity 99%, separated by 50 cm. With its help the bandwidth of the waveguide laser could be reduced to 1 MHz, single mode operation was obtained and maintained since the reported results (sharp spectral features and background absorption) depend on this single mode operation. The mode-structure of a waveguide laser is discussed in [18]. The 230 MHz free spectral range (FSR) of the waveguide laser could be covered by scanning the etalon. Along with the CO₂ radiation also a stabilised HeNe-laser [19] was aligned through the FPI in order to produce fringes (separated by 9 MHz) when the FPI was scanned. In this way the relative frequency differences between absorption peaks could be determined with an accuracy of 1 MHz.

An AOM (Intra Action Corp.) permits a frequency shift of 100 MHz. This shift is achieved by reflections of the laser beam from moving Bragg planes, which are produced by an acoustic wave of 100 MHz in a germanium crystal. The AOM can be used with single or double passage of the laser beam, the frequency is up or down shifted yielding shifts of +200, +100, -100 or -200 MHz. Together with the FSR of the waveguide laser a tuning range of about 0.6 GHz around each CO₂ transition could thus be achieved. Conversion efficiencies of nearly 55% of the incoming laser intensity have been realised, for every single

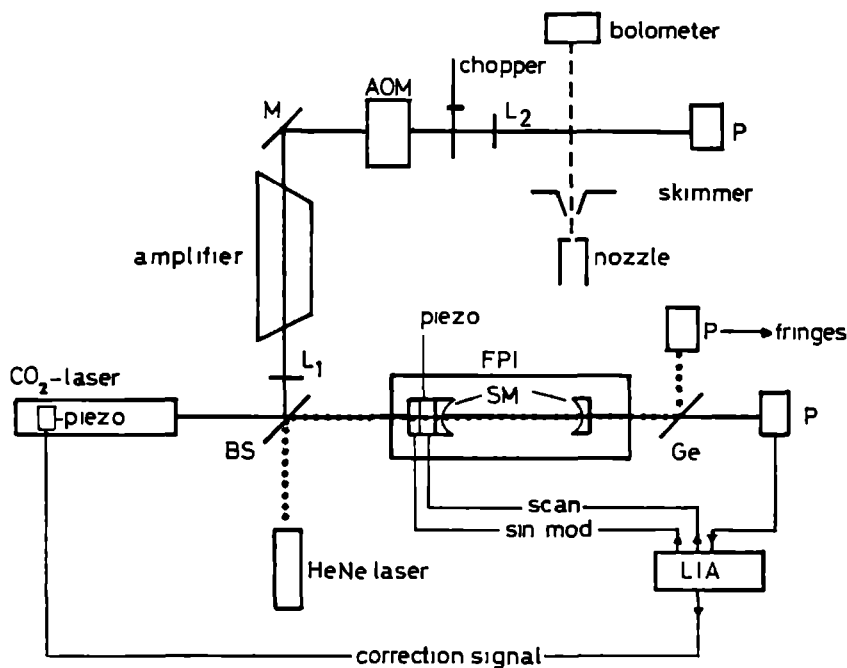


Figure 1 Experimental set-up B_s = beamsplitter ($R=90\%$), $L_{1,2}$ = lens ($f_1 = 75$ cm, $f_2 = 20$ cm), M = flat mirror, AOM = Acousto Optic Modulator, P = power meter, FPI = Fabry-Perot interferometer, SM = spherical mirror, Ge = Germanium plate, LIA = Lock-In amplifier

pass

In order to increase the power of the waveguide laser (typical output power of 8 Watts) an amplifier was installed. This amplifier consists of a 1 m long, water cooled CO_2 discharge tube with an inner diameter of 14 mm, flowed with a mixture of CO_2 , He and N_2 . Since the pressure of the gas mixture in the amplifier was about a factor 3 less as compared to the waveguide laser, the amplification was not constant for the total scanning range, at the center (edge) of the gain profile a maximum amplification factor 2 (1.2) has been achieved. The resulting radiation has been focussed near to the crossing point with the molecular beam, to an approximate waist of 0.1 mm radius. For the double pass configuration through the AOM, a maximum laser power of 5 Watts was obtained resulting in a fluence (i.e. laser intensity times interaction time) of 2.1 mJ/cm² for an average velocity of 1500 m/s of the seeded SF_6 molecules.

The laser beam has been chopped for lock-in detection of the opto-thermal signal from a bolometer, sensitive to the energy of the molecules impinging on its cold surface. By

cooling the bolometer from 4.2 K to approximately 1.7 K, the signal to noise ratio (S/N) is improved by a factor 5

Throughout the reported measurements the molecular beam conditions are characterised by a stagnation pressure $P_0=1000$ Torr and a stagnation temperature $T_0=300$ K, the nozzle diameter has been 50 μm and 2% SF₆ in He has been used

2.3 Experimental results

In fig 2 experimental results are presented for a frequency scan around the 10P16 CO₂-line. Similar measurements are performed around the 10P12-10P24 CO₂-lines, the resulting data are listed in table 1^a-1^g. Theoretically predicted lines from the literature (for the covered frequency region) are given. The R(66) and the R(67) multiplets (10P12), the R(28)-quartet (10P14), the P(4)-quadruplet (10P16) and the P(33)-sextet (10P18), as measured by the Bordé-group [1, 2], served for absolute frequency calibration. These are all one photon transitions. For the 10P20 the relative distances between successive absorption lines were compared with the theoretically predicted distances to obtain an assignment and an absolute frequency calibration. For the 10P22 and 10P24 the top of the laser gain profile (with amplifier) was used to estimate the line center frequency, resulting in an uncertainty of ± 5 MHz.

Most of the earlier measured one photon [1, 2] and two photon transitions [9] in the CO₂ laser region 10P12-10P20 could be identified. These authors could cover a frequency region of 500 MHz around a CO₂ line. They achieved remarkably narrow linewidths by saturation spectroscopy. Using bulk-gas absorption at room temperature they were able to excite molecules especially with high J-values, two photon resonances with large detunings (up to 50 GHz) were observed, however with the limitation $J \geq 14$. On the contrary we mainly observe two photon transitions on cold molecules ($J \geq 3$) which are scarcely populated in bulk and have not been observed by Patterson *et al* [9]. Transitions which were already measured by [1-7] and [9] are indicated by ¹⁾ and ²⁾ respectively in table 1^a-1^g, note that theoretical, not experimental results are listed.

All one photon transitions have recently been recalculated by Bobin *et al* for $0 \leq J \leq 100$ [20]. Agreement with earlier measurements [1, 2] exists within 1 MHz. In our tables all calculated values for one photon transitions are taken from [20]. Our measurements reproduce the earlier experimental results within 2 MHz. At the limit of our tuning range about 20 new transitions were observed indicated by • in table 1^a-1^g, these transitions agree with the calculation of [20] within 1 MHz. One result of the extension of the tuning range with the aid of the AOM is the appearance of the fourth most blue shifted component of the P(4)-quadruplet (see section 4).

About 35 new two photon transitions were observed, especially for $J < 14$. Older experimental results on two photon transitions were obtained only for $J \geq 14$ transitions, these

and, for some high J -values, the assigned J -value differs by 2. Since the laser lines coincide mostly with one and two photon transitions of relatively high J -values ($J \geq 35$) not all of the calculated transitions could be observed; the main reason is that molecular levels with J -values ≥ 35 are hardly populated. Note that different authors use different conventions in characterising two photon transitions. Patterson gives the final J -value (and the final n -value) whereas Bobin et al. refer to the initial J -value. We have chosen for the latter

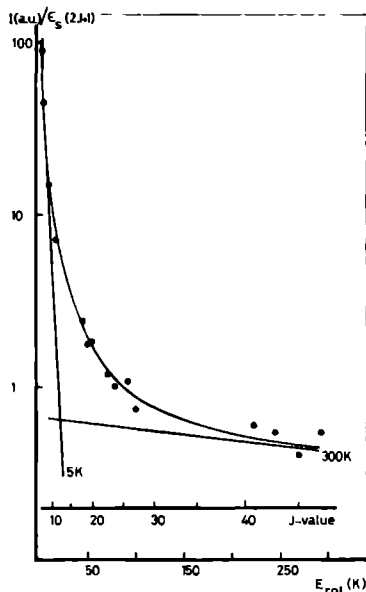


Figure 3: The Boltzmann plot, derived from the equation

$I \sim \epsilon_S \cdot (2J + 1) \cdot \exp\{-BJ(J + 1)/kT\}$, where I is the absorption strength, ϵ_S the symmetry weight (for F_1 , F_2 , E , A_1 , A_2 respectively 6,6,8,2,10 [24]), J the rotational quantum number and B the rotational constant (0.09184 cm^{-1} [21]). The J -values of the first four points from left to right are $J = 4$, $J = 7$, $J = 9$ and $J = 11$. The four points with $J \geq 40$ correspond to one photon transitions, all other to two photon transitions. The error in the points with $J \geq 40$ (25%) is much bigger than the error in the other points (5%). This is caused by two effects: first the intensity of a one photon transition is a factor two less compared to a two photon transition. Secondly, the poor population because of the high J -values decreases the signal, resulting in a smaller S/N ratio.

convention and e.g. increased J by one unit for two photon P-transitions with respect to Patterson. Rotational cooling is illustrated in a Boltzmann plot (fig 3) which was obtained from the relative intensities of the assigned one and two photon transitions around the 10P16 CO₂ laser line. The one photon transitions with high J -values could only be observed with a "fresh" bolometer, i.e. before a layer of condensed SF₆ molecules started to decrease the sensitivity of the bolometer.

The feature in fig 3 standing out is the non-Maxwellian rotational distribution of our expansion. If one looks at the derivative of the Boltzmann-plot, for the lowest observed J -values a temperature of 5 K is obtained, in agreement with [22]. However, for large J -values, $J \geq 40$, the rotational cooling is very poor ($T_{\text{ROT}} \approx 300$ K). Note that here the energy gap for two neighbouring J -states amounts to about 10 cm^{-1} and more and causes inefficient cooling, this works in our favour, since otherwise we would not be able to observe transitions from levels with $J \geq 14$ (for high J -values the level population decreases less than 10% by the expansion cooling). Evidently we have obtained a consistent set of level populations, derived from saturated one and two photon transitions.

Based upon these results we can distinguish non saturated transitions, e.g. two photon transitions with a large detuning of the intermediate level. In general, two photon resonances with detunings not exceeding 15 GHz (section 5) could be saturated for maximum laser powers using the CO₂ amplifier and the sharp focussing resulting in local laser intensities of 50 kW/cm^2 ($\Phi = 6.4 \text{ mJ/cm}^2$). In the case of larger detunings or less laser power (by using the AOM), only two photon transitions can be observed where the initial level is reasonably populated, most of the two photon transitions with $J < 14$ belong to this group. Examples are the P(7)-doublet and the Q(9)-doublet (both 10P16 CO₂ line) which appear at the calculated spectral position within 10 MHz (fig 2).

Decreasing the laser power to 5 mW we were able to narrow the one photon transitions with low J -values, e.g. the P(4)-quadruplet. An instrumental resolution of 2 MHz FWHM has been obtained. Besides the 1 MHz bandwidth of the stabilized laser, another contribution comes from the Doppler residue of about 0.5 MHz for the collimated molecular beam. The maximum obtainable fluence of waveguide laser plus amplifier hardly suffices to broaden the two photon transitions, thus resulting in small line widths. On the other hand, all one photon transitions were significantly broadened, for maximum laser intensities. To discriminate between one and two photon transitions the power dependence was measured as well as the line widths. Note that the FWHM for one photon transitions at maximum fluence ($I = 50 \text{ kW/cm}^2$) still remains far below the value calculated from conventional power broadening expressions ($\text{FWHM} \approx \sqrt{2} \cdot \Omega_{\text{Rabi, max}}^{(1)} / 2\pi \approx 1 \text{ GHz}$ [23]).

From table 1 it follows that besides the assigned one and two photon resonances in the 10P12-10P20 region other spectral features show up. Further, the presence of sharp resonances on the 10P22 and 10P24 lines were unexpected since these frequencies barely match with one or two photon steps on the ν_3 -ladder. We believe that all unidentified

transitions belong to hot-band or combination-band transitions. We do not attribute these to three photon transitions. First, the intensity does not show the correct power dependence, secondly the laser power seems to be insufficient to overcome an acceptable "three photon detuning", as can be estimated from $\Delta_{1,2} \cdot \Delta_{2,3} = 2.5$ [GHz]² (see appendix), for maximum laser power of 15 Watts; here $\Delta_{1,2}(\Delta_{2,3})$ is the detuning of the first (second) intermediate level.

The occurrence of a combined RAP/Rabi-effect in the interaction of the laser beam with the molecules deserves special attention. Different alignments cause different portions of molecules to be excited by RAP- or Rabi-mechanisms, resulting in different lineshapes. Characteristic for a pure RAP effect is the doubled absorption intensity due to inversion (which is independent of the laser power within large limits as discussed in section 4) and the absence of power broadening. RAP transitions take place due to a frequency sweep as experienced by the molecules caused e.g. by the curved wave front in a Gaussian power profile normally encountered in a convergent or divergent laser beam; transitions of the Rabi-type occur in a constant frequency field, e.g. precisely in the focus of the laser beam [13, 15]. In order to get reproducible results standardized alignment procedures were followed.

For the Rabi-type transitions the laser focus was aligned to coincide with the molecular beam axis optimizing the cluster dissociation signal on the 10P8 CO₂ line ($P_0=4.0$

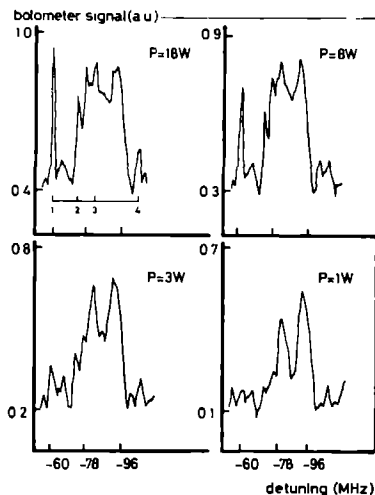


Figure 4: "Blob" structure on the 10P16 CO₂ laser line. The numbers 1 to 4 mark the frequencies of respectively the Q(18), Q(25), Q(26) and Q(29) transitions (see table 1^c).

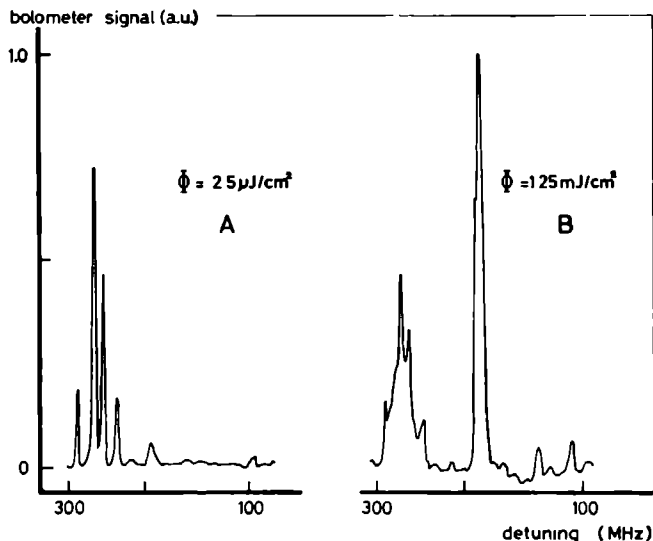


Figure 5: From RAP regime, left, to Rabi regime, right, due to increasing power. The frequency offset is given in MHz relative to the 10P16 CO₂ laser-line. Note the non-linearity of the frequency-scale.

bar, $T_0=300$ K, lens L_2 (fig.1) in "position B"). The alignment yielding maximum cluster dissociation ensures that the laser minimum waist is at the center of the molecular beam. Since the constant frequency condition in the laser focus is realized only for a limited dimension, it was not possible to suppress RAP-effects totally; because of the dimensions of the bolometer, 5 mm horizontal x 1 mm vertical, molecules cross the laser beam at different locations and partially "see" curved wave fronts.

Transitions of nearly pure RAP-type were realized by shifting the lens L_2 by 20 ± 5 mm to position A with respect to the optimum Rabi position discussed in the last paragraph; now all molecules interact with the curved wavefronts. The alignment was tested with well defined one and two photon transitions, showing an increase in intensity of more than 50 % when the lens L_2 was shifted from position B to A. One has to take into account the laser intensity which decreases when the lens is shifted, due to the divergence of the laser beam.

A remarkable fact is the appearance of "blobs" which show spectral sensitivity. These blobs appear, for growing laser power, on top of a relatively broad structure and are characterised by steep flanks as can be seen in fig.4. The blobs show up also at certain frequencies where at low laser power no absorption was observed.

2.4 The P(4) one-photon transitions

According to theoretical predictions, the quadruplet of P(4)- transitions, see fig.5^a, should show saturated intensities in the ratio of 1 : 3 : 4 : 3 [24]. Three of these transitions were observed before, with the best resolution of 10 kHz [1, 2]. The positions are shifted respectively 221 (A₁(0)), 238 (F₁(0)), and 250 (E(0)) MHz relative to the 10P16 CO₂ line (28,412,589 MHz) [25]. The observed relative line positions, see fig.5^a, lift any doubt that we deal with the P(4)-quadruplet. From the positions of the three well-known transitions, e.g. A₁(0), F₁(0), and E(0), we calibrate our frequency scale and observe a value of 286 ± 1 MHz for the fourth component (F₂(0)) of the P(4)-quadruplet. This position is in good agreement with the predicted value of [25]. To get an accurate estimate of the frequencies of the measured absorption lines, care has been taken to measure under RAP conditions, in order to avoid line broadening.

As for the intensities, note that the peak of the quadruplet shifted most to the blue in fig.5^a is on the limit of the tuning range. With an improved alignment of the laser we were able to determine the relative intensities. Averaging a series of measurements yielded the ratio values 1 : 2.9 : 3.7 : 2.6 which are in good agreement with the theoretical ratios mentioned above. The intensities were measured under RAP-conditions, L₂ in position A, with a laser fluence of $0.4 \mu\text{J}/\text{cm}^2$ (P = 5mW, $w = 0.5$ mm), enough to invert the population.

This value should be compared with the Rabi-frequency for a single 2π pulse, i.e. $\Omega_{\text{Rabi}}^{(1)} = \mu \cdot E_0/\hbar = 2\pi/\tau$ [s⁻¹] for Rabi-type transitions, lens L₂ in position B ($w_0 = 0.1$ mm). Here μ is the dipole moment, $\mu = 0.21$ Debye (for J = 4) [7], and τ is the transition time of the molecules through the laser field. The E-field in this equation can be expressed by $\sqrt{2P/\epsilon_0 c \pi w_0^2}$, where P is the laser power, ϵ_0 the dielectric constant, w_0 the minimum laser beam radius and c the speed of light in vacuum. Substituting the appropriate values, we find a 2π -cycle for a (circular) Rabi frequency for a one photon transition, $\Omega_{\text{Rabi}}^{(1)} = 50$ MHz for P = 3.2 mW. Note that the laser power for a 2π -cycle is independent of $w \geq w_0$. The conclusion then is that slightly more power (ca. 30 %) than necessary for a 2π -cycle yields almost complete inversion, under RAP conditions.

With a two laser pump and probe arrangement ($I_{\text{pump}} : I_{\text{probe}} = 7:3$) we actually tested that inversion by the pump laser has been achieved for low laser power, leading to negative double resonance bolometer signals (fig.6) [11]. To make sure that we dealt here with transitions of the RAP-type and not with a π pulse the laser fluence was doubled several times up to $13 \mu\text{J}/\text{cm}^2$. No decrease of the signal was found, indicating the absence of Rabi oscillations. Double resonance experiments are discussed in detail in section 6.

When the laser intensity (I) and thus also the fluence (Φ) is increased by a factor 500, two things happen to the one photon signals. First, considerable broadening is observed (but still less than expected for conventional power broadening), and second, the signals are reduced by about a factor two, as can be clearly seen in fig.5^b. Both phenomena follow from

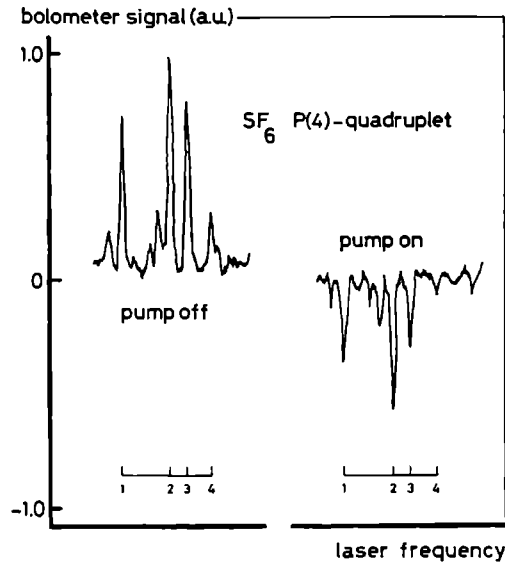


Figure 6: Stimulated deexcitation of the SF_6 $P(4)$ -quadruplet. On the left side the bolometer signal is shown for a (chopped) probe laser crossing the molecular beam. On the right an unchopped pump laser first produces inversion, resulting in stimulated deexcitation by the chopped probe laser. The positions of the $P(4)$ lines are indicated with numbers 1 to 4.

the fact that a change from the RAP regime to the (dephased) Rabi regime occurs by this drastic increase of laser intensity. In case of fig.5^b the FWHM due to power broadening is found to be about 15 MHz. At the same time the inversion which is typical for RAP processes ceases to occur, thus a maximum of 50% population for the upper level is found; this explains the loss of signal strength in fig.5^b as compared to fig.5^a. For a more detailed discussion of the RAP/Rabi transition see [26].

2.5 Two photon transitions with $J \leq 14$

For a two photon transition the Rabi frequency can be estimated from the one photon Rabi frequency, $\Omega_R^{(2)} = \Omega_R^{(1)} \cdot \Omega_R^{(1)} / 4\pi\Delta$ (see appendix). Using the saturation fluence of the $P(4)$ -quadruplet ($2.0 \mu\text{J}/\text{cm}^2$) and maximum (amplified) laser power (section 2), it follows that two photon resonances with maximum detuning of respectively 15, 8 and 4 GHz can be saturated for the zero, single and double pass configuration of the AOM. This condition is illustrated for some two photon resonances on the 10P16 CO_2 line. Since many of the

two photon resonances with low J-value are found around this line we will restrict us here mainly to this spectral area ($10P16 \pm 0.3$ GHz), if not mentioned otherwise.

The Q(9) doublet ($\Delta = 6$ GHz) could only be saturated when focussing exactly on the molecular beam (L_2 in position B). The $F_1(0)$ component was observed at a position of +235 MHz, about 8 MHz red shifted relative to the calculated value of +227 MHz. The E(0) component at +170 MHz was found in better agreement with the theoretically predicted value of +167 MHz. Similar small discrepancies have been observed for the P(4) E(0) transition (which showed already some power broadening, because of the smaller detuning, $\Delta = 1.7$ GHz) predicted at 164 MHz but observed at 174 MHz. Because of the saturation fluence of the P(4) transition, which is a factor 3 smaller than that of the Q(9) doublet, and the correct observed relative intensities of the Q(9) doublet, respectively 3:4, we are sure of this assignment. The P(4) $F_2(0)$ transition was also observed; it shows a redshift of 10 MHz relative to the predicted value. The P(7) $F_1(0)$ transition ($\Delta = 6.6$ GHz) on top of the

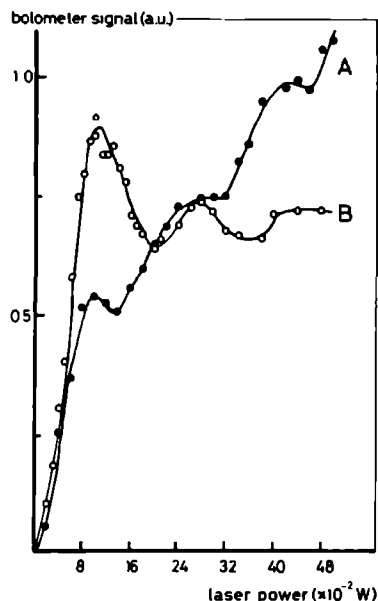


Figure 7: Power dependence of the P(4) E(0) transition shifted 174 MHz from the 10P16 CO₂ line taken under two different conditions (i.e. alignments). Curve A: the laser is aligned to maximum bolometer signal of the P(4) transition (RAP conditions). Curve B: the laser is aligned to maximum cluster signal on top of the 10P8 CO₂ line (Rabi conditions).

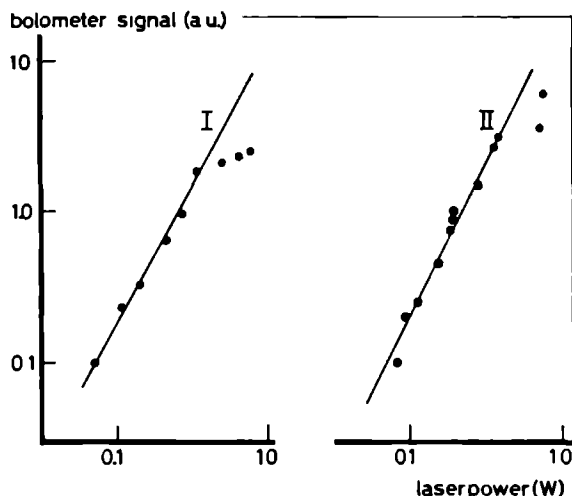


Figure 8 Absorption signal for increasing laser power, for transition I and II of fig 2 For an isolated n -photon transition, the absorption signal is proportional to the n^{th} power of the laser intensity The scales are logarithmic, the drawn lines correspond to $n=2$ Note that the laser fluence is smaller by about a factor 10 with respect to that of fig 7 due to different alignments

P(4) quadruplet and the P(7) $F_2(0)$ ($\Delta = 2.2$ GHz) were only observed with maximum laser intensity, at the expected spectral position (see table 1^c) The S-type transitions ($\Delta J = +2$) with relatively large detunings of 30 GHz (see table 1^c) could only be observed with sub-saturation intensities

Because of the low saturation fluence of the P(4) $E(0)$ transition the double resonance experiment could be repeated, for this two photon transition About 50% negative bolometer signal was found indicating 75% inversion Using this experimental set-up (L_2 in position A) the power dependence of the absorption intensity was investigated The result is shown in fig 7^a Only a small remainder of a Rabi oscillation is observed When focussing again exactly on the molecular beam (L_2 position B) a much more pronounced Rabi oscillation was observed, indicating that we had entered the Rabi regime, fig 7^b As far as we know this is the first time a two photon Rabi oscillation is observed Note the 50% increase of the "RAP saturation" going from L_2 position B to A

Dephasing behaviour of the oscillations results in a decreased absolute population (fig 7^b), this is in good agreement with numerical calculations done in our laboratory using the

optical Bloch equations. This simulation was performed using a Gaussian shaped intensity profile in a uniform frequency field. An active participation of the intermediate level in the process of populating the upper level is responsible for this behaviour, from this level both excitation to the two photon state and deexcitation to the ground state are possible. Dephasing becomes very important when the intermediate detuning gets smaller than the power broadening of a one photon transition. In case of random dephasing 33% of each level will be populated.

From the Rabi frequency in fig 7^b the power for the P(4) 2 π -pulse-transition could be calculated. The measured value, 200 mW, differs about a factor two from the calculated value (see appendix, especially the last paragraph). Entering the sub-saturation domain, the quadratic response of a two photon transition is illustrated in fig 8.

These two photon saturation measurements resemble the findings in [7] where similar experiments with one photon transitions were performed.

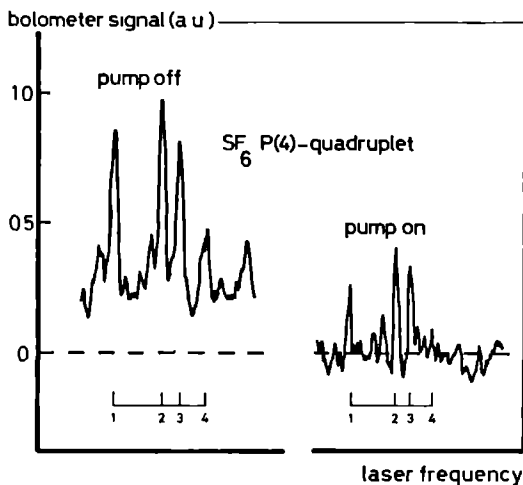


Figure 9 Double resonance signal of the SF₆ P(4)-quadruplet ($P = 400$ mW). On the left side the bolometer signal is shown for a (chopped) probe laser crossing the molecular beam. On the right an unchopped pump laser first induces a Rabi oscillation corresponding roughly to the action of a $(2\pi n + \pi/3)$ -pulse, yielding further excitation by the chopped probe laser, resulting in positive bolometer signal. The positions of the P(4) lines are indicated with numbers 1 to 4.

2.6 Inversion vs saturation, illustrated by double resonance experiments

This section serves to demonstrate clearly, though qualitatively, RAP-processes and their (partial) disappearance for increasing laser power. To start we go back to fig.6, where for weak laser power of 10 mW ($I = 1.3 \text{ W/cm}^2$, $\Phi = 8.5 \text{ } \mu\text{J/cm}^2$, L_2 in position A) RAP-inversion and stimulated deexcitation (by a second probe laser) are shown for the P(4)-quadruplet. Note the narrow line width and the 75% inversion obtained. In [11] similar one photon results were reported for a $\text{C}_2\text{H}_4 - \nu_7$ - transition.

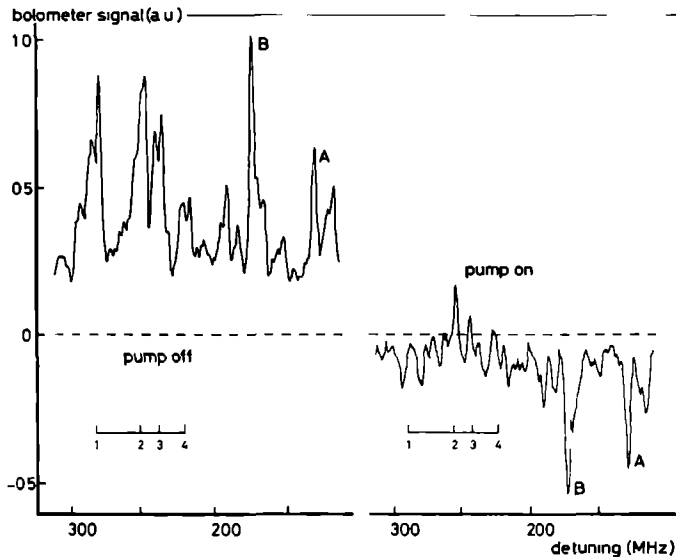


Figure 10: Inversion vs. saturation on the 10P16 CO_2 laser line (+200 MHz), for a laser power of 1.6 W. On the right side the two photon transitions A and B invert, while the P(4) one photon quadruplet is completely saturated, showing zero bolometer signal. The positions of the P(4) lines are indicated with numbers 1 to 4. The P(4) two photon transition is indicated with "B" whereas "A" is an unassigned two photon transition at 133 MHz detuned relative to the 10P16 CO_2 line center.

Next, the experiment has been repeated with a laser power of 400 mW ($I = 51 \text{ W/cm}^2$, $\Phi = 34 \text{ } \mu\text{J/cm}^2$, L_2 in position A), see fig.9. Two effects occur; most strikingly, the inversion (as proved by the negative signal in fig.6, with pump laser "on") is gone, for the P(4) quadruplet;

the RAP inversion starts disappearing at about 40 mW laser power. Secondly, some line broadening starts to show up. We take both effects as evidence for Rabi oscillations. The relative strength of the two laser signal of fig.9 suggests that the first laser excites about a 25% fraction of the ground state population with $J = 4$, i.e. the molecules see a $(2\pi n + \pi/3)$ -pulse. The laser power of 400 mW corresponds to a n -value of about 11. Note that underneath the pump-off signal of fig.9 one observes a background, which has disappeared in the pump-on mode. Apparently the background stems from (the flanks of) many saturated one photon transitions.

Finally, the laser power was further increased to 1.6 W ($I = 200 \text{ W/cm}^2$, $\Phi = 136 \mu\text{J/cm}^2$, L_2 in position A); the result is shown in fig.10. For the pump-off signal the P(4) quadruplet is still visible, but significantly broadened (although not to 1 GHz as expected conventionally [23]). The narrow peaks on top of the quadruplet probably are due to two photon transitions. The power is not large enough to saturate these transitions. Consequently, the left part of the pump-on signal averages to zero (the small peaks and valleys are not due to noise, but their origin is difficult to ascertain). Note that the laser power of 1.6 W corresponds to about 22 full Rabi cycles. On the left side of fig.10 interesting features start to appear. Peak B corresponds to the well assigned P(4)-two photon transition, 174 MHz detuned from the center of the 10P16 CO₂ laser transition, with the relative small Δ -value of 1.7 GHz. This two photon transition is strongly inverted (i.e. not saturated in the conventional way); it shows about 75% inversion, yielding the negative signal for the pump-on mode. Analogously, peak A is determined as a two photon transition, which could not be assigned and probably therefore belongs to a hot band transition. Note the narrow line width of the two photon transitions and the background which disappears for the pump-on signal.

2.7 Outlook

There is one straightforward extension of the measurements discussed above. Since we were neither particularly successful with, nor especially interested in efficient expansion cooling, we did not change the SF₆ concentration in He. Increasing the concentration one can obtain stronger signals and longer interaction times (by diminishing the drift velocity). It looks interesting to investigate under these conditions the changes in the Boltzmann plot because SF₆-SF₆ collisions just after the nozzle become more important. We also will search further for isolated three photon transitions by increasing the laser fluence and by performing double resonance experiments.

Next, we will try to solve the riddle of the spectral blobs. The most interesting explanation to be found would be that for strong laser fluences we reach highly excited states which couple so strongly that local quasi-continua show up.

There has been another puzzling question we were not able to solve yet. Since we can virtually label states with every J -value up to 50, we tried to investigate which were the

ground state levels from which the molecules depart most easily during multi-photon excitation processes. These experiments were more difficult than expected, we could not detect any ground state level with a very strongly preferent excitation probability. Consequently we have to improve our detection sensitivity, there will be another attempt.

Finally, experiments are underway to investigate the influence of high vibrational excitation on reactive and surface scattering properties in collaboration with the group of Duren in Gottingen and Iannotta in Trento, respectively, especially the angle distribution will be looked at.

2.8 Table

nr	transitions	n	Δ [GHz]	ν_{th} [MHz]	ν_{exp} [MHz]	FWHM [MHz]	I
1					-326	4	w
2					-316	9	w
3					-302	9	w
4					-288	5	w
5	R(93) F ₁ (0), F ₂ (0)	1	-	285			
6					-281	5	w
7 •	R(69) F ₁ (2)	1	-	-270	-271	2	w
8 •	R(68) F ₁ (3)	1	-	-264	266	-	w
9 •	R(68) E(2)	1	-	-260	-261	14	w
10 •	R(68) F ₂ (3)	1	-	-256	-257	-	w
11					-249	5	w
12					-244	3	m
13					-239	3	w
14					-235	3	w
15	R(70) F ₂ (7)	1	-	-231			
16					-227	4	w
17					-221	4	w
18					-212	4	m
19					-208	2	w
20					-204	3	w
21					-199	2	w
22 •	R(70) F ₁ (7)	1	-	-190	-190	5	w
23	R(72) E(6), F ₂ (10), A ₂ (3)	1	-	-183			
24					-175	6	m
25 ¹⁾	R(74) E(8), F ₂ (12), A ₂ (3)	1	-	-169	-168	3	m
26					-165	3	w
27					-155	3	w
28					-147	8	m
29					-134	4	w
30					-128	4	w
31 ¹⁾	R(89) E(0), F ₁ (1), A ₁ (0)	1	-	-117			
32 ¹⁾	R(73) E(4), F ₁ (7), A ₁ (2)	1	-	-113	-112	9	w
33					-101	4	w
34					-93	5	m
35					-79	4	w
36					-63	8	w
37					-60	8	w
38					-50	4	w
39					-29	3	w
40 ¹⁾	R(66) F ₁ (0), F ₂ (0), A ₁ (0), A ₂ (0)	1	-	-23	-23	4	m
41					-13	4	w
42					-4	6	m
43					7	6	w
44					17	6	w
45					22	2	w
46 ¹⁾	R(83) E(1), F ₁ (2), A ₁ (0)	1	-	25			
47					31	3	w
48					41	7	m
49					50	3	w
50 ¹⁾	R(77) F ₁ (5), F ₂ (4)	1	-	54	54	3	w
51					63	3	w
52	R(94) E(15), F ₂ (23), A ₂ (7)	1	-	65			
53					70	3	w
54					74	3	w
55					79	3	w
56					87	7	w
57					90	4	m
58					99	4	m
59					103	2	w

nr	transitions	n	Δ [GHz]	ν_{th} [MHz]	ν_{exp} [MHz]	FWHM [MHz]	I
60 ¹⁾	R(70) A ₁ (2)	1	-	106	107	6	w
61 ¹⁾	R(86) E(13), F ₁ (19), A ₁ (6)	1	-	109			
62					121	3	w
63					127	10	m
64					139	6	w
65					143	2	w
66					148	2	m
67					150	2	m
68					156	4	w
69					162	2	w
70					166	2	w
71					171	5	w
72					178	3	w
73 •	R(69) F ₂ (12)	1	-	187	185	10	w
74 ¹⁾	R(70) F ₁ (6)	1	-	197			
75					202	3	w
76	R(71) F ₁ (9)	1	-	209			
77	R(69) E(8)	1	-	210			
78 •	R(67) F ₁ (15), F ₂ (15), A ₁ (4), A ₂ (5)	1	-	214	214	-	m
79 •	R(71) F ₂ (9)	1	-	220	219	-	m
80					221	-	m
81 •	R(69) F ₁ (13)	1	-	228	227	-	w
82					230	-	w
83					234	-	w
84 •	R(81) F ₁ (3), F ₂ (3)	1	-	240	241	5	w
85					244	5	w
86	R(70) E(4)	1	-	249			
87	R(79) E(2), F ₂ (4), A ₂ (1)	1	-	250			
88					254	3	w
89					261	5	w
90					266	4	m
91					272	3	m
92					288	4	m
93					294	2	w
94					297	2	w
95	R(90) F ₁ (21)	1	-	308			

nr	transitions	n	Δ [GHz]	ν_{th} [MHz]	ν_{exp} [MHz]	FWHM [MHz]	I
1					-285	4	m
2					-276	5	m
3					-270	2	w
4 •	R(29) E(0), F ₁ (1), A ₁ (0)	1		-264	-264	12	m
5	S(25) F ₁ (1)	2	5 3	-258			
6	R(28) F ₁ (2)	1	-	-256			
7					252	9	w
8					-245	3	m
9					-241	4	m
10 ••	Q(40) E(4)	2	14	-231	-233	2	w
11					-225	3	m
12 ••	Q(30) F ₂ (2)	2	<1	-220	-220	9	m
13 ••	Q(30) F ₁ (1)	2	<1	-216			
14	Q(34) F ₂ (3)	2	5	-216			
15					-211	5	m
16					-203	2	w
17					-193	9	m
18					-182	2	w
19	Q(34) F ₁ (3)	2	5	-178			
20 ¹⁾	R(28) E(1)	1	-	-167	-168	5	m
21 ••	R(18) E(2)	2	15	160	-160	9	m

Tabel 1 ^s . (continued)							
nr	transitions	n	Δ [GHz]	ν_{ex} [MHz]	ν_{exp} [MHz]	FWHM [MHz]	I
22	S(52) A ₁ (2)	2	31	-158			
23					-152	2	m
24 ¹⁾	R(28) F ₂ (2)	1	-	-144	-143	4	m
25					-138	2	m
26	S(52) E(4)	2	31	-134			
27	S(53) A ₂ (1)	2	31	-130			
28	S(53) E(3)	2	31	-128			
29 ^{••}	R(6) E(0)	2	33	-125	-126	-	m
30					-115	6	m
31 ²⁾	S(47) F ₂ (9)	2	29	-94	-94	3	w
32					-89	3	w
33 ²⁾	S(46) F ₁ (1)	2	28	-79	-79	6	w
34 ²⁾	S(46) E(0)	2	28	-77			
35 ²⁾	S(46) F ₂ (1)	2	28	-74			
36	Q(37) A ₁ (1)	2	10	-73			
37 ²⁾	S(47) E(6)	2	29	-72			
38					-71	3	m
39	R(58) E(7), A ₂ (3)	2	34	-64			
40					-62	2	w
41					-58	2	w
42					-54	2	w
43 ²⁾	S(47) F ₁ (10)	2	29	-53			
44					-49	2	w
45 ^{••}	R(6) F ₁ (1)	2	34	-43	-42	3	w
46 ^{••}	Q(39) A ₁ (1)	2	11	-35	-36	2	w
47					-31	4	w
48					-20	2	w
49					-16	2	w
50					-13	2	w
51					-9	2	w
52					0	4	w
53					5	2	w
54					13	2	w
55 ¹⁾	R(28) A ₂ (0)	1	-	18	18	5	m
56					29	5	m
57					34	2	w
58 ¹⁾	R(28) F ₂ (1)	1	-	39	39	5	m
59 ¹⁾	R(28) F ₁ (1)	1	-	55	55	5	m
60	Q(46) F ₁ (10)	2	25	66			
61 ¹⁾	R(28) A ₁ (0)	1	-	68	68	10	w
62	Q(46) E(6)	2	25	71			
63	Q(46) F ₂ (10)	2	25	75			
64	Q(56) A ₁ (3) ⁻⁾	2	40	78			
65					80	10	w
66					93	3	w
67					101	10	w
68					112	2	w
69					117	2	w
70 ²⁾	S(48) F ₁ (3)	2	29	119			
71					122	5	m
72					128	5	m
73					132	5	m
74					138	5	m
75					148	2	w
76					158	2	w
77					162	2	m
78					167	4	s
79					176	2	w
80 ¹⁾	R(29) F ₁ (2), F ₂ (1)	1	-	185	185	5	m
81					193	2	w
82					198	2	w

nr	transitions	n	Δ [GHz]	ν_h [MHz]	ν_{exp} [MHz]	FWHM [MHz]	I
83 ●●	R(6) A ₁ (0)	2	34	217	217	2	w
84					225	2	w
85	S(50) E(2)	2	29	228			
86					228	2	w
87 ●●	Q(14) E(1)	2	20	234	237	10	m
88	S(47) E(7), F ₁ (11), F ₂ (11)	2	25	237			
89	S(51) F ₁ (7)	2	30	244			
90					239	2	m
91					247	2	w
92					253	4	m
93					264	4	w
94					271	4	m
95					276	2	w
96 ●●	R(18) F ₁ (4)	2	16	282	281	2	w
97	S(50) F ₂ (3)	2	29	291			
98					291	2	w
99	Q(14) F ₂ (2)	2	20	296			
100					302	2	w

nr	transitions	n	Δ [GHz]	ν_h [MHz]	ν_{exp} [MHz]	FWHM [MHz]	I
1	Q(44) F ₂ (2)	1	-	-320			
2 ●●	Q(23) F ₂ (5)	2	4.8	-297	-300	-	m
3 ●●	Q(46) E(2)	1	-	-291	-291	-	w
4	Q(30) A ₂ (0)	2	4.2	-288			
5	Q(44) A ₂ (0)	1	-	-288			
6	R(42) E(3)	2	1.3	-278			
7 ●●	Q(31) E(4)	2	2.4	-276	-277	-	s
8 ●●	P(7) F ₂ (0)	2	4.7	-269	-267	-	s
9	S(11) F ₂ (1)	2	27	-269			
10 ●●	Q(27) A ₁ (1)	2	3.7	-255	-256		m
11 ¹⁾	Q(55) F ₂ (6)	1	-	-249			
12	R(37) F ₁ (6), F ₂ (7)	2	<1	-246			
13 ¹⁾	Q(55) F ₁ (6)	1	-	-242			
14 ●●	Q(31) F ₁ (7)	2	2.4	-238	-237	-	s
15 ●●	Q(30) F ₂ (0)	2	3.7	-237	-237	-	s
16	R(42) F ₁ (5)	2	1.3	-229			
17 ●●	Q(29) F ₂ (6)	2	4.2	-227			
18 ●●	Q(25) F ₂ (5)	2	4.5	-226	-228	-	s
19 ¹⁾	Q(46) F ₁ (3)	1	-	-213			
20 ●●	Q(26) F ₁ (0)	2	4.0	-210	-210	-	-
21 ¹⁾	Q(49) F ₁ (7)	1	-	-207			
22 ●●	Q(28) F ₁ (0)	2	4.2	-206	-205	-	s
23	R(52) F ₂ (3)	2	<1	-205			
24 ¹⁾	Q(47) F ₁ (7)	1	-	-193	-195	-	-
25 ●●	Q(16) F ₁ (0)	2	6.0	-186	-191	-	s
26 ●●	Q(30) F ₁ (0)	2	3.6	-189	-187	-	-
27					-181	-	m
28					-177	-	
29 ²⁾	Q(21) F ₁ (5)	2	5.1	-172	-174	2	m
30					-170	1	-
31 ●●	P(4) F ₂ (0)	2	0.35	-173	-164	2	s
32 ²⁾	Q(29) E(4)	2	3.3	-162			
33 ²⁾	R(46) F ₂ (7)	2	<1	-160			
34 ¹⁾	Q(49) E(4)	1	-	-159			
35 ²⁾	Q(24) F ₂ (0)	2	4.5	-155	-156	-	-
36 ²⁾	R(47) E(2)	2	<1	-152			
37 ²⁾	Q(27) F ₁ (6)	2	3.6	-149	-151		m
38 ¹⁾	Q(54) A ₂ (2)	1	-	-147			
39 ²⁾	Q(14) F ₁ (0)	2	6.3	-144	-146		-
40 ²⁾	Q(30) A ₁ (0)	2	3.6	-141			

Tabel 1^c: (continued)

nr	transitions	n	Δ [GHz]	ν_{th} [MHz]	ν_{exp} [MHz]	FWHM [MHz]	I
41 ●●	R(42) A ₁ (2)	2	1.4	-140	-141	-	-
42 1)	Q(54) F ₂ (7)	1	-	-137	-136	-	m
43 1)	Q(54) E(4)	1	-	-132	-	-	-
44 2)	R(24) F ₁ (0), F ₂ (0)	2	4.4	-132	-	-	-
45 2)	Q(28) E(0)	2	4.0	-128	-127	2	m
46	R(52) E(2)	2	<1	-127	-	-	-
47 1)	Q(41) F ₁ (9)	1	-	-122	-122	2	-
48 1)	Q(41) E(5)	1	-	-117	-118	2	s
49 1)	Q(48) F ₁ (4)	1	-	-115	-115	2	-
50 1)	Q(41) F ₂ (8)	1	-	-111	-111	2	m
51 2)	Q(29) F ₁ (7)	2	3.2	-103	-103	2	s
52				-96	-96	6	s
53	S(20) E(3), F ₁ (4), A ₁ (1)	2	40	-87	-	-	-
54				-86	-86	4	s
55 2)	Q(44) F ₁ (5)	2	<1	-81	-81	5	-
56 2)	Q(26) E(0)	2	3.9	-79	-79	2	s
57 2)	Q(25) E(3)	2	4.1	-75	-75	2	m
58	S(19) A ₂ (0)	2	39	-71	-	-	-
59				-70	-70	2	w
60	S(19) F ₂ (1)	2	39	-66	-	-	-
61 1)	Q(45) A ₂ (2)	1	-	-63	-65	4	w
62 2)	Q(18) F ₂ (0)	2	5.6	-60	-62	-	s
63				-59	-59	2	s
64 2)	Q(27) F ₂ (6)	2	3.5	-52	-	-	-
65 2)	Q(28) F ₂ (0)	2	4.0	-51	-51	5	s
66 2)	Q(22) E(0)	2	4.8	-50	-	-	-
67	R(52) F ₁ (3)	2	<1	-50	-	-	-
68				-46	-46	-	s
69 2)	Q(23) E(3)	2	4.5	-39	-38	-	m
70 2)	R(45) A ₂ (1)	2	<1	-34	-35	-	-
71 1)	Q(53) F ₂ (6)	1	-	-30	-30	-	-
72				-25	-25	-	-
73 1)	Q(53) F ₁ (6)	1	-	-17	-18	-	s
74 1)	Q(38) F ₂ (0)	1	-	-8	-	-	-
75 1)	Q(38) E(0), F ₁ (0)	1	-	-7	-8	10	w
76				-2	-2	-	m
77 ●●	R(49) A ₂ (2)	2	<1	2	3	-	w
78 ●●	Q(11) F ₁ (1)	2	6.5	8	10	2	e
79 1)	Q(43) F ₁ (8)	1	-	9	-	-	-
80 1)	Q(45) F ₂ (7)	1	-	13	-	-	-
81 ●●	S(11) E(0)	2	27	24	20	3	w
82 2)	Q(24) F ₁ (0)	2	4.3	27	25	2	s
83 2)	Q(26) F ₂ (0)	2	3.8	32	30	2	s
84 2)	R(35) F ₁ (4)	2	<1	33	-	-	-
85 1)	Q(48) F ₂ (5)	1	-	36	-	-	-
86 2)	R(35) F ₂ (5)	2	<1	36	-	-	-
87 2)	Q(27) A ₂ (2)	2	3.4	38	37	2	s
88 1)	Q(43) E(5)	1	-	38	-	-	-
89				43	43	2	m
90 2)	Q(19) E(2)	2	5.3	50	48	2	s
91				52	52	-	-
92				56	56	2	m
93				62	62	2	m
94 2)	Q(20) E(0)	2	4.4	71	70	2	s
95 2)	Q(25) F ₁ (6)	2	4.0	72	72	2	s
96 1)	Q(43) F ₂ (8)	1	-	72	-	-	-
97 1)	Q(47) E(4)	1	-	73	-	-	-
98 2)	R(43) F ₂ (5)	2	<1	81	79	2	m
99 1)	Q(52) E(4)	1	-	86	86	2	w
100 1)	Q(52) F ₁ (6)	1	-	95	93	8	-
101				96	96	3	s

nr	transitions	n	Δ [GHz]	ν_{th} [MHz]	ν_{exp} [MHz]	FWHM [MHz]	I
102	Q(46) A ₁ (1)	1	-	96	-	-	-
103	Q(45) F ₁ (8)	1	-	100	100	4	-
104	S(12) F ₁ (3)	2	28	103	102	8	w
105	Q(52) A ₁ (2)	1	-	112	110	2	w
106					116	2	-
107					122	3	s
108					125	3	m
109					133	4	s
110	Q(21) F ₂ (4)	2	4.8	142	142	2	s
111	Q(47) F ₁ (7)	1	-	147	147	2	-
112	Q(23) F ₁ (5)	2	4.4	153	152	2	s
113					160	-	w
114					168	6	s
115	Q(9) E(0)	2	6.8	167	170	2	s
116	P(4) E(0)	2	0.076	164	174	2	s
117	Q(24) A ₁ (0)	2	4.1	188	185	4	m
118					192	6	s
119	Q(51) F ₂ (6)	1	-	206	207	6	m
120	Q(22) F ₂ (0)	2	4.5	214	215	-	-
121	P(4) A ₁ (0)	1	-	221	221	-	s
122	Q(9) F ₁ (1)	2	6.4	227	235	-	s
123	Q(51) F ₁ (6)	1	-	228	-	-	-
124	P(4) F ₁ (0)	1	-	238	238	-	s
125	Q(40) A ₁ (0)	1	-	247	245	-	-
126	P(4) E(0)	1	-	250	250	-	s
127	Q(45) A ₁ (2)	1	-	251	-	-	-
128	P(7) F ₁ (0)	2	5.3	252	254	-	-
129	Q(40) F ₁ (1)	1	-	253	-	-	-
130	R(38) F ₁ (0)	2	<1	257	-	-	-
131	Q(40) F ₂ (1)	1	-	259	259	-	m
132	R(38) F ₂ (0)	2	<1	260	-	-	-
133	Q(40) A ₂ (0)	1	-	266	265	-	-
134	R(53) E(6)	2	<1	267	-	-	-
135	R(49) F ₂ (7)	2	<1	273	-	-	-
136	R(39) F ₂ (3)	2	<1	276	-	-	-
137	Q(47) A ₂ (2)	1	-	276	276	-	-
138	Q(46) F ₁ (4)	1	-	282	-	-	-
139	S(12) E(1)	2	28	286	-	-	-
140	P(4) F ₂ (0)	1	-	286	286	-	s
141	R(39) F ₂ (3)	2	<1	289	-	-	-
142	R(47) A ₂ (2)	2	<1	293	295	-	w
143	Q(50) A ₂ (1)	1	-	313	-	-	-

nr	transitions	n	Δ [GHz]	ν_{th} [MHz]	ν_{exp} [MHz]	FWHM [MHz]	I
1					-315	4	m
2					-308	4	m
3					-297	4	m
4	R(21) F ₂ (2)	2	69	290	-	-	-
5					-290	8	w
6					283	2	w
7	P(42) F ₁ (6)	2	19	-278	-	-	-
8	P(57) E(0), A ₁ (0)	2	52	277	-	-	-
9					-274	10	m
10	P(49) E(1), F ₂ (2), A ₂ (0)	2	31	288	-	-	-
11					-266	8	m
12	P(42) F ₂ (6)	2	19	-262	-	-	-
13	P(37) F ₂ (5)	2	7.7	260	-	-	-
14					259	2	w
15					-252	10	w
16					-243	5	m

Table 1 ^d : (continued)							
nr	transitions	n	Δ [GHz]	ν_{ch} [MHz]	ν_{exp} [MHz]	FWHM [MHz]	I
17					-231	5	m
18	P(39) F ₂ (5)	2	12	-227			
19	P(35) F ₁ (6)	2	3 5	-221			
20					-217	-	-
21	O(26) F ₂ (1)	2	14	-215	-212	-	-
22					-207	-	-
23					-203	-	-
24					-198	-	-
25					-190	6	m
26					-174	3	s
27	O(11) A ₂ (0)	2	41	-169			
28					-168	2	m
29					-163	2	s
30					-161	2	s
31					-154	2	w
32	R(21) F ₁ (2)	2	59	-150			
33					-149	3	w
34					-144	3	w
35					-139	2	w
36	Q(55) E(0), A ₂ (0) **)	2	43	-137			
37					-134	6	m
38 ²⁾	O(26) E(2)	2	13	-130			
39 ²⁾	O(26) F ₂ (4)	2	13	-126			
40 ¹⁾	P(33) F ₁ (5)	1	-	-126	-127	2	-
41					-123	2	m
42 ²⁾	O(26) A ₂ (1)	2	13	-117			
43 ¹⁾	P(32) F ₁ (6), F ₂ (7)	1	-	-117	-117	4	m
44					-115	2	w
45					-112	2	w
46					-109	2	w
47					-107	2	w
48					-102	-	m
49					-100	-	m
50					-98	-	m
51					-91	2	m
52					-88	2	m
53 ¹⁾	P(33) F ₂ (4)	1	-	-85	-85	3	m
54					-81	4	m
55					-75	2	w
56					-69	2	w
57	R(22) F ₂ (3)	2	59	-62			
58					-62	2	w
59					-59	2	m
60					-54	2	w
61					-49	6	m
62					-42	2	w
63					-39	2	w
64					-36	2	w
65					-30	2	w
66					-28	3	m
67					-25	2	w
68					-17	5	m
69 ^{••}	P(39) F ₁ (4)	2	12	-15	-13	2	w
70					-7	4	m
71					-2	2	w
72					3	2	w
73 ¹⁾	P(33) A ₂ (1)	1	-	6	7	-	m
74					14	2	w
75					18	4	w
76					31	10	m
77					45	2	w

Tabel 1 ^d (continued)							
nr	transitions	n	Δ [GHz]	ν_{th} [MHz]	ν_{exp} [MHz]	FWHM [MHz]	I
78					49	5	m
79					53	2	w
80	P(45) F ₁ (3), F ₂ (3)	2	28	55			
81					63	10	m
82					68	2	w
83					75	4	w
84					80	4	w
85					85	2	w
86					89	2	w
87					91	4	m
88					95	2	w
89	R(18) E(0)	2	60	98			
90					99	3	m
91	P(36) A ₁ (1)	2	60	102			
92	R(18) F ₁ (1)	2	60	105			
93 ¹⁾	P(33) F ₂ (5)	1		108	107	2	w
94					113	9	m
95	P(19) A ₂ (0)	2	26	114			
96	P(20) A ₁ (0)	2	27	119			
97					121	2	w
98					126	5	w
99					130	2	w
100	R(24) F ₂ (5)	2	57	131			
101••	P(35) A ₁ (1)	2	35	138	136	2	w
102					140	9	m
103 ¹⁾	P(33) E(3)	1	-	141			
104					147	2	w
105					150	2	w
106					156	3	m
107					160	2	w
108					162	2	w
109	R(24) E(3)	2	57	163			
110					166	2	w
111					170	2	w
111	R(16) F ₁ (0)	2	59	171			
112	R(16) F ₂ (0)	2	59	174			
113					175	2	w
114					180	3	m
115					184	3	m
116 ¹⁾	P(33) F ₁ (6)	1		187	188	2	w
117	R(24) F ₁ (5)	2	57	191			
118••	P(32) F ₂ (1)	2	21	193	193	4	w
119					197	2	w
120					203	2	w
121					208	3	m
122					215	2	w
123					219	3	m
124					224	3	m
125••	O(14) F ₁ (2)	2	35	231	230		w
126					237	-	-
127					240	2	m
128					246	6	m
129					252	2	w
130					255		m
131					260		w
132	R(22) E(2)	2	59	260			
133					264	-	-
134					272	2	w
135					277	2	w
136••	P(32) E(1)	2	21	275	278	2	m
137					284	2	m
138					290	2	w

Tabel 1 ^d . (continued)						
nr	transitions	n	Δ [GHz]	ν_{th} [MHz]	ν_{exp} [MHz]	FWHM [MHz]
139					295	-
140					297	2
141					302	4
142					304	2
143					312	2

Tabel 1 ^e . 10P20 CO ₂ laser line 28,306,225 MHz						
nr	transitions	n	Δ [GHz]	ν_{th} [MHz]	ν_{exp} [MHz]	FWHM [MHz]
1					-317	4
2					-311	3
3					-299	4
4	Q(50) F ₁ (7) ⁻	2	12	-298		
5					-294	4
6	Q(50) F ₂ (6) ⁻	2	12	-294		
7	O(8) E(0)	2	103	-292		
8	Q(37) F ₁ (4) ⁻⁻	2	42	-279		
9	Q(42) E(6), F ₁ (8), A ₁ (3) ⁻⁻	2	31	-279		
10					-274	4
11					-268	2
12					-258	3
13	Q(49) E(1), F ₁ (3) ⁻	2	15	-258		
14	Q(49) F ₂ (2) ⁻	2	15	-257		
15					-244	4
16					-231	2
17 ¹⁾	P(57) F ₁ (3), F ₂ (3)	1	-	-226		
18	O(25) F ₂ (1)	2	72	-223		
19					-216	4
20	Q(51) F ₁ (7), F ₂ (8) ⁻	2	10	-209		
21					-207	4
22					-203	3
23 ¹⁾	P(58) F ₁ (8), F ₂ (9)	1	-	-197		
24					-191	3
25	Q(50) E(4), F ₁ (6), A ₁ (2) ⁻	2	12	-185		
26					-183	3
27	O(20) F ₂ (0)	2	79	-175		
28					-165	3
29					-159	3
30					-150	2
31 ²⁾	Q(43) E(0), F ₂ (1), A ₂ (0) ⁻⁻	2	29	-148		
32	O(47) E(1), F ₁ (2), A ₁ (0)	2	22	-146		
33	Q(49) F ₁ (5)	2	19	-144		
34	O(47) F ₂ (4)	2	22	-143		
35 ¹⁾	P(59) F ₁ (8)	1	-	-141		
36 ²⁾	Q(49) A ₂ (3) ⁻	2	15	-134		
37 ²⁾	Q(49) F ₂ (10) ⁻	2	15	-131		
38 ²⁾	Q(49) F ₁ (11) ⁻	2	15	-126		
39					-125	2
40 ²⁾	Q(49) A ₁ (3) ⁻	2	15	-121		
41	Q(37) F ₂ (5) ⁻⁻	2	42	-115		
42					-115	3
43					-100	3
44	P(14) E(0)	2	89	-92		
45	Q(38) F ₂ (3) ⁻⁻	2	40	-78		
46 ¹⁾	P(60) F ₁ (1)	1	-	-75		
47 ¹⁾	P(60) E(0), F ₂ (1)	1	-	-74		
48 ¹⁾	P(59) F ₂ (9)	1	-	-72		
49 ²⁾	Q(49) F ₁ (7) ⁻	2	15	-66		
50 ²⁾	Q(44) E(7), F ₁ (10), A ₁ (3) ⁻⁻	2	26	-64		
51	P(30) F ₁ (2)	2	59	-64		
52	P(30) F ₂ (1)	2	59	-63		
53 ²⁾	Q(49) E(4) ⁻	2	15	-58		

Table 1* (continued)

nr	transitions	n	Δ [GHz]	ν_{rh} [MHz]	ν_{exp} [MHz]	FWRM [MHz]	I
54					56	3	m
55 ²⁾	Q(49) F ₁ (10)	2	15	-54			
56 ²⁾	Q(49) E(5)	2	15	50			
57	Q(38) F ₁ (3) --)	2	40	-49			
58					46	5	m
59 ²⁾	Q(49) E(6)	2	15	-45			
60	O(46) E(6), F ₁ (9), A ₁ (3)	2	27	-41			
61 ²⁾	Q(50) F ₁ (5), F ₂ (5) -)	2	12	-37			
62					-35	4	w
63					-19	5	m
64 ²⁾	Q(52) E(5), F ₂ (8), A ₂ (2) --)	2	7.5	-19			
65 ²⁾	Q(49) F ₂ (9) -)	2	15	-17			
66 ²⁾	Q(53) E(2), F ₁ (4), A ₁ (1) --)	2	5.0	-14			
67					-10	3	m
68	O(25) E(0)	2	68	2			
69 ²⁾	Q(49) F ₁ (6) -)	2	15	2	2	3	m
70					9	3	m
71					15	2	w
72					26	4	m
73 ¹⁾	P(59) A ₂ (3)	1		28			
74					32	2	w
75 ²⁾	Q(51) E(3), F ₁ (5), A ₁ (1) --)	2	10	40			
76					48	2	w
77					55	3	w
78 ²⁾	Q(54) E(6), F ₂ (10), A ₂ (3) --)	2	2.5	60	63	3	w
79 ²⁾	Q(49) A ₂ (1) -)	2	15	61			
80	Q(49) E(3) -)	2	15	64			
81 ²⁾	Q(49) E(5)	2	15	66			
82 ²⁾	Q(49) F ₂ (7) -)	2	15	67			
83 ²⁾	Q(49) F ₂ (8)	2	15	70			
84 ²⁾	Q(49) E(6) -)	2	15	72			
85 ²⁾	Q(49) A ₂ (2) -)	2	15	75			
86 ²⁾	Q(49) F ₂ (9) -)	2	15	76			
87					80	4	w
88 ¹⁾	P(55) F ₁ (0), F ₂ (0)	1	-	88	88	2	w
89 ²⁾	Q(49) A ₂ (3) -)	2	15	89			
90	Q(19) F ₁ (0)	2	79	91			
91	Q(19) F ₂ (0)	2	79	92			
92					100	4	m
93					112	4	m
94 ¹⁾	P(56) E(8), F ₂ (12), A ₂ (3)	1	-	128			
95					129	3	w
96 ²⁾	Q(48) F ₁ (0), A ₁ (0) -)	2	17	131			
97 ²⁾	Q(48) F ₂ (0), A ₂ (0) -)	2	17	132			
98					134	4	w
99					141	4	w
100 ²⁾	Q(39) F ₁ (3) --)	2	38	147			
101	P(35) F ₂ (3)	2	49	148			
102	O(31) E(4), F ₂ (7), A ₂ (2)	2	57	149			
103					149	2	w
104 ²⁾	Q(39) F ₂ (3) --)	2	38	151			
105 ²⁾	Q(50) E(4), F ₂ (6), A ₂ (1) -)	2	12	154			
106					155	4	w
107					161	4	m
108 ²⁾	Q(49) F ₁ (8), F ₂ (7) -)	2	15	175			
109					179	3	m
110					196	4	m
111					209	8	m
112	Q(55) E(8), A ₁ (3) --)	2	<1	212			
113	Q(36) F ₁ (4) --)	2	44	217			
114					223	2	w

Tabel 1 ⁶ : (continued)							
nr	transitions	n	Δ [GHz]	ν_{th} [MHz]	ν_{exp} [MHz]	FWHM [MHz]	I
115	O(43) F ₁ (0), F ₂ (0)	2	28	224			
116 ¹⁾	P(59) F ₂ (10)	1	-	226			
117	O(27) F ₁ (3)	2	65	230			
118					240	2	w
119	Q(48) F ₂ (8) ⁻⁾	2	17	243			
120					243	3	m
121	Q(48) E(5) ⁻⁾	2	17	247			
122					250	3	w
123	Q(48) F ₁ (8) ⁻⁾	2	17	263			
124					258	4	w
125	O(50) F ₂ (5)	2	19	261			
126					265	3	w
127	P(59) E(6)	1	-	270			
128					283	2	w
129	O(8) F ₂ (0)	2	100	287			
130					291	3	w
131	O(20) F ₁ (0)	2	79	300			
132					300	2	w
133					306	3	w

Tabel 1 ⁷ : 10P22 CO ₂ laser line 28,251,942 MHz							
nr	transitions	n	Δ [GHz]	ν_{th} [MHz]	ν_{exp} [MHz]	FWHM [MHz]	I
1					-276	4	m
2					-263	3	m
3					-252	3	m
4					-240	3	m
5					-231	4	m
6					-222	4	m
7					-205	4	s
8	P(83) F ₁ (13)	1	-	-192			
9					-185	4	s
10					-173	4	s
11					-161	3	m
12					-153	5	m
13					-133	3	m
14					-119	3	m
15					-105	6	m
16	P(82) F ₁ (10)	1	-	-86			
17					-75	3	w
18					-45	3	w
19					-23	4	m
20					39	4	w
21					49	3	w
22	P(81) F ₁ (8), F ₂ (7)	1	-	58			
23	P(83) F ₂ (14)	1	-	114			
24	P(83) F ₁ (14)	1	-	236			
25					237	5	w
26					285	3	m

nr	ν_{exp} [MHz]	FWHM [MHz]	I	nr	ν_{exp} [MHz]	FWHM [MHz]	I	nr	ν_{exp} [MHz]	FWHM [MHz]	I
1	-297	3	m	14	-8	3	m	27	180	3	s
2	-286	3	w	15	-1	3	m	28	184	3	s
3	-279	3	w	16	17	4	m	29	188	3	m
4	-271	3	m	17	37	3	m	30	208	4	m
5	-248	9	w	18	53	5	s	31	223	4	m
6	-221	3	m	19	71	5	m	32	232	2	m
7	-203	5	m	20	80	7	s	33	241	3	m
8	-164	4	m	21	95	5	m	34	257	3	m
9	-150	3	m	22	123	3	m	35	265	2	m
10	-135	4	m	23	140	3	m	36	264	4	m
11	-113	4	m	24	147	4	w	37	272	3	m
12	-41	3	w	25	159	2	m	38	278	3	m
13	-23	3	m	26	167	3	s				

Table 1: All calculated SF₆ one [20] and two [9, 21] photon transitions around the 1CP12 to 10P24 CO₂ laser lines (each ± 320 MHz) are listed in column two, with their symmetry type. If more than one symmetry is given, different transitions coincide within our accuracy; earlier measured one photon transitions, [1, 2], are indicated by ¹⁾, the two photon transitions, [9], by ²⁾. The newly measured one and two photon transitions which we could assign are marked with • and ••, respectively. The Q-transitions marked with *) indicate $\Delta l = 0$; the **) indicates that both $\Delta l = 0$ and $\Delta l = 2$ transitions coincide within our accuracy. If there is no indication, only a $\Delta l = 2$ transition is present. The number of photons participating in the transition is given in column three. The fourth and fifth column show respectively the calculated [9, 20] and measured frequencies in MHz relative to the center of the CO₂ laser line. The center frequencies are taken from [28]. The intensity in the seventh column gives only a rough indication of the strength of the absorption lines relative to each other; w = weak, m = medium, s = strong.

2.9 Appendix

The n-photon Rabi frequencies, $\Omega_R^{(n)}$, are related approximately to the one photon Rabi frequency, $\Omega_R^{(1)}$, by [27]

$$\frac{\Omega_R^{(n)}}{2} = \frac{\Omega_R^{(1)}}{2} \cdot \left(\frac{\Omega_R^{(1)}}{2 \cdot 2\pi\Delta} \right)^{n-1} \quad (2.1)$$

In equation 1, the one photon frequencies are taken to be step- independent; similarly, the intermediate levels are assumed to possess the same (average) detuning Δ .

We will use equation 1 to estimate the maximum acceptable Δ -value, for two and three photon processes (in view of our maximum realized laser power $P_{\max} = 15$ Watts) and to

find the laser power for which typically a two photon 2π -Rabi cycle is expected.

For maximum laser power (P_{\max}) equation 1 becomes

$$\Omega_{\text{R}}^{(n)}(P_{\max}) = \Omega_{\text{R},s}^{(1)} \cdot \left(\frac{P_{\max}}{P_{1,s}} \right)^{n/2} \cdot \left(\Omega_{\text{R},s}^{(1)} \right)^{n-1} \cdot (4\pi\Delta)^{1-n} \quad (2.2)$$

$\Omega_{\text{R},s}^{(1)}$ stands for the one photon Rabi frequency at the laser power $P_{1,s}$, where a 2π -pulse is completed during the interaction time, $\tau = 130$ ns. Next we multiply both sides of equation 2 by τ and put $\Omega_{\text{R},s}^{(1)} \cdot \tau = \Omega_{\text{R}}^{(n)}(P_{\max}) \cdot \tau$, i.e. we postulate a 2π -Rabi cycle for P_{\max} . Then

$$(4\pi\Delta)^{n-1} = \left(\frac{P_{\max}}{P_{1,s}} \right)^{n/2} \cdot \left(\Omega_{\text{R},s}^{(1)} \right)^{n-1} \quad (2.3)$$

For $n = 2$, the acceptable detuning is given already in section 5. For $n = 3$ we derive $\Delta \leq 2.5$ GHz in order to find at least a 2π -Rabi cycle.

The two photon Rabi frequency for which a 2π -cycle is performed during τ , corresponds to a laser power $P_{2,s}$. We then find from equation 1

$$4\pi\Delta = \frac{P_{2,s}}{P_{1,s}} \cdot \Omega_{\text{R},s}^{(1)} \quad (2.4)$$

For the P(4) two photon transition, Δ amounts to 76 MHz. From here follows that $P_{2,s}$ is approximately 100 mW. If this result is compared to the position of the first minimum in fig. 7^b, at 200 mW, we find a factor 2 discrepancy, which is acceptable for these measurements because the focused laser intensity is not well known.

2.10 Acknowledgement

This work has greatly profited from the permanent and skilful technical assistance of Cor Sikkens, Frans van Rijn and John Holtkamp. Information on unpublished work has been vital; we thank C.W. Patterson (Los Alamos), F. Herlemont (Lille) and M. Bobin, C.I. Pierre and G. Pierre (Dijon). In the initial phase, Coen Liedenaum and Steven Stolte contributed significantly to the project. The Dutch organisation N.W.O. and the European Community (Brussels) made this investigation possible by generous financial support.

References

- [1] A van Lerberghe, S Avrillier and C J Bordé, I E E E J Quantum Electron , **QE-14**, 481 (1978)
- [2] J Bordé and C J Bordé, Chem Phys **71**, 417 (1982)
- [3] C J Bordé, M Ouhayoun and J Bordé, J Mol Spec **73**, 344 (1978)
- [4] C J Bordé, M Ouhayoun, A van Lerberghe, C Salomon, S Avrillier, C D Cantrell and J Bordé, Laser Spectroscopy IV, H Walther, K W Rothe, ed , Springer-Verslag, 142 (1979)
- [5] J Bordé, C J Bordé, C Salomon, A van Lerberghe, M Ouhayoun and C Cantrell, Phys Rev Letters **45**, 14 (1980)
- [6] C Salomon, C Breant, A van Lerberghe, G Camy and C J Bordé, Appl Phys B, **29**, 153 (1982)
- [7] C J Bordé, Développements récents en spectroscopie infrarouge a ultra-haute résolution, Revue du Cethedec-Ondes et Signal **NS83-1** (1983)
- [8] M Bobin, C J Bordé, J Bordé and Bréant, J Mol Spec , **121**, 91 (1987)
- [9] C W Patterson, F Herlemont, M Azizi and J Lemaire, J Mol Spec **108**, 31 (1984)
- [10] C W Patterson, B J Krone and A S Pine, J Mol Spec **88**, 133 (1981)
- [11] C Liedenbaum, S Stolte and J Reuss, Chem Phys **122**, 443 (1988)
- [12] C Liedenbaum, S Stolte and J Reuss, Infr Phys **29**, 397 (1989)
- [13] C Liedenbaum, S Stolte and J Reuss, Phys Rep **178**, 1 (1989)
- [14] T E Gough, R E Miller and G Scoles, Appl Phys Letters **30**, 338 (1977)
- [15] S Avrillier, J M Raimond, C J Bordé, D Bassi and G Scoles, Opt Comm **39**, 311 (1981)
- [16] M Snels, R Fantoni, M Zen, S Stolte and J Reuss, Chem Phys Letters **124**, 1 (1986)
- [17] M Quack, J Chem Phys **69**, 1282 (1978)
- [18] H Steffen and F K Kneubuhl, I E E E J Quantum Electron **QE-4**, 992 (1968)

- [19] R Bulhorn, H Kunzmann and F Lebowsky, Appl Optics **11**, 742 (1972)
- [20] M Bobin, private communications, autumn 1989
- [21] C W Patterson, private communications, spring 1990
- [22] P K Chakraborti, R Talukdar, P N Bajor, A Joshi and V B Kartha, Chem Phys **95**, 145 (1985)
- [23] R Loudon, The quantum theory of light, Clarendon Press, p 65 (1983)
- [24] C D Cantrell and H W Galbraith, J Mol Spec **58**, 158 (1975)
- [25] G Herzberg, Molecular spectra and molecular structure, II, Infrared and Raman spectra of polyatomic molecules, Van Nostrand, p 101 (1945)
- [26] B Wichman, C Liedenbaum and J Reuss, to be published in Appl Phys (sept 1990)
- [27] V N Bagratashvili, V S Letokhov, A A Makarov and E A Ryabov, Multiple Photon Infrared Laser Photophysics and Photochemistry, Harwood academic publishers, p 150 (1985)
- [28] C Freed, L C Bradley and R G O'Donnell, I E E E J Quantum Electron **QE-16**, 1195 (1980)

Calculation of two photon transitions in SF₆, fit to measured frequencies

**S. te Lintel Hekkert, A.F. Linskens, B.G. Sartakov[†],
G. Pierre^{††} and J. Reuss**

Department of Molecular and Laser Physics, University of Nijmegen
Toernooiveld, 6525 ED Nijmegen, The Netherlands

[†] General Physics Institute, Vavilov street 38, 117942 Moscow Russia

^{††} Laboratoire de spectrométrie moléculaire et instrumentation laser, Université de Bourgogne, bd Gabriel 6, 21100 Dijon, France

Abstract

Two photon transitions of the ν_3 band of SF₆ have been fit utilizing two different representations of the Hamiltonian. The strong transitions predicted around the 10P16 CO₂ laser line can all be observed within 3 MHz from the calculated frequencies. For the other measured spectral regions (i.e. the regions around the 10P12, 10P14, 10P18, 10P20, 10P22 and 10P24 CO₂ laser lines), we are less certain of the assignment of the two photon transitions, because in these regions almost no strong lines are predicted. The constants utilized to produce the best fit of the two photon transitions are presented.

3.1 Introduction

In this paper an updated table of the $2\nu_3$ transitions of SF_6 will be discussed. A table of calculated and measured one and two photon transitions was already presented in [1]; however, in that case our measured frequencies were not included in the fitting procedure. In the meantime two fitting programs for the measured two photon transitions were developed; both methods start from the same Hamiltonian, which will be discussed in section 2, but utilize different representations of the tensorial components in this Hamiltonian.

In section 3 the difference in the results of the two fitting procedures will be discussed. In the fitting procedure also transitions measured with two different lasers interacting simultaneously with the molecules are included. These measurements are discussed elsewhere [2]. In order to make it possible to compare the theoretically predicted strengths of the transitions with the measured ones, we included a multiplication factor for each J-value. This multiplication factor is derived from the Boltzmann plot presented in fig.3 of [1]. From this we know that we deal with a non thermal rotational energy distribution; therefore it is possible to measure transitions with J-values up to approximately 40, if their strength factors are large enough. Of course, the transitions starting from low J-values are much easier to observe in our set-up utilizing a molecular beam. In section 4 the results of the fitting procedure will be discussed.

3.2 Calculation of two photon transitions

$$H = \sum H_{(i)}, \text{ with} \quad (3.1)$$

						energy (J=10)
$H_{(0)} =$	$H_{02} +$	H_{20}				1000 cm^{-1}
$H_{(1)} =$		H_{21}				1 cm^{-1}
$H_{(2)} =$	$H_{04} +$	$H_{22} +$	H_{40}			1 cm^{-1}
$H_{(3)} =$		$H_{23} +$	H_{41}			10^{-3} cm^{-1}
$H_{(4)} =$	$H_{06}^{\odot} +$	$H_{24}^{\odot} +$	$H_{42} +$	H_{60}		10^{-2} cm^{-1}
$H_{(5)} =$		$H_{25}^{\odot} +$	$H_{43} +$	H_{61}^*		10^{-5} cm^{-1}
$H_{(6)} =$	$H_{08}^{\odot} +$	$H_{26} +$	$H_{44} +$	$H_{62}^* +$	H_{80}^*	10^{-6} cm^{-1}
$H_{(7)} =$		$H_{27}^{\odot} +$	$H_{45}^* +$	$H_{63}^* +$	H_{81}^*	10^{-10} cm^{-1}
			1	2	3	

In [3, 4] a general way to write down the Hamiltonian for the rotations and vibrations of a molecule is proposed. Starting from these conventions it is possible to calculate the

energy levels and eigenfunctions describing the ro-vibrational behaviour of the ν_3 -mode in SF_6 [5].

Eq.1 represents the Hamiltonian split into the different orders ($H_{(0)}$ second order, $H_{(1)}$ third order, etc.). H_{ij} means that the vibration parameters are of order i and the rotation parameters are of order j . For example H_{20} represents the pure vibration, $v\hbar\omega$ with $\hbar\omega$ the energy of one vibrational quantum and v the number of vibrational quanta, while H_{02} represents the rigid rotor $B_0J(J+1)$, with B_0 the rotational quantum number and J the number of rotational quanta. H_{21} represents the Coriolis coupling of the ro-vibrational momenta; $H_{21} = -2B_0\zeta(\vec{J} \cdot \vec{l})$ in which ζ is the Coriolis constant. Higher order terms consist of a combination of terms; they always include tensorial factors. As an example H_{40} is given in eq.2 utilizing the representation of [6].

$$H_{40} = X_{33}v(v-1) + G_{33}[l(l+1) - 2v] + \sqrt{120}T_{33}\hat{T}^{404} \quad (3.2)$$

where X_{33} is the factor responsible for the anharmonic shift of the ν_3 levels.
 G_{33} is the factor responsible for the splitting into different l sublevels.
 T_{33} is the factor responsible for the splitting of each l sublevel into octahedral sublevels.
 \hat{T}^{abc} is a tensor operator with vibrational part of rank a ,
rotational part of rank b , resulting in a total tensor rank c .

For the two different predictions of the frequencies of the two photon transitions, the same Hamiltonian is used but different representations lead to different expressions for the H_{ij} .

In eq.1, the terms left from line 1 are important for the calculations of the frequencies of one photon transitions. With the aid of the commutation relation it is easily shown that the terms right from this line can be left out in the fitting procedure. Higher order perturbation terms, causing processes like $1\nu_3 \leftarrow 2\nu_3 \leftarrow 0\nu_3$ do not change the constants left from line 1 within our experimental accuracy. In the same way it is possible to prove that the terms right from line 2 can be excluded in the calculations of the two photon transitions, the terms right from line 3 have no influence on the prediction of the three photon transitions.

For each Hamiltonian term $H_{(i)}$ an estimate of the order of magnitude of the energy involved is shown; if more components contribute, the largest one is taken into account in this listing. To calculate these energies eq.3 is used in which E_{nm} is the component of the Hamiltonian with vibrational order n , and rotational order m ; C_{nm} is a constant taken from table 2 (section 4). To calculate the energies listed in eq.1; $v=2$ and $J=10$ are used.

$$E_{nm} = C_{nm}v^n J^m \quad (3.3)$$

In order to predict the two photon transitions within our experimental accuracy of 2 MHz, we need to include all the terms left from line 2 in eq.1. However, the terms marked

with * are estimated to be very small and can be neglected, e.g. the H_{45} term can be excluded. In this way a Hamiltonian including 67 fit parameters can be constructed for the two photon transitions.

The terms marked with \odot are very small, however, they can not be excluded. In the fitting procedure for the one photon transitions as measured by the Bordé group they are important and are determined with very high accuracy [7, 8, 9, 10], this is of great help for the fitting procedure of the two photon transitions. The one photon measurements were performed at room temperature, as a result, the rotational population of the molecules extends to much higher J-values than in our measurements where the molecules are cooled.

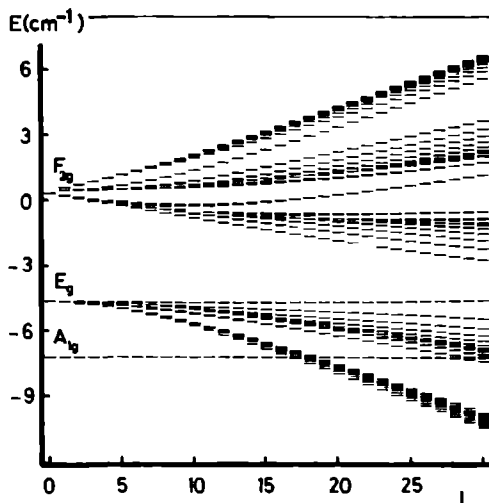


Figure 1 Energy level diagram for the $2\nu_3$ transitions of SF_6 . For each J-value up to 30 the relative energy of the different sublevels is plotted. The vibrational symmetries of the three branches are indicated, for the A_{1g} symmetry branch $l=0$, for the E_g and F_{2g} branches $l=2$.

during the expansion through the nozzle [11, 12]. In order to fit these one photon transitions properly, it is necessary to include the terms marked with \odot , because they will be much larger for higher J-values than the values indicated in the last column of eq 1. For the two photon transitions the predicted energy level scheme is given in fig 1. To fit all the parameters of the Hamiltonian it is necessary to measure transitions with different J-values for all of the symmetry branches. For the A_{1g} symmetry (see fig 1) we could not measure and assign two photon transitions, accordingly, the predicted frequencies of this symmetry branch will not

be very accurate (± 200 MHz). On the contrary, we measured many transitions with $\Delta J=0$ and vibrational symmetry F_{2g} so that other transitions of this symmetry type can now be predicted with an accuracy of 3 MHz.

Due to the enormous number of parameters it is sometimes possible to predict a set of transitions with two different sets of parameters. Obviously one of these sets of parameters is not correct. The only way to find out which one is to include more lines in the fitting procedure.

From eq.1 it is clear that in predicting three photon transitions only one extra term, i.e. the H_{60} which contains another 5 extra parameters, has to be included. This will raise the number of parameters which have to be fit to a total of 72. For four photon transitions it is not necessary to include new parameters anymore, they will be predicted with the same set of parameters as the three photon transitions.

3.3 Fitting procedure

In [1] a listing of predicted one [13] and two [14, 15] photon transitions, together with the measured frequencies is presented. Numerous measured lines match within 2 MHz with predicted transitions; from this we derived their assignments. However, we did not include our measured two photon transitions in the fitting procedure. The transitions Patterson used for his fit are the one photon transitions measured by the Bordé group in Paris [16], and the two photon transitions presented in [17]. Both measurements are performed in an absorption cell at room temperature; accordingly especially higher J-values were observed. On the contrary, we perform our measurements in a molecular beam in which low rotational energy levels are favoured. Another difference is the use of Acousto Optic Modulators to extend the tuning range of the lasers; in this way many new transitions could be measured and included in the fitting procedure.

In assigning the experimental data, doublets and triplets of transitions starting from the same level, with the same ΔJ , are very important. If they are saturated, their intensity depends entirely on their ro-vibrational symmetry ($A_1:A_2:E:F_1:F_2=1:5:4:3:3$) [19]; the distance between the transitions in such a group is fixed within $\pm 10\%$. Transitions with J-values not too far apart from each other, with the same ΔJ , can be used in a similar way. Utilizing the Boltzmann plot it is possible to estimate the intensity of a predicted transition with a certain J-value from other already assigned transitions with other J-values.

If, because of the large detuning, a transition is not saturated, the strength factor predicted by theory give a rough indication of the intensities of the transitions in the measured spectra. Especially transitions starting from the same J-value, with the same ΔJ and symmetry but with different counting indices (see e.g. the Q(23) E doublet on the 10P16 CO₂ laser line, shifted -39 MHz from the CO₂ line centre, table 1) sometimes are not predicted with the same relative strength factors S_S and S_P . From this and similar multiplets only

the transition with the highest intensity factor is used in the fitting procedure.

Transitions not belonging to a multiplet can only be used in the fitting procedure if they are strong and measured in a frequency region where no other strong unassigned spectral features are observed.

Starting with the transitions measured by the Bordé group [16] and Herlemont et al [14, 18] (in a first attempt to fit our data) reasonable agreement is found for the P and Q transitions with F_{2g} vibrational symmetry on the 10P16 CO₂ laser line. This is due to the fact that many of these lines are also measured by Herlemont et al, and had thus been already included in the fitting procedure. For the other vibrational symmetries there was often only very poor agreement between the calculated and measured transition frequencies; this is due to the fact that there were almost no transitions of this symmetry which could be assigned before. In order to fit the transitions possessing these symmetries it is often necessary to put into the fitting procedure measured frequencies which are shifted more than 100 MHz from the predicted frequencies.

3.4 Results of the fitting procedure

The results of the fitting procedure are given in table 1, in which the measured and calculated transitions are listed, and table 2, in which the constants used to calculate the frequencies of table 1 are listed. In column 2 of table 1, the transitions are listed with their ro-vibrational symmetries. The vibrational symmetries are listed in column 3, being meaningful only for transitions starting from J-values up to approximately 20. For higher J-values strong mixing between the different vibrational symmetries occurs; this mixing of symmetries is responsible for shifts of the energy levels (see fig.1). Especially mixing with transitions possessing A_{1g} vibrational symmetry give rise to high uncertainties in the predicted frequencies because there are not yet many transitions measured with this symmetry. Transitions marked with • are used in the fitting procedure.

In columns 5 and 6 the theoretically predicted two photon transition frequencies of the co-authors B.G. Sartakov and G. Pierre, respectively, are listed. Their strength factors are shown in column 4 and 7. The strength factors are calculated utilizing formula 4.

$$S = I(J)\varepsilon_s \left(\sum \frac{a_{01}a_{12}}{\Delta} \right)^2 \quad (3.4)$$

$I(J)$ is a factor depending on the population of the rotational energy levels, derived from the Boltzmann plot as presented in [1]; ε_s is the ro-vibrational symmetry factor ($A_1:A_2:E:F_1:F_2=1:5:4:3:3$); a_{01} and a_{12} are the dipole transition moments between the initial and intermediate and the intermediate and final levels, respectively; Δ is the detuning of the laser frequency with respect to the intermediate level. In the calculation of the strength of a transition, all the possible pathways have been included, accordingly, the sum being taken over all possible intermediate levels.

Some transitions are listed with either ν_S or ν_P ; this does not mean that these transitions are not predicted in the other listing. In order to make the listing of calculated transitions not too long, the transitions with strength factors so low that they are not expected to be observable in our spectra, are excluded. Due to the fact that in both calculation other conventions are utilized for the dipole transition moments a_{01} and a_{12} , the two predicted strength factors differ approximately by two orders of magnitude. For ν_S strength factors smaller than 0.1 and for ν_P strength factors smaller than 10 are left out. Often transitions possessing a low intensity factor ν_P have an intensity factor ν_S smaller than .1 and consequently have been excluded from the table.

In column 8 the experimental frequencies of the transitions are listed. Transitions for which it is not possible to find spectral features in the spectra which can be used in an assignment, are marked by a *. Sometimes ν_S and ν_P are not the same and differ so much that it is not clear which calculated transition has to be used in the assignment. But more often both predicted frequencies can be used to find the assignment. For the multiplets starting from the same J-value with the same ΔJ and symmetry, mostly one of the transitions is much stronger than the other ones. It is not possible to assign the weaker transitions in such a multiplet because either they are too weak to be observed or they are too close to the transition with high intensity to be resolved within our experimental resolution.

For the transitions around the 10P16 CO₂ laser line there is not much difference between the predicted frequencies ν_S and ν_P ; also the measured frequencies match within 3 MHz the theoretically predicted values. Three discrepancies between the two calculations and the experimental values still occur. First, the transitions possessing A₁ ro-vibrational symmetry have a relatively much stronger S_P than S_S factor. Because the Q(24) transition 190 MHz shifted from the 10P16 CO₂ laser line center can be observed in the spectrum, the strength factor as proposed in S_P seems to be alright. Second, the R(38) triplet 250 MHz shifted from the 10P16 CO₂ laser line center is estimated much stronger in S_P than in S_S . However, in this case measured transition frequencies have not been found to match the predicted values; we conclude that these strength factors are overestimated. The third discrepancy is on transitions possessing E_g vibrational symmetry; they are predicted with low accuracy. Utilizing the two strongest components of the S(19) triplet, it is possible to fix some extra parameters and get the ν_S and ν_P in reasonable agreement (± 20 MHz) with each other and the experimental data.

For the 10P14 CO₂ laser line, only the Q(30) and the R(6) F₁ transitions are predicted to possess strong S_P and S_S values. For both transitions it is possible to find measured frequencies which are in good agreement with the predicted ones. For the other transitions, all expected to be weak, the most probable experimental frequency is listed. However their assignment is not certain enough to include these lines in the fitting procedure. Similar arguments hold for the transitions around the 10P20 CO₂ laser line.

In order to fit the O-transitions around the 10P18 CO₂ laser line, the O(24) triplet is used. For the P-transitions in this spectral region, the discrepancy between the two calculated frequencies is very large, therefore it is not possible to assign these transitions. About the A_{1g} vibrational symmetry only very little is known, this is the reason why the R(16) triplet can not be fitted uniquely.

For each term of the Hamiltonian in eq 1, the constants used to predict the frequencies of ν_3 in table 1, are listed in table 2. From this table it can be seen that some of the constants are fit with large accuracy (e.g. the Z_{3t}), while other constants are effectively not fit at all (e.g. $D_{t_{vj}}$). In order to fit the set of transitions measured up to now, the terms in the Hamiltonian described by parameters possessing poor accuracies can be excluded. However, new experimental data on transitions possessing e.g. E_g vibrational symmetry cause these parameters to become important. Because of the large number of interactions participating in the excitation process of SF₆ it is impossible to predict which term of the Hamiltonian is important in the fit of a certain set of transitions. Accordingly, if new experimental data are included in the fitting procedure, none of the terms of the Hamiltonian can be excluded, it is only afterwards that it can be decided which terms were unimportant.

3.5 Tables

tabel 1 ⁴ : 10P14 CO ₂ laser line 28,464,674 MHz							
nr	transitions	vib sym	S _S a u	ν _S [MHz]	ν _P [MHz]	S _P a u	ν _{exp} [MHz]
1	S(25) F ₁ (1)	F _{2g}			-264	56	-264
2	R(20) F ₂ (3)				-259	53	
3	Q(34) F ₂ (7)				-253	18	-257
3	Q(30) F ₂ (7)		.13	-233	-231	318	-233
4	Q(30) F ₁ (7)		13	-230	-228	320	
5	Q(34) F ₁ (6)				-215	19	-212
6	R(18) E(1)	F _{2g}			-155	11	-152
7	R(6) E(1)	F _{2g}			-92	23	-94
8	R(6) F ₁ (1)	F _{2g}	8 10	-18	-10	60	-16
9	R(6) A ₁ (1)	F _{2g}			250	84	247
10	Q(14) E(3)	F _{2g}	12	251			253

Tabel 1 ⁵ : 10P16 CO ₂ laser line 28,412,590 MHz							
nr	transitions	vib sym	S _S a u	ν _S [MHz]	ν _P [MHz]	S _P a u	ν _{exp} [MHz]
1	Q(23) F ₂ (1)	F _{2g}	1 80	-296	-296	1605	-298
2	Q(23) F ₂ (2)	F _{2g}	1 64	-296			
3	Q(30) A ₂ (1)		17.58	-287	-289	1703	-291
4	Q(31) E(1)		8.23	-276	-278	8684	-277
5	Q(27) A ₁ (1)				-254	944	
6	P(7) F ₂ (1)	F _{2g}	235 00	-254	-253	1427	
7	P(7) F ₂ (2)	F _{2g}	671.14	-254	-253	4010	-256
8	Q(31) F ₁ (4)				-243	11	
9	Q(31) F ₁ (1)		2 65	-238	-239	6720	-237
10	Q(30) F ₂ (1)		2 19	-237	-238	5302	
11	Q(29) F ₂ (1)		2 02	-226	-227	4200	-228
12	Q(29) F ₂ (2)		2 27	-226			
13	Q(25) F ₂ (1)		1 77	-226	-226	2189	
14	Q(26) F ₁ (1)		1.73	-210	-209	2556	-210
15	Q(28) F ₁ (1)		1.85	-206	-206	3498	-205
16	Q(30) F ₁ (1)		2 30	-188	-190	5499	-191
17	Q(30) F ₁ (3)		2.31	-188			
18	Q(16) F ₁ (1)	F _{2g}	4.13	-188	-186	1210	-187
19	Q(16) F ₁ (2)	F _{2g}	7 37	-186	-186	121	
20	Q(16) F ₁ (3)	F _{2g}	.43	-186			
21	Q(21) F ₁ (3)				-172	12	
22	Q(21) F ₁ (2)				-172	17	
23	Q(21) F ₁ (1)		2 14	-171	-171	1480	-170
24	Q(29) E(3)				-166	11	
25	Q(29) E(2)		6.40	-162			
26	Q(29) E(1)		7 16	-162	-163	5851	
27	P(4) F ₂ (1)	F _{2g}	4 10 ⁶	-161	-162	1 10 ⁶	-164
28	Q(24) F ₂ (1)		1 75	-154	-154	1989	-156
29	Q(27) F ₁ (1)		1.74	-149	-149	3010	-151
30	Q(14) F ₁ (3)	F _{2g}	7.03	-145			
31	Q(14) F ₁ (1)	F _{2g}	5.89	-145	-144	1146	-146
32	Q(14) F ₁ (2)	F _{2g}	.26	-145	-144	50	
33	Q(30) A ₁ (1)				-143	1900	-141
34	R(25) F ₂ (6)		.29	-134	-133	375	-136
35	R(25) F ₁ (7)		.29	-132	-134	375	
36	Q(28) E(2)				-130	10	
37	S(20) E(4)	E _g	.28	-129	-123	78	*
38	Q(28) E(1)		6 03	-128	-128	4903	-127
39	S(20) A ₁ (2)	E _g			-123	20	
40	S(20) F ₁ (5)	E _g			-123	59	
41	S(19) A ₂ (2)	E _g	88	-107	-106	21	-107
42	Q(29) F ₁ (1)		2 02	-104	-104	4575	-103
43	S(19) F ₂ (4)	E _g	11	-102	-100	62	

Table 1 ^b (continued)							
nr	transitions	vib sym	S_S a u	ν_S [MHz]	ν_P [MHz]	S_P a u	ν_{exp} [MHz]
44	S(19) E(3)	E_g	36	99	97	82	-98
45	Q(26) E(3)				-81	14	
46	Q(26) E(2)				79	12	
47	Q(26) E(1)		5 65	-79	-78	3664	-79
48	Q(25) E(1)	F_{2g}	5 67	-76	74	3165	-75
49	Q(25) E(2)		12	-74	-76	18	
50	Q(18) F ₂ (3)				61	22	
51	Q(18) F ₂ (2)		13	-60	-61	49	
52	Q(18) F ₂ (1)	F_{2g}	3 27	-60	-60	1422	-62
53	Q(27) F ₂ (1)		1 74	-53	-52	3193	-51
54	Q(22) E(2)				-51	28	
55	Q(28) F ₂ (1)		1 96	-52	51	3867	
56	Q(22) E(1)	F_{2g}	6 07	-50	-50	2168	
57	Q(23) E(2)	F_{2g}	4 66	-39	-39	26	
58	Q(23) E(1)	F_{2g}	5 58	-39	38	2414	-38
59	S(11) E(2)	E_g	12	21			
60	Q(11) F ₁ (2)	F_{2g}	11 59	11	11	1368	10
61	Q(24) F ₁ (3)				26	13	
62	Q(24) F ₁ (1)		1 84	28	28	2186	25
63	Q(26) F ₂ (3)				31	13	
64	R(36) F ₁ (5)		13	31	34	630	
65	Q(26) F ₂ (1)		1 82	32	33	2935	30
66	R(36) F ₂ (6)		13	36	37	630	
67	Q(27) A ₂ (1)		13 74	37	38	1126	37
68	R(36) F ₂ (3)				42	13	
69	Q(19) E(2)	F_{2g}	22	49	50	50	
70	Q(19) E(1)	F_{2g}	9 61	49	50	2162	48
71	Q(20) E(3)	F_{2g}			70	20	
72	Q(20) E(2)	F_{2g}	26	71	70	66	
73	Q(25) F ₁ (4)				71	18	
74	Q(20) E(1)	F_{2g}	8 29	71	71	2342	70
75	Q(25) F ₁ (1)		1 77	73	73	2574	72
76	Q(21) F ₂ (3)	F_{2g}			141	18	
77	Q(21) F ₂ (2)	F_{2g}			142	17	
78	Q(21) F ₂ (1)	F_{2g}	2 15	142	143	1717	142
79	Q(23) F ₁ (3)				152	20	
80	Q(23) F ₁ (1)		1 82	153	153	2002	152
81	Q(9) E(1)	F_{2g}	145 14	172	172	2033	
82	P(4) E(1)	F_{2g}	3 10 ⁷	175	174	8 10 ⁷	174
83	Q(24) A ₁ (1)				190	796	192
84	Q(22) F ₂ (4)	F_{2g}			214	21	
85	Q(22) F ₂ (1)	F_{2g}	1 95	215	215	1850	215
86	Q(9) F ₁ (1)	F_{2g}	29	233	232	68	
87	Q(9) F ₁ (2)	F_{2g}	13 82	233	232	1415	235
88	R(38) F ₁ (7)				253	643	*
89	R(38) F ₂ (8)				256	643	*
90	R(38) F ₁ (4)				264	24	*
91	P(7) F ₁ (1)	F_{2g}	18 71	266	268	42	
92	P(7) F ₁ (2)	F_{2g}	905 11	266	268	2159	265

nr	transitions	vib sym	S_S a u	ν_S [MHz]	ν_P [MHz]	S_P a u	ν_{exp} [MHz]
1	O(26) E(2)	F _{2g}	79	-305	-300	413	-297
2	O(26) E(3)		88	-305			
3	O(26) E(4)		1 01	-305			
4	P(37) F ₂ (4)		11	-270	-312	474	*
5	P(39) F ₂ (5)				-290	168	*
6	P(35) F ₁ (4)				-268	22	*
7	P(35) F ₁ (3)		46	-234	-267	2538	*
8	O(26) F ₂ (2)		25	-212	-207	313	-207
9	O(26) F ₂ (3)		29	-212			
10	O(26) F ₂ (4)		33	-212			
11	O(11) A ₂ (1)	F _{2g}	57	-167			-168
12●	O(24) E(3)		66	-131	-131	259	-134
13●	O(24) F ₂ (5)		21	-126	-126	194	-127
14●	O(24) A ₂ (2)		1 59	-117	-117	65	-117
15	P(39) F ₁ (6)				-78	160	*
16	P(36) A ₁ (2)				54	234	*
17	P(35) A ₁ (1)				92	674	*
18	P(19) A ₂ (1)		35	113			113
19	R(16) F ₁ (1)	A _{1g} +E _g	78 20	125			*
20	R(16) F ₂ (1)	A _{1g} +E _g	78 23	129			*
21	R(16) F ₂ (2)	A _{1g} +E _g	98 52	130			*
22	P(32) F ₂ (5)	F _{2g}			152	42	*
23	P(32) F ₂ (4)				154	14	*
24	P(32) F ₂ (2)		1 92	179	156	7199	*
25	P(32) E(4)				233	22	*
26	P(32) E(3)				236	52	*
27	P(32) E(2)		6 44	261	238	10419	*
28	O(20) A ₁ (2)				281	42	
29	O(20) F ₁ (5)		28	288	281	125	
30	O(20) E(4)		86	289	282	166	284

nr	transitions	vib sym	S_S a u	ν_S [MHz]	ν_P [MHz]	S_P a u	ν_{exp} [MHz]
1	Q(38) F ₂ (6)	E _g	21	218	-77	19	-74
2	Q(38) F ₁ (6)				-48	19	-46
3	Q(39) F ₁ (7)				146	30	149
4	Q(39) F ₂ (7)				150	30	
5	O(8) F ₂ (2)						223
6	Q(40) F ₂ (8)				304	43	308
7	Q(40) F ₁ (8)				305	43	

Table 1: Calculated and measured $2\nu_3$ transitions of SF₆. The assignment of the transitions with ro-vibrational symmetry is given in column 2. Column 3 contains the vibrational symmetries of the transitions. It is not possible to assign the vibrational symmetries of transitions with J-values higher than 20, because for these transitions there will be mixing of states of different symmetries which influences strongly the energy levels and thus the transition frequencies. In column 5 and 6 the transition frequencies resulting from the two different calculations are listed, the strength factors are listed in column 4 and 7, respectively. The frequency of the experimental lines are listed in column 8. Only the transitions marked with ● are used in the fitting procedure. Transitions which are not yet satisfactorily assigned and fit or for which the two calculations predict a largely different frequency are marked by *.

H ₂₀ :	F ₀₁	=948.102509	$\pm 1 \cdot 10^{-6}$	H ₄₃ :	M _{33j}	=-1.4·10 ⁻⁸	$\pm 3 \cdot 10^{-9}$
H ₀₂ :	B ₀	=9.10771·10 ⁻²	$\pm 7 \cdot 10^{-7}$		N _{33tj}	=-7·10 ⁻⁹	$\pm 2 \cdot 10^{-9}$
H ₂₁ :	2B ₀ ζ	=1.26128·10 ⁻¹	$\pm 1 \cdot 10^{-6}$		F _{3tv}	=6·10 ⁻¹⁰	$\pm 8 \cdot 10^{-10}$
H ₀₄ :	D _s	=7·10 ⁻⁹	$\pm 1 \cdot 10^{-9}$		T ₃₃₆	=-1.4·10 ⁻⁸	$\pm 1 \cdot 10^{-9}$
	D _t	=1.54·10 ⁻¹⁰	$\pm 3 \cdot 10^{-12}$	H ₀₈ :	D _{sjj}	=7·10 ⁻¹⁹	$\pm 2 \cdot 10^{-17}$
H ₂₂ :	Y ₃	=-1.31056·10 ⁻⁴	$\pm 8 \cdot 10^{-9}$		D _{tjj}	=3.4·10 ⁻¹⁸	$\pm 3 \cdot 10^{-19}$
	Z _{3s}	=9.1747·10 ⁻⁵	$\pm 5 \cdot 10^{-9}$		ξ _j	=1·10 ⁻²¹	$\pm 3 \cdot 10^{-20}$
	Z _{3t}	=3.75466·10 ⁻⁵	$\pm 1 \cdot 10^{-10}$		H ₀₈	=4·10 ⁻¹⁷	$\pm 5 \cdot 10^{-17}$
H ₄₀ :	X ₃₃	=-1.7467	$\pm 1 \cdot 10^{-4}$	H ₂₆ :	X _{vjjj}	=-1.2·10 ⁻¹⁵	$\pm 4 \cdot 10^{-16}$
	G ₃₃	=9.2532·10 ⁻¹	$\pm 1 \cdot 10^{-5}$		Z _{3sjj}	=2.1·10 ⁻¹⁵	$\pm 4 \cdot 10^{-16}$
	T ₃₃	=-2.4896·10 ⁻¹	$\pm 1 \cdot 10^{-5}$		Z _{3tjj}	=-1.4·10 ⁻¹⁶	$\pm 1 \cdot 10^{-17}$
H ₂₃ :	F _{3s}	=3.9·10 ⁻⁸	$\pm 5 \cdot 10^{-9}$		D _{twj}	=5.58·10 ⁻¹⁶	$\pm 4 \cdot 10^{-18}$
	F _{3t}	=-1.63·10 ⁻⁹	$\pm 1 \cdot 10^{-11}$		ξ _v	=1.01·10 ⁻¹⁷	$\pm 2 \cdot 10^{-19}$
H ₄₁ :	M ₃₃	=1.39·10 ⁻⁴	$\pm 1 \cdot 10^{-6}$		T _{246j}	=-3.2·10 ⁻¹⁶	$\pm 2 \cdot 10^{-17}$
	N _{33t}	=1.38·10 ⁻⁵	$\pm 8 \cdot 10^{-7}$		T ₂₆₈	=1.7·10 ⁻¹⁴	$\pm 1 \cdot 10^{-15}$
H ₀₆ :	π	=-1·10 ⁻¹³	$\pm 5 \cdot 10^{-13}$	H ₄₄ :	X _{33jj}	=1.4·10 ⁻¹⁰	$\pm 4 \cdot 10^{-11}$
	ρ	=4.8·10 ⁻¹⁴	$\pm 1 \cdot 10^{-15}$		G _{33jj}	=-4·10 ⁻¹¹	$\pm 2 \cdot 10^{-11}$
	ξ	=1.0·10 ⁻¹⁶	$\pm 2 \cdot 10^{-17}$		T _{33jj}	=-8·10 ⁻¹¹	$\pm 1 \cdot 10^{-11}$
H ₂₄ :	ΔD _s	=-4.8·10 ⁻¹¹	$\pm 7 \cdot 10^{-12}$		Z _{3svj}	=-9·10 ⁻¹⁰	$\pm 2 \cdot 10^{-10}$
	ΔD _t	=8.1·10 ⁻¹²	$\pm 2 \cdot 10^{-13}$		Z _{3slj}	=-1·10 ⁻¹⁰	$\pm 1 \cdot 10^{-10}$
	ΔZ _{3sj}	=4.7·10 ⁻¹¹	$\pm 6 \cdot 10^{-12}$		Z _{3tvj}	=-2·10 ⁻¹²	$\pm 4 \cdot 10^{-11}$
	ΔZ _{3tj}	=3.28·10 ⁻¹²	$\pm 9 \cdot 10^{-14}$		Z _{3tlj}	=3·10 ⁻¹¹	$\pm 2 \cdot 10^{-11}$
	T ₂₄₆	=7.21·10 ⁻¹²	$\pm 6 \cdot 10^{-14}$		T _{246v}	=7.3·10 ⁻¹¹	$\pm 8 \cdot 10^{-12}$
H ₄₂ :	ΔY _{3v}	=-2.6·10 ⁻⁷	$\pm 5 \cdot 10^{-8}$		T _{246t}	=1.4·10 ⁻¹¹	$\pm 6 \cdot 10^{-12}$
	ΔY _{3l}	=-2.9·10 ⁻⁷	$\pm 4 \cdot 10^{-8}$		T _{426j}	=1.1·10 ⁻¹⁰	$\pm 3 \cdot 10^{-11}$
	ΔZ _{3s}	=2.1·10 ⁻⁶	$\pm 3 \cdot 10^{-7}$		T ₄₄₀	=2·10 ⁻¹⁰	$\pm 1 \cdot 10^{-10}$
	ΔZ _{3t}	=-1.4·10 ⁻⁷	$\pm 5 \cdot 10^{-8}$		T ₄₄₈	=-2.3·10 ⁻⁸	$\pm 2 \cdot 10^{-9}$
	T _{l220}	=-1·10 ⁻⁷	$\pm 2 \cdot 10^{-7}$		D _{tvv}	=3.2·10 ⁻¹¹	$\pm 6 \cdot 10^{-12}$
	T _{l224}	=-1.9·10 ⁻⁷	$\pm 2 \cdot 10^{-8}$		D _{tlj}	=2.2·10 ⁻¹¹	$\pm 4 \cdot 10^{-12}$
	ΔT _{33j}	=3.7·10 ⁻⁷	$\pm 2 \cdot 10^{-8}$	H ₂₇ :	a _{5j}	=2·10 ⁻¹⁸	$\pm 7 \cdot 10^{-17}$
	T ₄₂₆	=-2.7·10 ⁻⁷	$\pm 1 \cdot 10^{-8}$		b _{5j}	=8.9·10 ⁻¹⁸	$\pm 9 \cdot 10^{-19}$
H ₂₅ :	a ₅	=6·10 ⁻¹³	$\pm 2 \cdot 10^{-12}$		d _{5j}	=-3·10 ⁻¹⁹	$\pm 9 \cdot 10^{-19}$
	b ₅	=-2.57·10 ⁻¹³	$\pm 5 \cdot 10^{-15}$		e ₇	=3·10 ⁻¹⁶	$\pm 4 \cdot 10^{-16}$
	d ₅	=-1.05·10 ⁻¹⁴	$\pm 5 \cdot 10^{-16}$				

Table 2: Constants utilized in the Hamiltonian (equation 1) to predict the frequencies ν_S in table 1. The constants are ordered according to the terms of the Hamiltonian in which they participate.

References

- [1] A F Linskens, S te Lintel Hekkert and J Reuss, *Infrared Phys* 32 (1991) 259
- [2] S te Lintel Hekkert, A F Linskens, B G Sartakov, G Pierre and J Reuss, to be published
- [3] M R Alev and J K G Watson, *J Molec Spec* 61 (1976) 29
- [4] M R Alev and J K G Watson, *Mol Spectrosc modern research* 3 (1985) 1
- [5] B G Sartakov, *Infrared laser field resonant interactions with polyatomic molecules*, Moscow Nauka 27 (1990) 3
- [6] K T Hecht, *J Molec Spec* 5 (1960) 355
- [7] B Bobin, C J Bordé, J Bordé and C Bréant, *J Molec Spec* 121 (1987) 91
- [8] J Bordé and C J Bordé, *Chem Phys* 71 (1982) 417
- [9] J Bordé, C J Bordé, C Salomon, A van Lerberghe, M Ouhayoun and C D Cantrell, *Phys Rev Lett* 45 (1980) 14
- [10] C Salomon, C Bréant, A van Lerberghe, G Camy and C J Bordé, *Appl Phys B* 29 (1982) 3
- [11] P K Chakraborti, V B Kartha, R K Talukdar, P N Bajar and A Joshi, *Chem Phys Lett* 101 (1983) 397
- [12] B J C Wu, P P Wegener and G D Stein, *J Chem Phys* 68 (1978) 308
- [13] M Bobin, private communications
- [14] C W Patterson, F Herlemont, M Azizi and J Lemaire, *J Molec Spec* 108 (1984) 31
- [15] C W Patterson, private communications
- [16] C J Bordé, M Ouhayoun, A van Lerberghe, C Salomon, S Avrillier, C D Cantrell and J Bordé, *Laser Spectroscopy 4* (Edited by H Walther and K W Rothe), Springer, New York (1979) 142
- [17] C W Patterson, R S McDowell, P F Moulton and A Mooradian, *Opt Lett* 6 (1981) 93
- [18] F Herlemont, M Lyszyk and J Lemaire, *Appl Phys* 24 (1981) 369
- [19] C D Cantrell and H W Galbraith, *J Molec Spec* 58 (1975) 58

Multiphoton experiments on SF₆, molecular quantum electronics with infrared radiation

**S. te Lintel Hekkert, A.F. Linskens, B.G. Sartakov[†],
G. Pierre^{††} and J. Reuss**

Department of Molecular and Laser Physics, University of Nijmegen
Toernooiveld, 6525 ED Nijmegen, The Netherlands

[†] General Physics Institute, Vavilov street 38, 117942 Moscow Russia.

^{††} Laboratoire de spectrométrie moléculaire et instrumentation laser, Université de Bourgogne, bd Gabriel 6, 21100 Dijon, France.

Abstract

Multiphoton experiments on SF₆ in a molecular beam are performed utilizing cw CO₂ waveguide lasers. In this paper the emphasis will be on the non-spectroscopic aspects. - The saturation dip in one photon transitions is measured. -To investigate which rotational states participate in the multiphoton process, an intra cavity laser is used as a pump laser, followed by a waveguide laser. Only hot band transitions seem to be depleted. -With the aid of two counter propagating CO₂ waveguide laser beams, new spectral regions were entered to investigate two photon transitions. In this way it is also possible to investigate three and more photon transitions, because of the higher intensity (two lasers) and smaller intermediate detunings (two colours).

4.1 Introduction

Since a few years the possibility of introducing rapid adiabatic processes (RAP) in spectroscopic and collision studies has been exploited by the Nijmegen group [1-6]. There are at least two ways to realize RAP. Either a (linear) frequency chirp is applied, a method useful for one colour $1h\nu$ or $n h\nu$ transitions, or, in case of two or more colour excitation, a counter intuitive sequence of laser interactions is introduced [7-12], i.e. in a pump-probe experiment the probe laser comes first followed by the pump laser with temporal (in our case of a molecular beam, partial spatial) overlap [4].

In this paper results obtained for SF_6 are discussed. The emphasis will be on the non-spectroscopic aspects of the investigations; under RAP-conditions, the absence of saturation broadening, in general (and specifically for $1h\nu$ saturation dips) and measurements of two and more photon transitions utilising two different lasers will be discussed. In section 2

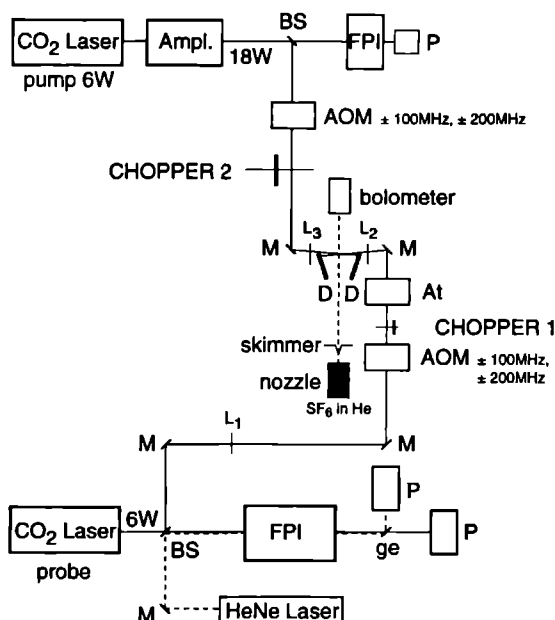


Figure 1: Experimental set-up. BS, beam splitter ($R=90\text{cm}$); M, flat mirror; AOM, Acousto Optic Modulator; P, power meter; FPI, Fabry-Perot interferometer; ge, germanium plate; D beam dumps; ampl, CO_2 amplifier; At, attenuator.

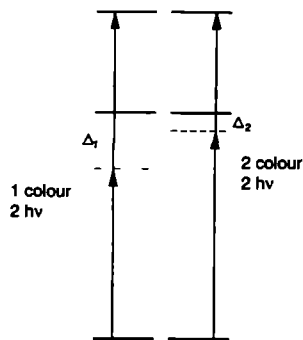


Figure 2 The intermediate detuning of a two photon transition can be reduced, utilizing two colour instead of one colour excitation

the experimental set-up will be described briefly. Depletion measurements utilizing an intra cavity laser as a pump and a wave guide laser as a probe laser are discussed in section 3. In section 4 two level systems, in section 5 three level systems and in section 6 four and more level systems are considered.

4.2 Experimental set-up

The experimental set-up used in the present experiments has been described before [6]. There are two new aspects. From the point of view of laser interactions we realized two colour fields, where two single mode laser fields interact simultaneously with the SF₆ molecules of a molecular beam. The realization of this concept is not a trivial task because we work with cw CO₂ waveguide lasers, in most experiments this radiation is focused to a waist of 0.1 mm diameter in order to obtain enough laser fluence (laser power \times time of flight of molecules through the laser field) to induce multiphoton effects.

We work with two counterpropagating laser beams - both orthogonal to the molecular beam axis - just inclined so little that they do not disturb the well functioning of the opposite laser (see fig 1). The alignment is facilitated by the observation of intense two colour multiphoton excitations. One laser is fixed in frequency and chopped, whereas the second laser is not chopped but scanned in frequency. Thus transitions are produced and observed as a result of the combined action of both lasers. The simultaneous character makes it possible to cope with transitions where large detuning Δ occurs for the intermediate level(s). First the use of two different colours can decrease the intermediate detuning (see

fig.2) and secondly the radiation intensity is increased by a factor 2, allowing a larger detuning. Since e.g. the $2h\nu$ Rabi frequency goes linearly with $\Delta^{-1} \times P_{laser}$ both effects contribute to render a relatively weak transition observable.

It is evident that the simultaneous presence of two colour laser fields opens new spectral regions for the final states, very similar to what has been postulated and realized in earlier low resolution experiments employing pulsed lasers in multiphoton excitation of molecules [13, 14]. In the present experiment we exploit the about 1 MHz resolution of our cw lasers (tunable over about ± 125 MHz around the strong CO₂ laser transitions) to obtain one, two and three photon excitation spectra with 2 MHz resolution.

A second new aspect of our experimental set-up is the installation of CO₂ waveguide amplifiers, instead of the conventional amplifier used in [6]. This permits us to obtain amplification over the full tuning range of the laser oscillator, with a maximum power of 25 W. Other advantages are a reduction of coupling losses and conservation of the TEM₀₀ mode.

We use Acousto Optic Modulators (AOM's) to increase the tuning range above ± 125 MHz, in steps of 100 MHz per passage around the fundamental laser transition. We loose about a factor of 2 in laser power per passage. Using two sideband shifters together with the tuning range of the waveguide laser, allows a total tuning range of 1 GHz around a CO₂-transition, with a factor 4 drop in laser power.

To investigate saturation dips in our molecular beam signal, a single laser is retro-reflected and crosses the molecular beam again, so that SF₆ molecules travelling parallel to the molecular beam axis have the possibility to interact with the unreflected and reflected laser radiation. In this way the Doppler residue of the molecular beam is eliminated. The FWHM of $1h\nu$ saturation dips is now solely determined by the time of flight broadening (± 500 kHz) and laser stability. It appears that our lasers have a stability better than 500 kHz, during several seconds.

Since we are interested in the consequences of RAP, the minimum waist is mostly chosen to be very narrow (about 0.1 mm diameter) and normally does not coincide with the molecular beam axis. In earlier experiments [6] where we wanted to observe $2h\nu$ Rabi oscillations this coincidence between minimum waist and molecular beam axis was achieved.

4.3 Depletion measurements

Two colour excitation has been performed with two in space separated laserfields to investigate depletion effects on single rovibrational states due to a strong pump field. To investigate the participation of various initial states of the ν_3 -ladder in the multiphoton process in SF₆, we first cross the molecular beam with an intra-cavity laser (300 Watt) set on the 10P24 CO₂ laser line, i.e. on maximum multiphoton signal. A few centimeters downstream, we probe the same molecules with a waveguide laser, set on the 10P16 line with

double passage through the AOM. Within our experimental accuracy of 10%, we could not detect any depletion of the P(4) two photon transitions (peak A in fig 3), this in contrast with measurements of V M Apatin et al [15], from which we expected depletions up to 30%. The measurements of [15] are critically discussed, theoretically [16]. On the other hand, the unassigned spectral features (peaks B and C in fig 3), coming probably from hot band transitions, vanish almost completely. This and similar findings suggest that thermally excited vibrational states form very effective departure levels for multiphoton excitation.

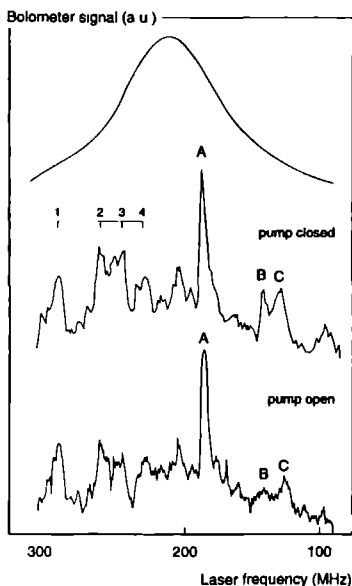


Figure 3 Pump-probe experiment with an intra cavity laser set on the 10P24 CO₂ laser line as a pump laser (300 Watt), and a 200 MHz shifted waveguide laser (1.5 Watt), scanned around the 10P16 CO₂ laser line. The numbers 1 to 4 mark the position of the P(4) quadruplet, peak A is the P(4)E(0) 2hν transition and B and C are two not assigned 2hν hot band transitions. When the pump laser is opened, no dramatic changes in the spectrum are observed except for the two hot band transitions B and C, which disappear almost completely.

Excitation of a molecule either from the ground or from a thermally populated vibrational level may yield a very different number of possible transitions due to the difference in selection rules. There are well known selection rules $\Delta J=0, \pm 1$, $\Delta R=0$ and $\Delta p=0$ for the fundamental vibrational transition of the ν_3 mode [17]. Here R is the rotational angular-momentum quantum number and p the quantum number to assign octahedral sublevels of the same symmetry. If we deal with initially already excited vibrational states where strong

R mixing takes place, the selection rules $\Delta R=0$ and $\Delta p=0$ can be violated. It is known e.g. for the $2\nu_3$ transition of CH_4 [18] and for the $3\nu_3$ transition of SF_6 [19], that these selection rules are violated due to the strong anharmonic coupling of the levels in the excited vibrational state. For example, if for SF_6 the departure level is ν_6 , the selection rule $\Delta R=0$ becomes invalid due to the R mixing in the $\nu_3+\nu_6$ final vibrational state. The vibrational degeneration of the ν_6 level is 3, and of the $\nu_3+\nu_6$ level 9. The number of allowed transitions due to $\Delta R \neq 0$ is 9 times larger than for the fundamental ν_3 transition. If one takes into account the violation of the $\Delta p=0$ selection rule, this difference is even more enhanced by about a factor of $J/2$. This great enhancement of allowed transitions makes it relatively easy to find laser coincidences for transitions from thermally populated vibrational levels such like ν_6 , $2\nu_6$ and ν_5 , which possess low energy and high degeneracy.

4.4 Two level systems, $N=2$

Before starting the discussion on the new points we want to draw attention once more to the double resonance experiments which demonstrate the occurrence of RAP inversion through the first laser interaction with C_2H_4 molecules in a molecular beam. This demonstration is based on the use of a second laser interaction downstream, where the population inversion is undone and stimulated emission occurs, producing a bolometer signal about equally strong as and negative with respect to the absorption signal induced by the first laser interaction alone [1]. In the meantime, this experiment has been repeated also for the $P(4)$ one and two photon resonances of SF_6 (fig. 6 and 10 of [6]). There, too, the reversal of the inversion by stimulated emission has been observed together with the nearly complete absence of power broadening of the RAP signal.

On this last issue we want to add new information. Theoretically, once the conditions for RAP are established, an increase in laser power does not lead to anything but inversion. Experimentally things are slightly different. Some power broadening occurs if the laser power is increased about thousand times over the lower limit value needed for complete inversion, but this broadening is 2 orders of magnitude lower than expected from the standard expression for power broadening, i.e. $\text{FWHM} \approx \text{Rabi frequency}$. However, concomitantly with this rudimentary power broadening we observe the disappearance of the inversion to a point where the second laser interaction yields a zero effect. We thus conclude that by the increase of laser power a 50% population of both levels is achieved, without the effect of residence time broadening due to the increasing Rabi frequency [6]. This observation might be explained by the presence of various modes in our laser beam, which, even if they are a hundredfold less intense than the main gaussian mode, finally show up when the power level is increased more than a hundred times.

Another experiment was performed utilizing only one laser. The laser beam, however, crosses the molecular beam twice at practically the same spot, which induces a saturation

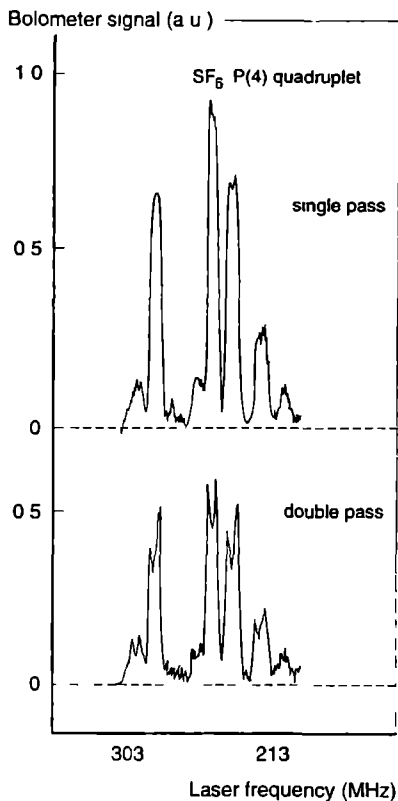


Figure 4 Saturation dip measurements on the P(4) one photon quadruplet in SF₆, upper spectrum taken with single passage of the laser through the molecular beam, lower spectrum taken with double passage, the saturation dips on top of the one photon transitions are clearly visible. The width of the dip corresponds to the time-of-flight broadening.

dip (see fig 4) that is caused by the molecules parallel to the molecular beam axis which "see" both laser fields. Under normal conditions this saturation dip is known to show power broadening of the order of $\frac{1}{2}\pi \Omega_{\text{Rabi}}$. In case of our RAP conditions (i.e. the laser beam is narrowly focussed both ways, but not precisely on the molecular beam) no broadening of the saturation dip has been found.

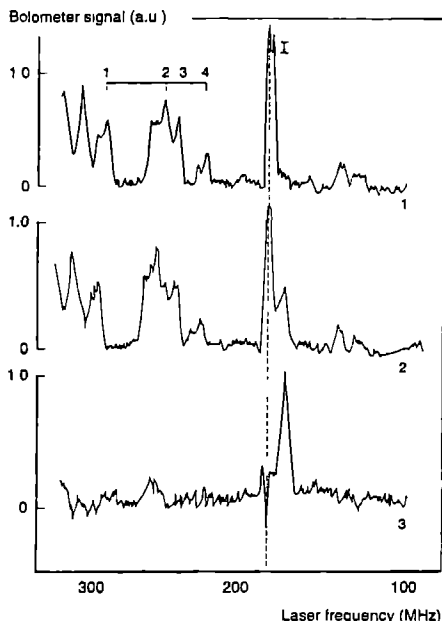


Figure 5: Pump-probe experiment utilizing two overlapping, counter propagating lasers. In spectrum 1, the chopped probe laser is scanned over the 10P16 CO₂ line and shifted 200 MHz (1.5 Watt). I marks the position of the P(4)E(0) $2h\nu$ transition and the numbers 1 to 4 mark the position of the P(4) one photon quadruplet. The unchopped pump laser, fixed on the 10P14 CO₂ laser line (18 Watt), is opened and again a spectrum is taken (spectrum 2). The chopper is moved from the probe laser to the pump laser, resulting in spectrum 3, where on top of a continuous background signal caused by the pump laser the spectral features produced by the interaction of the molecules with both lasers simultaneously are recorded.

4.5 Three level system, N=3

In [6], three level systems have been investigated with one colour $2h\nu$ excitation showing many new transitions in SF₆, amongst which the P(4)E(0) transition 174 MHz shifted from the 10P16 CO₂ line center, with an extraordinarily small detuning of the intermediate level (76 MHz), peak A in fig.3.

We present here our first results on two photon spectroscopy using two coincident counter propagating laser beams. To isolate the two colour signal from the one colour signal we chop

the laser that is fixed in frequency whereas the unchopped (probe) laser is scanned over the full tuning range. Since the bolometer is sensitive only to modulated signals the fixed laser alone will at most produce a non varying background. If a transition is made involving both laserfields the signal will be modulated due to the contribution of the fixed laser. In this way the spectra can be simplified showing only the $n h\nu$ transitions ($n \geq 2$) resulting from two colour interaction (spectrum 3 of fig.5). In the upper part of figure 5, the -still chopped- probe laser is scanned over the 10P16 CO₂ laser line, shifted 200 MHz. Then the pump laser is aligned counter propagating to the probe laser and set on the 10P14 CO₂ laser line; spectrum 2 is thus obtained showing both the structure produced by the probe laser and structures caused by both lasers simultaneously. To find the differences in the two spectra, instead of the probe laser, the pump laser is chopped. Now only the differences in spectra one and two are monitored (spectrum 3), which are exactly the structures we are looking for.

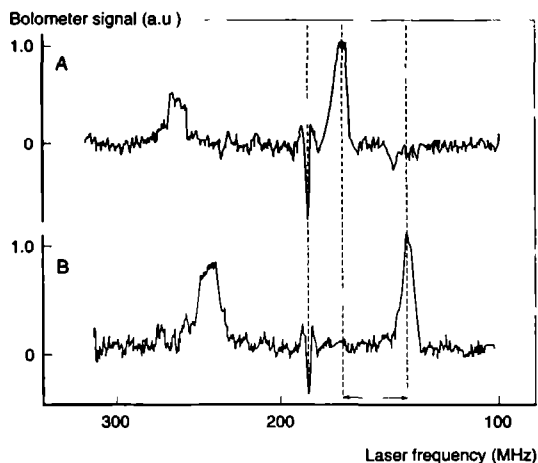


Figure 6: Spectra taken with two overlapping, counter propagating lasers. The probe laser was scanned around the 10P16 CO₂ line and shifted 200 MHz. In A the pump laser is fixed on the 10P14 CO₂ line center, the dip coincides with the $P(4)E(0) 2h\nu$ transition, the two positive peaks are two photon transitions. If we shift the pump laser approximately 50 MHz to the blue, the two photon transitions have to shift 50 MHz to the red to be on resonance again, see spectrum B.

To illustrate the dependence of the signal on both laserfields, the frequency fixed laser was displaced to the blue by about 30 MHz. Scanning the probe laser the two colour transition

frequency should shift to the red by the same amount (in case of a two photon transition) This is clearly shown in fig 6, where the pump laser is fixed on the 10P14 CO₂ line center (spectrum A) For spectrum B, the pump laser is shifted to the blue by approximately 30 MHz, producing a red shift for $2h\nu$ -peaks, with respect to the one-colour $2h\nu$ transition dip For A and B the probe laser is scanned around the 200 MHz shifted 10P16 CO₂ laser line The dip coincides exactly with the P(4)E(0) two photon transition in the probe laser scan and is not shifted

In fig 7 a dense spectrum of multiphoton transitions is presented using a strong pump (18 Watts) and a relatively weak (5 Watts) CO₂ probe laser, set on the 10P14 and 10P16 CO₂ laser transitions, respectively The weak laser is scanned The two strong features we assigned as the Q(21)F₂ at 72 MHz and the Q(17)F₂ at -46 MHz two photon transitions Similar spectra have been made for other combinations of CO₂ laser lines, showing many new transitions Their assignment is discussed in a separate paper [20]

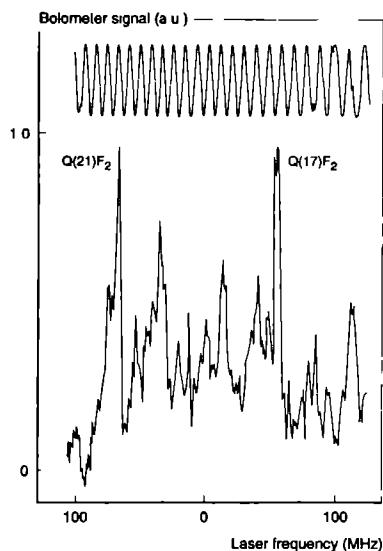


Figure 7 Two colour spectrum, taken with the pump laser (18 Watt) fixed on the 10P14 CO₂ line, the probe laser is scanned around the 10P16 CO₂ line (6 Watt) The two assigned transitions are two photon transitions, predicted in theoretical calculations Above the spectrum, the distance between two fringes is 9 MHz

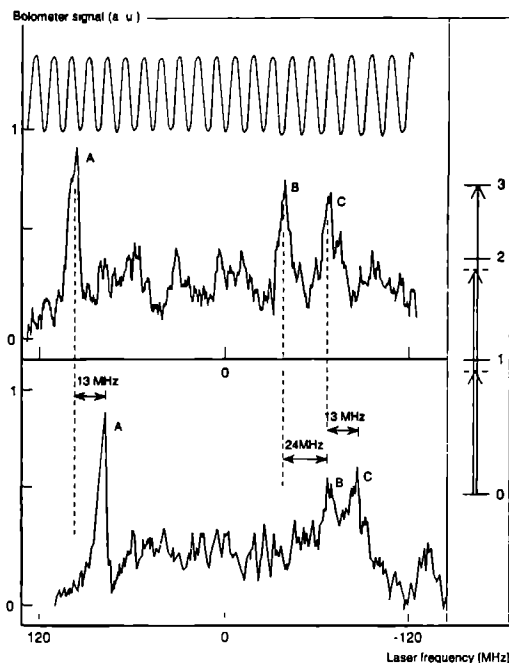


Figure 8: Spectra taken with the probe laser scanned around the 10P14 CO₂ line (5.5 Watt). In the upper spectrum, the pump laser (18 Watt) is set on the 10P16 line center; in the lower spectrum, the pump laser is shifted 13 MHz to the blue. Transitions A and C, assigned as two photon transitions (Q(21)F₂ and Q(17)F₂, respectively) shifted 13 MHz to the red to compensate for the shift of the pump laser. Transition B, however, shifts twice as fast to the red; thus we deal with a three photon transition, utilizing two photons from the pump and one photon from the probe laser, as indicated in the energy level diagram at the right.

4.6 N > 3 level systems

An interesting phenomena showed up interchanging the role of the two lasers of fig.7. The chopped pump laser at the 10P16 line centre has now an intensity of 18 Watt, the probe laser is scanned around the 10P14 line center, with 5.5 Watt intensity (upper part of fig.8). At -30 ± 10 MHz detuning a new very strong transition is observed (peak B). Apparently

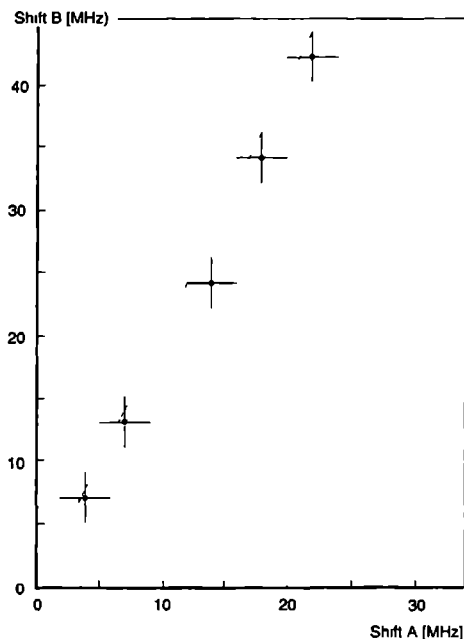


Figure 9 Shift of transition B, relative to the shift of transition C in figure 8. The dotted line is what is expected for a three photon transition according to the energy level diagram in figure 8, the data fit very well within the experimental accuracy.

one step in the excitation depends strongly on the intensity of the 10P16 laser. This fact forms an indication that peak B is due to a $(n h \nu_{10P16} + h \nu_{10P14})$ -type transition with $n > 1$. For $n=1$, the interchange of laser characteristics would show no big influence as observed for peak A and C. In addition the position of peak B does match neither with calculated one nor with two photon frequencies. A R(16)E three photon transition of the type $(2 h \nu_{10P16} + h \nu_{10P14})$ is predicted almost exactly coinciding with the observed transition B.

To prove that we definitely deal here with a three photon transition we shifted the pump laser frequency by varying amounts, each time taking a new spectrum by scanning the probe laser (see e.g. the lower part of fig 8 where the shift amounts to 13 MHz). Every time the shift of the two photon two colour transitions is measured and compared with the shift of peak B. If this peak is due to a three photon transition there are two possibilities, a) either the peak shifts twice as fast as the two photon transitions, indicating that two photons from

the pump laser are needed to make the transition, or b) the peak shifts twice as slowly as the two photon transitions, indicating that only one photon is needed from the pump laser to produce the transition.

In fig.9 the shift of transition B is plotted against the shift of the two photon transitions; the theoretically predicted shift for alternative a) is indicated by the dotted line. From this, we conclude that we really deal here with a three photon transition, utilizing two photons from the pump and one photon from the probe laser, as indicated in the energy level scheme in fig.8.

For $N > 3$ level systems, the experimental possibilities are subject to certain restraints. With one colour excitation of SF₆ two things have been shown experimentally. There is a vibrational bottleneck at $n=5$ (i.e. under RAP conditions inverted populations can be created up to the fifth level of the ν_3 mode; higher up one either runs out of resonance or the high density of states prevents RAP-processes to occur [1]). Furthermore, at this bottleneck level no spectral features have been resolved. This second point might render experiments where the bottleneck is overcome employing two or more colour excitation less interesting, from a spectroscopic point of view.

On the other hand, with one colour excitation and fluences up to 0.01 J/cm² (typical for our waveguide lasers with an amplifier stage focused to 0.1 mm \varnothing) no three or four photon excitations have been identified. However, with two colour excitation (simultaneous excitation by two overlapping CO₂ laser foci) sharp spectral structures due to at least three photon excitation have been found in the present work. This opens the way for new spectroscopy at excitation up to 3000 or even 4000 cm⁻¹.

4.7 Acknowledgement

We would like to thank Cor Sikkens, Frans van Rijn and John Holtkamp for their permanent and skilful technical assistance. The dutch organisations N.W.O. and S.T.W. made this investigation possible by generous financial support.

References

- [1] C Liedenbaum, S Stolte and J Reuss, *Chem Phys* 122 (1988) 443
- [2] C Liedenbaum, S Stolte and J Reuss, *Infrared Phys* 29 (1989) 397
- [3] C Liedenbaum, S Stolte and J Reuss, *Phys Rep* 178 (1989) 1
- [4] N Dam, S Stolte and J Reuss, *Chem Phys* 135 (1989) 437
- [5] J Reuss and N Dam, *Applied Laser Spectroscopy*, Eds W Demtroder and M Inguscio, Plenum Press, New York (1990)
- [6] A Linskens, S te Lintel Hekkert and J Reuss, *Infrared Phys* 32 (1991) 259
- [7] F T Hioe, *Phys Lett* 99A (1983) 150
- [8] J Oreg, F T Hioe and J H Eberly, *Phys Rev A* 29 (1984) 690
- [9] U Gaubatz, P Rudecki, M Becker, S Schiemann, M Kultz and K Bergmann, *Chem Phys Lett* 149 (1988) 463
- [10] J R Kuklinski, U Gaubatz, F T Hioe and K Bergmann, *Phys Rev A* 40 (1989) 6741
- [11] U Gaubatz, P Rudecki, S Schiemann and K Bergmann, *J Chem Phys* 92 (1990) 5363
- [12] G Z He, A Kulin, S Schiemann and K Bergmann, *J Opt Soc Am B* 7 (1990) 1960
- [13] S S Alimpiev, N V Karlov, E M Khokhlov, S M Nikiforov, B G Sartakov and A L Shtarkov, *J of Mol Struct* 115 (1984) 229
- [14] S S Alimpiev, G S Baronov, D K Bronnikov, A E Varfolomeev, I I Zasavitski, S M Nikiforov, B G Sartakov and A P Shotov, *Opt Spektrosc* 67 (1989) 625
- [15] V M Apatin, V M Krivtsun, Yu A Kuritsyn, G N Makarov and I Pak, *Opt Com* 47 (1983) 251
- [16] D P Hodgkinson, A J Taylor, *Opt Com* 50 (1984) 214
- [17] J. Moret-Bailly, *Ibid* 15 (1965) 344
- [18] K Fox, *J Mol Spectrosc* 9 (1962) 381
- [19] C W Patterson, B J Krohn and A S Pine, *J Mol Spectrosc* 88 (1981) 133
- [20] S te Lintel Hekkert, A F Linskens, B G Sartakov, G Pierre and J Reuss, to be published in *Chem Phys*

Multiphoton multi laser excitation of the ν_3 mode of SF_6 in a molecular beam

S. te Lintel Hekkert, A.F. Linskens, I. Holleman,
B.G. Sartakov[†], G. Pierre^{††} and J. Reuss

Department of Molecular and Laser Physics, University of Nijmegen
Toernooiveld, 6525 ED Nijmegen, The Netherlands

[†] General Physics Institute, Vavilov street 38, 117942 Moscow Russia

^{††} Laboratoire de spectrométrie moléculaire et instrumentation laser, Université de Bourgogne, Bd Gabriel 6, 21100 Dijon, France

Abstract

Results are presented of measurements utilizing two counter propagating CO_2 waveguide lasers interacting simultaneously with SF_6 molecules in a molecular beam. 95 two photon transitions were observed and assigned, for combinations of two different CO_2 laser lines. Especially transitions to levels of E_g vibrational symmetry provided new information on the parameters of the Hamiltonian because older one colour measurements could barely access these levels. Still no transitions were found to levels with A_{1g} vibrational symmetry. Some results are presented on three and four photon transitions.

5.1 Introduction

Two counterpropagating c.w. CO₂ lasers are applied simultaneously to SF₆ molecules in a molecular beam. The frequencies can be continuously tuned over ± 500 MHz. With this technique it is possible to enter new spectral regions at about 10 μm . Many new transitions are measured which allow to fit the SF₆ Hamiltonian.

These new lines lead to a better understanding of the Hamiltonian of SF₆. Previously, the group of Bordé [1, 2] has determined 310 one photon transitions with extremely high accuracy. The restriction to levels at about 1000 cm⁻¹ is compensated by the small value of the FWHM, 3 kHz. The initially populated and measurable levels possess rotational quantum numbers $12 \leq J \leq 95$, since the measurements were performed at room temperature.

In addition, Herlemont et al [3, 4] observed two photon transitions by saturation spectroscopy (FWHM 200 kHz, room temperature measurements). Both these series of measurements form the basis of the determination of the parameters in the SF₆ Hamiltonian by G. Pierre who recently also included many transitions observed by us; these new measurements are reported in [5] (two photon one colour (TPOC) spectra) and in this work (two photon two colour (TPTC) spectra). Independently, and using a slightly different but in principal equivalent form of the SF₆ Hamiltonian [6] the other co-author of this paper, B.G. Sartakov, bases predictions of transitions on older work of the group of Bordé, and the here presented TPTC spectra.

The measurements were extended to the 3000 cm⁻¹ region; even the first observation of four photon transitions are reported below. Already in 1980 A.S. Pine et al [7, 8] reported 3h ν_3 overtone measurements for SF₆, observed in a molecular jet, $5 \leq J \leq 35$. These measurements possess linewidth of 30 MHz and are not taken into account in the fits presented in this paper. They agree within their linewidth with Sartakov's calculated values.

In section 2, the experimental set-up as well as some tricks to determine the frequencies of the multiphoton transitions are presented. The experiments aim at the observation of discrete multiphoton transitions with MHz resolution. It is well known that e.g. with pulsed lasers, but also with c.w. lasers interacting with vibrationally hot SF₆ molecules, unstructured background-like multiphoton excitation has been observed [9]. In section 3, the interaction by a c.w. 150 Watt CO₂ laser (Apollo, Sales Laser Photonics, Carlsbad U.S.A.) is described. The laser is not fine tuned, but set to the maximum of different CO₂ laser transitions. Especially for the 10P24 transition, depletion measurements are discussed which demonstrate that only the already thermally excited energy levels are depleted. Transitions starting from the ground state level of SF₆ show no signal decrease by the interaction with the Apollo laser; accordingly we conclude that the molecules in the ground state of SF₆ barely participate in the background-like multiphoton process.

Our interest is directed towards multiphoton transitions. Therefore, possible power broadening forms an interesting issue. Note that normally we work with laser powers up to

600 times larger than what is needed for complete saturation of one photon transitions. To clarify the saturation issue, the Apollo laser has been employed (possessing even 6000 times the intensity needed for saturation) to investigate power broadening effects of the assigned two photon transitions; no power broadening is observed, the results are discussed in section 4.

In section 5, dynamical Stark effects as observed in the spectra are discussed. These Stark effects are produced by the interaction of the pump laser with the levels of transitions in resonance with the probe laser. This probe laser is not chopped; accordingly transitions induced by the interaction of molecules with the probe laser only should not be observed in the spectra. For the strong one photon transitions (P(4) quadruplet on the 10P16 CO₂ laser line) and two photon transitions (P(4) doublet on the 10P16 CO₂ laser line), the dynamical Stark effect is observed very clearly and renders the probe laser transitions observable.

The assigned TPTC transitions are presented in section 6. Preliminary results on three and four photon transitions are presented in section 7. Some concluding remarks and suggestions are made in section 8: the outlook.

5.2 Experimental set-up

The experimental set-up is described in detail in [5, 6, 9, 10]; there are two new aspects. To investigate power broadening effects of the transitions and depletion of hot band transitions, high intensities are required. In order to achieve this, a commercially available Apollo laser is installed. This laser produces 150 W outcoupled power in a TEM₀₀ mode, on the strong 10P lines. This in contrast with the intra-cavity laser utilized in [5], which produces twice as much power with, however, rather poor beam qualities.

A second new aspect is the installation of a Lamb dip cell [11, 12]. In the two laser experiments, performed to investigate two and more photon transitions, the pump laser is fixed in frequency. To determine the distance between two transitions in a spectrum, it is necessary to keep the pump laser frequency fixed for more than 10 minutes, i.e. the time needed to scan the second laser (probe laser) over its total tuning range of 230 MHz. In order to do so, the pump laser is locked to the dip in fluorescence signal of a Lamb dip cell [13].

The rotational cooling of the molecules during the expansion through the nozzle is very sensitive on the stagnation pressure behind the 50 μ m nozzle [14, 15], as can be seen in fig.1. In fig.1, spectra taken with only one laser are shown with a background pressure of 300 Torr (upper spectrum) and 700 Torr (lower spectrum). All assigned two photon transitions are marked. Especially the Q(29) transition left in the spectra is difficult to find back in the lower spectrum. The Q(29) transition is a strong one [6]; with the laser intensities utilized to produce this spectrum, it is saturated. Its vanishing is caused by the depletion of the J=29 rotational energy level due to the better cooling of the molecules in the expansion.

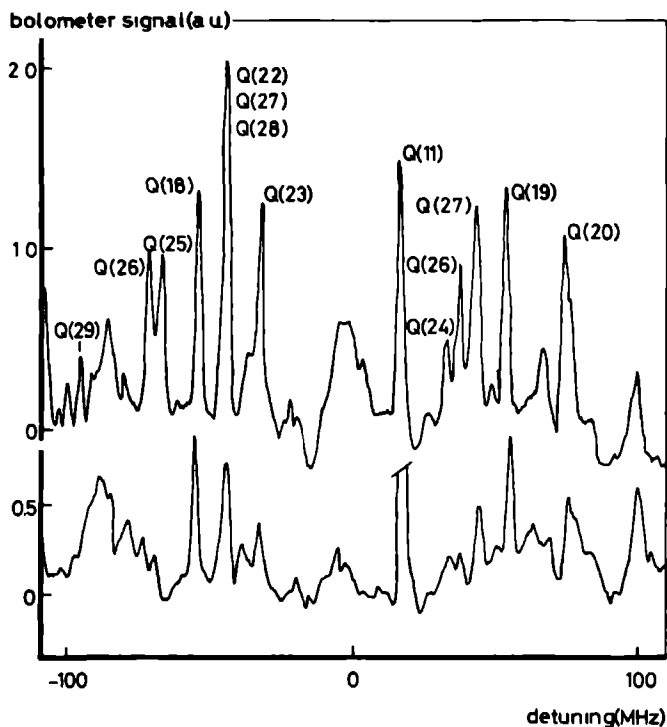


Figure 1 Dependence of the intensity of the measured two photon transitions on the 10P16 CO_2 laser line on the stagnation pressure behind the $50\ \mu\text{m}$ nozzle. The upper spectrum is taken with 300 Torr stagnation pressure, the lower spectrum with 700 Torr resulting in a much better rotational cooling. In the lower spectrum the transitions starting from low J -values are relatively much higher than the transitions starting from higher J -values. In the assignment of the transitions, the dependence on the background signal is very useful.

To find transitions starting from high J -values with low strength factors, it is important to take the spectra with lower background pressure. On the contrary, transitions starting from energy levels with low J -values, 700 Torr background pressure leads to optimum signals.

The measured spectral region can be covered in several ways choosing the right CO_2 laser line combination and configuration of Acousto Optic Modulators (AOM's). The AOM's shift

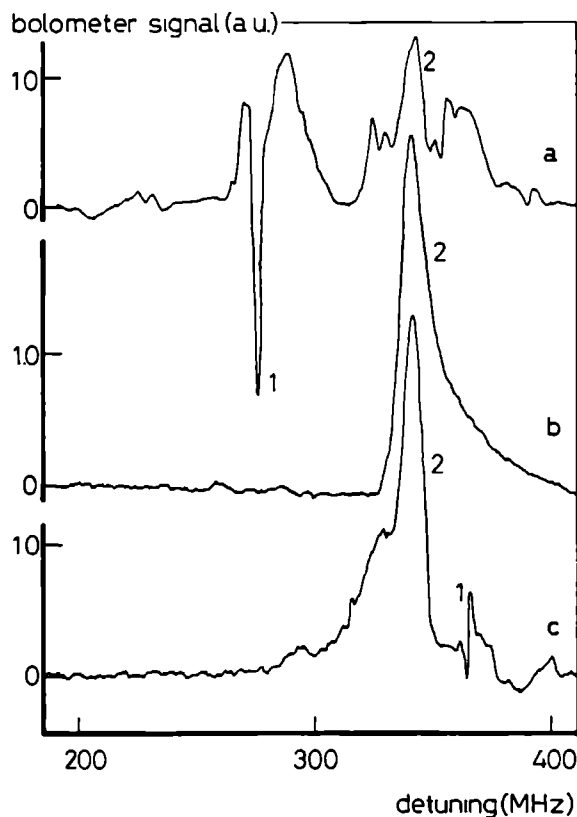


Figure 2: The spectral region shifted 300 MHz from the 10P16 CO_2 laser line center for the two colour, two photon transitions, taken with three different configurations of the AOM's. In the upper spectrum, the pump laser is shifted by 100 MHz and the probe laser is shifted by 200 MHz with respect to the 10P16 CO_2 laser line. The spectrum in the middle is taken with the pump laser shifted by 300 MHz, no AOM is aligned in the probe laser. In the lower spectrum, the pump laser is shifted by 200 MHz and the probe laser by 100 MHz. For two colour, two photon transitions these spectra should be the same, indeed, the strong $P(4) E(0)$ transition (peak 2) reproduces in all three spectra. Structure 1 is in resonance with the $P(4) E(0)$ transition frequency of the probe laser. This structure and the less narrow structure around transition 2 in the upper spectrum are due to the dynamic Stark effects (section 5).

the frequency of the CO₂ lasers 100 MHz up or down for a single passage of the laser beam through the AOM crystal. Providing a second pass through the modulator results in another 100 MHz shift, in this way it is possible to shift the frequency of the CO₂ laser 200 MHz. As an example the frequency region with a total shift for two colour, two photon transitions from 200 MHz to 400 MHz with respect to the 10P16 CO₂ laser line is presented in fig 2. In the upper spectrum, the scanned probe laser is shifted 200 MHz, while the chopped pump laser is shifted 100 MHz. In the spectrum in the middle, no AOM is inserted into the probe laserbeam, both AOM's are aligned in the pump laserbeam (one double and the other single pass), resulting in a total shift of 300 MHz. In the lower spectrum the role of the two lasers is interchanged with respect to the upper spectrum (i.e. the probe laser is shifted 100 MHz, while the pump laser is shifted 200 MHz).

Two spectral features reproduce very clearly in these spectra. The feature numbered 1, is in resonance with the P(4) E(0) two photon transition utilizing two photons of the probe laser, it appears in the spectra due to the dynamical Stark effect (see section 5). Because the frequency of this transition is well known, it can be used for absolute frequency calibration. The transition 2 is the same transition, but now produced utilizing one photon from each laser. This are the transitions we are interested in. The less narrow features in the upper spectrum around transition 2, caused by the dynamic Stark shift on the P(4) one photon quadruplet (as will be discussed in section 4), makes it difficult to assign transitions in this frequency region. On the contrary, in the middle spectrum nothing is left of the less narrow structures, only a tail on transition 2 is observed due to saturation of the transition (section 4). Now it is possible to enlarge the sensitivity of the lock-in detector without overload in the regions near the P(4) two photon transition and resolve other interesting transitions which are less intense.

5.3 Multiphoton depletion measurements

To investigate which energy levels participate mainly in the unstructured background-like multiphoton process, an Apollo laser set on top of the multiphoton signal (i.e. the 10P24 CO₂ laser line) is crossed with the molecular beam. Seventy mm downstream the molecules are probed by a chopped waveguide laser set on the 10P16 CO₂ laser line and shifted 100 MHz by a single pass through an AOM. First the spectrum without the Apollo laser is taken in fig 3^a with a background pressure of 300 Torr behind the nozzle and the nozzle at 300 K. Some of the two photon transitions possessing J-values from 4 to 27 are indicated. No changes in the intensities of the assigned two photon transitions are observed in the spectrum when the Apollo laser is turned on.

Heating up the nozzle to 400 K changes the spectrum dramatically (fig 3^b). The transitions starting from low rotational energy levels are decreased as compared with the transitions starting from higher J-values. Interesting are the two transitions marked A and

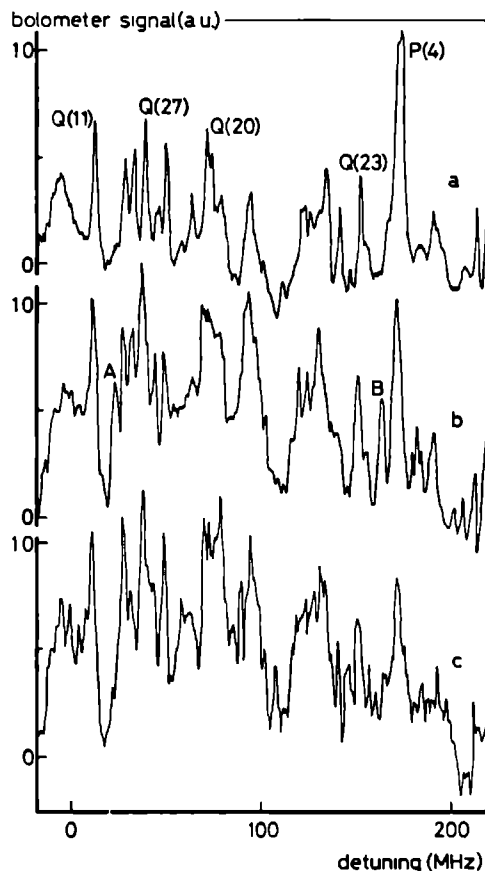


Figure 3 Pump-probe experiments with the Apollo laser (150 W) set on the 10P24 CO_2 laser line, i.e. on top of the multiphoton signal. Seventy mm downstream the interaction with the Apollo laser, the molecules are probed by a waveguide laser tuned to the 10P16 CO_2 laser line, its frequency is shifted 100 MHz utilizing an AOM. In fig 3^a the nozzle is at room temperature and the Apollo laser is turned off. Some of the assigned two photon transitions are indicated in the spectra. In fig 3^b the nozzle is heated up to 400 K, still the Apollo laser is off. As expected, the relative intensities of the transitions in the spectra change very much. Special attention is required for the two transitions marked A and B, they are not observed in fig 3^a. From this we conclude that they are hot band transitions. In fig 3^c the Apollo laser is turned on, now the two hot band transitions are gone, whereas the relative intensity of the assigned two photon transitions is not changed.

B in fig.3^b, they are on frequencies where no $2\nu_3 \leftarrow 0$ transition is expected and therefore they are assigned to hot band transitions. Opening the Apollo laser, almost the same spectrum (fig.3^c) is observed again, the relative intensities of the two photon transitions staying the same. However, the two hot band transitions vanish almost completely. From these measurements we conclude that for the multiphoton process, transitions starting from hot bands play an important role, while molecules in the ground state barely participate in the multiphoton process. This is in agreement with [6]. However, they are in contrast with measurements of V.M. Akulin et al [16], from which we expected depletions up to 30%. The measurements of [16] are critically discussed, theoretically [17]. Increasing the temperature of the nozzle again with 100 K up to 500 K, results in a broadband almost structureless spectrum. The hot band transitions come up very strongly and the spectrum becomes so dense that it is impossible to assign the ν_3 transitions anymore. Putting on the Apollo laser will decrease the signal but still no spectral features are resolved.

5.4 Absence of power broadening and background signals

In order to investigate power broadening effects of the transitions produced by the simultaneous interaction of two lasers with a molecule, a 150 W Apollo laser, set on the 10P16 CO₂ laser line center is used as a pump laser. The probe laser (6 W) is scanned around the 10P16 CO₂ laser line, the resulting spectrum is presented in fig.4. The assigned TPTC transitions are indicated in the spectrum. In conventional spectroscopy line widths exceeding 100 MHz are expected for the intensities utilized in our experiments. However, no significant power broadening is observed; the FWHM of the measured transitions is approximately 4 MHz. This is twice as much as the FWHM of the transitions measured with only one laser (TPOC) where both participating photons change frequency.

The absence of power broadening is due to the fact that we utilize curved wave fronts; in order to increase the fluence of our lasers to investigate the transitions with low intensity factors, the lasers are tightly focused on the molecular beam (minimum waist 0.1 mm). The curved wave fronts (together with the smooth Gaussian line profiles of our lasers) are responsible for the fact that we do not observe Rabi-type transitions but RAP-transitions, for which no power broadening is expected to take place [18, 19, 20, 21].

The 20 MHz broad dip in the center of the spectrum of fig.4, is caused by a depletion of initial levels by the pump laser. The pump laser produces a background-like signal; if the probe laser frequency coincides with the frequency of the pump laser, part of the molecules are not anymore available to become excited by the probe laser; accordingly, the pump laser produces less signal resulting in negative bolometer signal. This broad dip is not very dependent on the intensities of the lasers. It appears also in all spectra with two waveguide lasers on positions where the pump and probe laser frequencies are the same. An example of such a dip is shown in fig.6, where both waveguide lasers were shifted by -200 MHz.

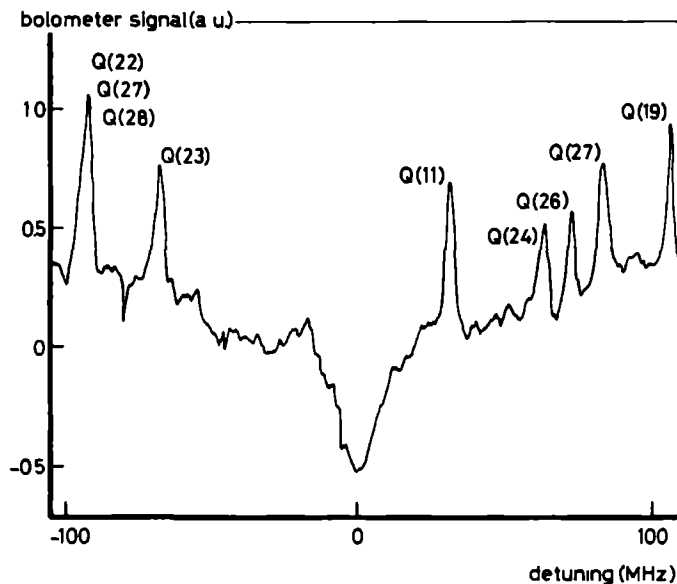


Figure 4 Two colour, two laser transitions measured with an Apollo laser tuned to the 10P16 CO₂ laser line (150 W) as a pump, and a waveguide laser also set on the 10P16 CO₂ laser line (6 W), as a probe laser. A broad dip appears in the spectra in the region where the frequencies of the pump and the probe laser are the same. The widths of the assigned two photon transitions is approximately 4 MHz.

5.5 Dynamic Stark effects

These effects are due to the working of the chopped strong pump laser and give rise to spectral features when the probe laser is scanned, the spectral features are observed at unshifted positions (for one- and two photon transitions) but were expected to remain undetected because the probe laser is not chopped.

The sharp dips in the spectra (e.g. structure 1 in fig 2 and fig 5) are caused by the dynamic Stark effect. The pump laser couples the excited energy states of transitions - in resonance with the frequency of the probe laser - with energy levels in the quasi continuum.

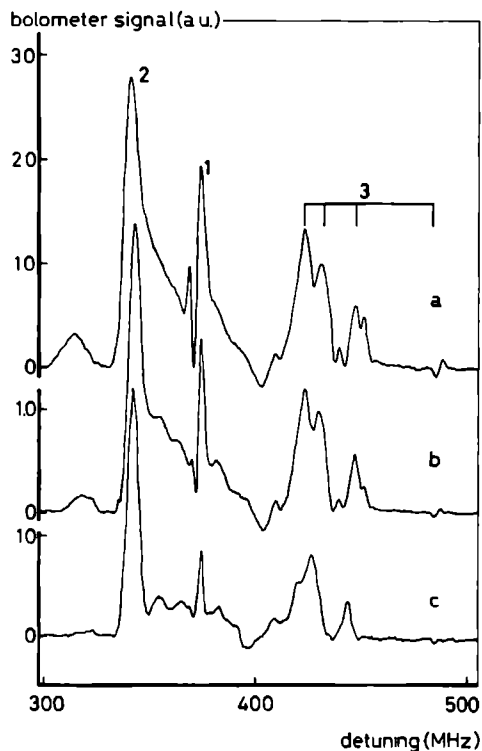


Figure 5: Power dependence of the tail on the strong $P(4) E(0)$ two colour, two photon transition and the Stark effects. Both the pump and the probe laser are shifted 200 MHz from the 10P16 CO_2 laser line. In spectrum a the intensity of the probe laser is 1 W; the pump laser is 6 W. In b the intensity of the pump laser is decreased till 3 W, in c the intensity of the pump laser is 1.5 W. The spectral feature marked 1 is due to the Stark effect of the $P(4) E(0)$ transition in resonance with the probe laser only. The resonance of the probe laser with the $P(4)$ one photon transitions, also causes structures to appear in the spectra. The frequencies of the $P(4)$ quadruplet are marked under 3. Peak 2 is the $P(4) E(0)$ two colour, two photon transition.

This may push the two photon transition slightly out of resonance resulting in negative bolometer signal. However, at a nearby frequency this two photon transition comes into

resonance again with the photons from the probe laser, resulting in positive bolometer signal. This effect is observed only for the strong two photon transitions, especially for the P(4) transitions on the 10P16 CO_2 laser line [6]. The levels participating in two photon transitions interact with energy levels in the quasicontinuum through the pump laser, over a wide range of pump laser frequencies. This is observed in the spectra, even if the pump laser is shifted several CO_2 laser lines the structures remain at the same probe laser frequency. The shape of the structure changes depending on the intensity of the pump laser.

Two other more obvious interactions of the pump laser with the final level of the transitions induced by the probe laser can give rise to signals. First, the pump laser can deplete the level which is populated by the probe laser, by de-exciting the molecules. However, the pump laser is fixed in frequency and the density of states in the ground state or the first excited state of the cooled molecules is not high. The pump laser has to be exactly in resonance with a transition from the excited state, what will rarely happen. Second, the pump laser can excite the molecule further up, either with one or two photons to a discrete level or to the quasicontinuum resulting in positive bolometer signal. This second effect is much more likely to happen because the density of states increases going up on the energy ladder, in the quasi continuum there is always a transition in resonance with the laser frequency.

It is difficult to distinguish in general between the dynamic Stark effects and the two possibilities discussed in the last paragraph. However, in all spectra the dip is accompanied by a positive peak, ruling out the de-excitation scheme. The de-excitation scheme leads to a dip which is not accompanied by a nearby peak. In all spectra this extra peak has been clearly observed, as one expects from dynamic Stark effects, thus, this mechanism is clearly present.

The excitation scheme is also rather improbable, the absence of peaks at the center frequency of transitions forms a contra-indication.

A strong argument in favour of the dynamic Stark effects mechanism and the de-excitation depletion mechanism derives from the observation that the observed less narrow features do not strongly depend on the value of the pump laser frequency.

In fig 5, the less narrow structure 3 is certainly due to the dynamical Stark effect. In this case not the final level of a two photon transition, but the final levels of the P(4) one photon transitions [5] are affected. The frequencies of the transitions of the P(4) quadruplet are marked under 3 in fig 5. The same effect is responsible for the less narrow structure around the P(4) TPTC transition (peak 2 in the upper part of fig 2). The pump laser has been shifted by 200 MHz and these features did not disappear. With the pump laser working on the 10P14 or 10P18 laser transitions, the less narrow feature 3 was not observed. The two photon structure 2, however, remained. This probably is connected to the fact that the $2h\nu_3$ level at about 2000 cm^{-1} can be coupled to the quasicontinuum by the pump laser at a greater variety of frequencies, as consequence of the increased density of states.

The TPTC P(4) transition on the 10P16 CO_2 laser line (peak 2 in fig 2 and fig 5)

possesses a very low detuning of the intermediate level with respect to the laser frequency. The intensities utilized in our experiments are more than two orders of magnitude higher than the intensities needed to saturate this transition [5]. This causes saturation effects to become visible, often a tail on one side of the transition is observed. Decreasing the fluence of the pump laser causes the tail to disappear much faster than the two photon transition itself. This can be seen in fig 5, in which the intensity of the pump laser is decreased each time by a factor two, going from 6 W in the upper spectrum, to 3 W in the middle spectrum, to 1.5 W in the lower spectrum. From these spectra it is clear that also the spectral features caused by the Stark effect on levels in resonance with the frequency of the probe laser, disappear much faster than the main signal from the TPIC transition itself.

5.6 Two colour, two photon transitions

With the two waveguide lasers interacting simultaneously with the beam molecules new two photon transitions have been measured. These transitions are included in the fitting procedure, the resulting constants for the Hamiltonian were already listed in table 2 of [6]. The predicted transitions together with the measured frequencies are listed in table 1. In this table in column 2, the transitions with their ro-vibrational symmetry are listed. Column 3 shows the vibrational symmetry for transitions for which coupling to other vibrational symmetries does not disturb the energy levels too much; this is only the case for transitions starting from low J -values. The calculated frequencies (ν_S and ν_P) and strength factors (S_S and S_P), predicted utilizing two different representations of the terms in the Hamiltonian, are listed in columns 4 till 7. In the last column the experimental frequency of the transition is listed.

The discrepancy in the two predicted frequencies ν_S and ν_P is mainly caused by the fact that the set of measured transitions, utilized in the fitting procedure is not identical in both calculations. Besides the measurements described here and in [22], also two photon transitions as measured by Herlemont et al [3, 4], and one photon transitions as measured by Borde et al [23] are included in the calculations of Pierre.

The two strength factors S_S and S_P differ by about 2 orders of magnitude due to the use of different conventions, in comparing the different transitions one should consider only the relative strengths. In order not to make the listing of two photon transitions too long, transitions with a strength factor smaller than 0.1 for S_S and 10 for S_P are excluded. These transitions are not expected to be observable in the spectra.

In the last column the experimental frequencies are listed, however, if the assignment is uncertain (i.e. either there are no measured structures or too many measured structures around the predicted frequency) a \star is listed. Transitions included in the fitting procedure resulting in ν_S are marked with \bullet .

Transitions possessing F_{2g} vibrational symmetry are in good agreement with the theo-

retically predicted frequencies. Especially for the 10P14-10P18 laser line combination, the transitions are predicted very accurately due to the fact that this frequency region partially overlaps with the frequency region covered by the one laser experiments (i.e. the 10P16 region). Especially for E_g vibrational symmetry, the measurements utilizing two lasers are of great importance; many new transitions are found with this symmetry. Though the predictions of the frequencies of transitions possessing this vibrational symmetry are already one order of magnitude better than the first estimates (based upon TPOC results), still work has to be done to improve the fit for the E_g vibrational symmetry. Transitions possessing pure A_{1g} vibrational symmetry are not predicted in the spectral regions of our measurements. For these transitions other measurements have to be performed. Utilizing N₂O or isotope lasers in combination with the TPTC technique, it seems possible to improve the 67 parameters necessary to describe the $2\nu_3$ transitions in SF₆.

5.7 Three and four photon transitions

Overtone measurements on the $3\nu_3$ transitions in SF₆ were performed previously, [7, 8]. From these measurements we know that it is possible to measure resolved discrete three photon transitions in SF₆. With our experimental set-up it is possible to determine frequencies with much higher accuracy (2 MHz instead of 30 MHz). Due to selection rules it is possible to measure many more multiphoton transitions leading to levels near to the $3\nu_3$ overtone levels. For overtone transitions to the third energy level, $\Delta J = -1, 0$ or 1 and the vibrational symmetry is restricted to F_{1u}, while for a three photon transition ΔJ can be $-3, -2, -1, 0, 1, 2$, or 3 and the vibrational energy of the final level can be either A_{2u}, F_{1u} or F_{2u}.

For three and four photon transitions, only preliminary results are presented. Because of the fact that the two photon transitions are not yet fitted completely, the predicted three and four photon transition frequencies ν_S and ν_P are separated often by more than 100 MHz. This makes it sometimes difficult to assign the transitions uniquely. Therefore, we approach this problem from the experimental side, in a first attempt.

To illustrate the method, the spectrum a) with both pump and probe laser shifted -200 MHz with respect to the 10P16 CO₂ laser line (fig.6^a), and the spectrum b) with the probe laser shifted -200 MHz and the pump laser shifted -100 MHz, both with respect to the 10P16 CO₂ laser line (fig.6^b) are compared. For TPTC transitions the right part of fig.6^a and the left part of fig.6^b are equivalent, and indeed the predicted two photon transitions in this region can be observed in both spectra. In the lower spectrum, a transition is observed between the Q(21) and the P(4) two photon transitions. This transition is not present in spectrum 6^b, indicating that one deals with a n photon transition with $n \geq 3$. If it is a three photon transition, from spectrum 6^a two possible frequency shifts can be predicted for spectrum 6^b. If the transition is produced utilizing two photons from the pump and one photon from the probe laser, the frequency of the transition is at $3\nu_{10P16} - 538$ MHz. Another

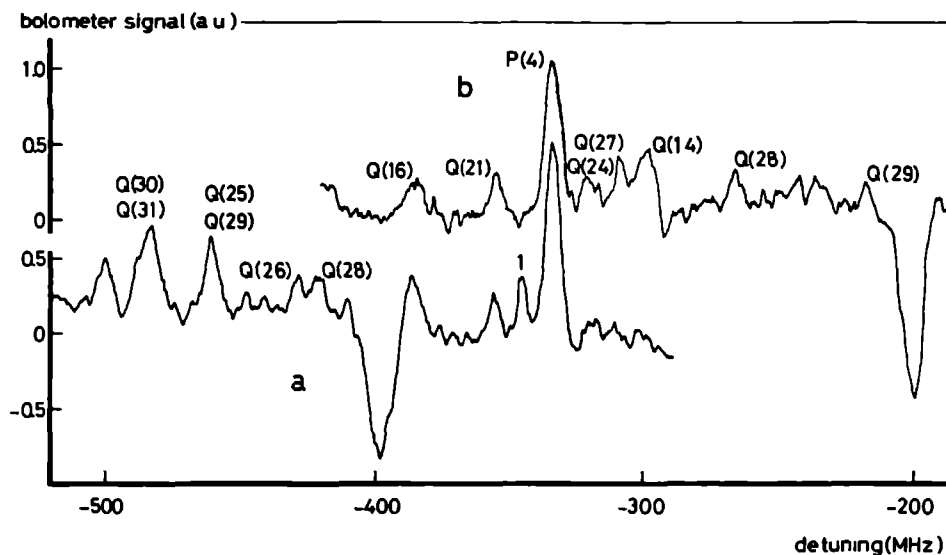


Figure 6 In the assignment of the three photon transitions, the shift of the pump laser is very important. In spectrum a and spectrum b the probe laser is scanned around the 10P16 CO₂ laser line and shifted -200 MHz, in spectrum a the pump laser is shifted -200 MHz with respect to the 10P16 laser line, in spectrum b this shift is only -100 MHz. The assigned two photon are indicated in the spectra. Transition 1 in spectrum a disappears in spectrum b, it can be assigned as a three photon transition.

possibility is that only one photon is utilized from the pump, and two photons from the probe laser, the frequency of the transition is $3\nu_{10P16} - 476$ MHz. Comparison of these frequencies with the calculated frequencies an assignment results for peak 1 in fig 6^a, as a R(10) F₂(1) transition utilizing one photon from the pump and two photons from the probe laser.

In a similar way other three and four photon transitions are assigned, they are listed in table 2. In the second column the laser line combination needed to enter the spectral region on which the transition presented in column 3 is found, is listed. The predicted frequencies (ν_S and ν_P) and strength factors (S_S and S_P), calculated utilizing two different representations of the terms in the Hamiltonian and two sets of different transitions in the fitting procedure, are listed in columns 4 to 7. The experimentally determined frequencies are listed in column 8.

The upper part of table 2 shows the three photon transitions. For ν_P only transitions ending on energy levels with $J \leq 10$ are available at the present time, for ν_S J-values up to 30 are predicted. If in column 4 **** is listed for the strength factor, this strength factor is higher than 10^5 . Four photon transitions are only predicted in ν_S ; this list is limited to J-values smaller than 10. For higher J-values the time needed to calculate the four photon increases considerably because the density of states increases very fast.

The three and four photon transitions are not included in the fitting procedure; this is one reason for the discrepancies in the two theoretical predictions. In order to make the prediction of the frequencies of the three and four photon transitions more reliable it is necessary to fit first all two photon transitions and then include also step by step the three and four photon transitions, in an interactive way.

5.8 Outlook

Utilizing the simultaneous interaction of two lasers with SF_6 molecules opens a wide range of frequency regions on where many new multiphoton transitions can be measured. The one laser experiments alone do not provide enough experimental data to determine the 67 constants of the Hamiltonian which describe the $2h\nu_3$ transitions in SF_6 [6].

Even the use of three independent CO_2 lasers is planned. Hereby, the investigation of what often is termed the onset of the quasicontinuum/stochastisation becomes feasible. One expects that spectral blobs appear for certain frequencies, whereas elsewhere discrete levels will be found even for much higher energies.

Once the two photon transitions have been fit properly, the predictions of the frequencies of the three and four photon transitions will improve. Only 5 new constants have to be fit to determine the three and four photon transitions within our experimental accuracy of 2 MHz. We have still about 20 of these transitions observed which will become assignable.

5.9 Tables

tabel 1 ^a 10P12-10P14 laser line combination							
nr	transition	vib sym	S_S a u	ν_S [MHz]	ν_P [MHz]	S_P a u	ν_{exp} [MHz]
1	S(14) E(3)	F _{2g}	0 26	238			*
2	S(9) E(1)	F _{2g}	0 25	233			*
3	S(14) A ₂ (1)	F _{2g}	0 66	177			*
4	R(11) F ₁ (2)	F _{2g}	0 10	302			*

Tabel 1 ^b 10P12-10P16 laser line combination							
nr	transition	vib sym	S_S a u	ν_S [MHz]	ν_P [MHz]	S_P a u	ν_{exp} [MHz]
1	R(18) F ₂ (3)	F _{2g}	0 13	-433	425	68	-440
2	R(31) F ₂ (8)				-367	308	*
3	R(31) F ₁ (8)				367	308	*
4	Q(13) A ₂ (1)	F _{2g}	3 60	393	-366	177	*
5	R(10) F ₁ (1)	F _{2g}	0 73	353	-337	38	*
6	R(10) F ₁ (2)	F _{2g}	0 53	353	-337	29	*
7	Q(32) E(6)				227	93	*
8	R(9) F ₁ (2)	F _{2g}	1 66	233	-216	58	
9	R(9) F ₁ (1)	F _{2g}	5 76	233	-215	221	-234
10	Q(32) F ₂ (7)				215	69	*
11	Q(37) E(4)		0 17	-216			*
12	Q(32) A ₂ (2)				-189	116	*
13	Q(32) A ₂ (1)		0 10	-183			*
14	R(26) F ₁ (6)		0 14	2	-24	332	27
15	R(26) F ₂ (6)		0 14	3	19	332	
16	R(20) F ₂ (3)	F _{2g}	0 22	208	213	170	209
17	R(20) F ₂ (1)	F _{2g}			215	29	*
18	Q(34) F ₂ (7)				225	97	*
19	Q(30) F ₂ (7)				270	44	*
20	Q(30) F ₁ (7)				276	44	*
21	Q(34) F ₁ (6)				301	97	*
22	R(18) E(1)	F _{2g}	0 26	414	421	53	*
23	R(18) E(2)	F _{2g}	0 11	414	420	23	*

Tabel 1 ^c 10P12-10P18 laser line combination							
nr	transition	vib sym	S_S a u	ν_S [MHz]	ν_P [MHz]	S_P a u	ν_{exp} [MHz]
1	Q(15) E(1)	F _{2g}	2 97	146			134

Tabel 1 ^d 10P12-10P20 laser line combination							
nr	transition	vib sym	S_S a u	ν_S [MHz]	ν_P [MHz]	S_P a u	ν_{exp} [MHz]
1	Q(10) F ₂ (1)	F _{2g}	0 18	-143			*
2	Q(10) F ₁ (2)	F _{2g}	0 12	36			*
3	S(17) A ₂ (1)	E _g	0 12	146			*

Tabel 1 ^e 10P12 10P22 laser line combination							
nr	transition	vib sym	S_S a u	ν_S [MHz]	ν_P [MHz]	S_P a u	ν_{exp} [MHz]
1	R(12) E(2)	E _g	0 12	-16			*
2	S(6) F ₂ (1)	E _g	10 06	4			*
3	S(6) F ₁ (1)	E _g	10 06	479			*

Tabel 1^f: 10P14-10P16 laser line combination

nr	transition	vib sym.	S _S a.u.	ν_S [MHz]	ν_P [MHz]	S _P a.u.	ν_{exp} [MHz]
1	Q(11) F ₁ (2)	F _{2g}	1.39	-484	-470	26	-481
2	Q(11) F ₁ (1)	F _{2g}	0.12	-484	-470	38	
3	R(9) F ₁ (3)	F _{2g}	30.02	-369	-368	1729	-373
4	S(33) E(3)		1.83	-128	-127	2798	-126
5	S(33) F ₁ (5)		0.57	-71	-69	2092	-69
6	Q(17) F ₂ (2)	F _{2g}			-37	98	
7*	Q(17) F ₂ (3)	F _{2g}	0.19	-48	-37	152	-47
8	S(33) A ₁ (2)				66	692	*
9	S(36) F ₂ (8)		0.24	28	89	916	*
10	S(36) E(5)		0.76	28	89	1220	*
11	S(36) A ₂ (3)		1.86	29	89	1526	*
12	S(32) F ₂ (3)		0.73	64	157	2786	*
13*	Q(21) F ₂ (1)	F _{2g}	0.19	76	86	371	76
14*	R(7) E(1)	F _{2g}	1212.79	127	130	11071	132
15	Q(4) F ₂ (1)	F _{2g}	118.94	140			141
16	Q(16) F ₂ (4)	F _{2g}	0.12	307	319	112	317
17	Q(16) F ₂ (2)	F _{2g}			320	59	
18	S(32) F ₁ (3)		0.76	359	351	2751	*
19	S(34) E(4)		1.29	404	418	2099	*
20	S(34) F ₂ (6)		.40	413	427	1673	*
21	S(35) E(5)		.94	413	448	1706	*
22	S(35) F ₁ (7)		.31	414	449	1280	*
23	S(34) A ₂ (2)		3.10	430	445	2620	*
24	Q(4) F ₁ (1)	F _{2g}	7 · 10 ⁵	435	443	5 · 10 ⁵	429
25	S(36) A ₁ (2)				451	427	*

Tabel 1^g: 10P14-10P18 laser line combination

nr	transition	vib sym.	S _S a.u.	ν_S [MHz]	ν_P [MHz]	S _P a.u.	ν_{exp} [MHz]
1	S(17) F ₁ (2)	E _g	0.63	-473			*
2	Q(34) F ₁ (1)		2.40	-419	-423	12980	*
3	Q(34) E(1)		7.54	-382	-385	17336	-382
4	Q(34) F ₂ (1)		2.40	-346	-349	13023	-347
5	Q(33) A ₁ (1)				-238	6605	-236
6	Q(33) F ₁ (1)		5.48	-187	-190	16796	-187
7	R(35) F ₂ (6)				-154	194	*
8	Q(13) A ₂ (1)	F _{2g}	0.61	-146			-148
9	Q(33) F ₂ (1)		5.47	-140	-143	16776	-143
10	R(35) F ₁ (6)				-138	195	*
11	Q(33) A ₂ (3)		9.27	-95			
12	Q(33) A ₂ (2)		1988.28	-95	-97	28141	-96
13	Q(33) A ₂ (1)		199.75	-95			
14	S(18) F ₁ (3)	E _g	0.61	-39			-59
15	Q(32) F ₁ (1)		0.97	-37	-40	1426	-40
16	R(31) F ₂ (6)		1.16	-8	-13	3286	*
17	R(31) F ₁ (7)		1.16	-3	-8	3287	*
18	Q(24) A ₂ (1)		0.92	-1	-2	345	-3
19	Q(24) A ₂ (2)		0.17	2			
20	Q(32) E(1)		3.11	24	21	1902	24
21	S(18) E(2)	E _g	2.00	37			16
22	Q(32) F ₂ (1)		1.03	82	80	1427	83
23	Q(22) F ₁ (1)	F _{2g}			91	64	92
24	Q(31) F ₂ (4)		0.23	103			
25	Q(31) F ₂ (1)		0.71	103	100	663	102
26	Q(31) F ₂ (2)		0.21	103			
27	Q(31) F ₂ (6)		0.26	103			
28	Q(23) F ₂ (1)	F _{2g}			140	109	139
29	Q(30) A ₂ (1)		6.53	158	155	2080	156
30	Q(30) A ₂ (2)		1.07	158			
31	Q(31) E(4)		0.80	179			
32	Q(31) E(1)		2.10	179	177	885	178
33	Q(31) E(2)		0.63	179			

nr	transition	vib sym	S_S a u	ν_S [MHz]	ν_P [MHz]	S_P a u	ν_{exp} [MHz]
34	Q(31) E(3)		0 70	179			
35	Q(27) A ₁ (1)				223	2512	222
36	Q(31) F ₁ (1)		0 71	256	253	665	253
37	Q(31) F ₁ (3)		0 20	256			
38	Q(31) F ₁ (4)		0 23	256			
39	Q(31) F ₁ (5)		0 26	256			
40	Q(30) F ₂ (1)		0 83	258	256	1249	257
41	Q(30) F ₂ (2)		0 11	258			
42	Q(30) F ₂ (3)		0 12	258			
43	Q(30) F ₂ (5)		0 14	258			*
44	Q(29) F ₂ (1)		1 86	279	278	3521	278
45	Q(25) F ₂ (1)		0 24	280	281	444	283
46	Q(26) F ₁ (1)		0 62	312	313	1259	312
47	Q(28) F ₁ (1)		36 93	320	320	78101	320
48	Q(30) F ₁ (3)		0 10	355			
49	Q(30) F ₁ (1)		0 83	355	353	1251	356
50	Q(30) F ₁ (6)		0 14	355			
51	Q(30) F ₁ (5)		0 12	355			
52	Q(29) E(1)		6 08	407	406	4698	407
53	Q(29) E(2)		0 20	407			
54	Q(29) E(3)		0 61	407			
55	Q(29) E(4)		0 31	407			
56	Q(24) F ₂ (1)		0 12	425	424	209	426
57	Q(27) F ₁ (1)		3 61	435	434	7592	436
58	Q(30) A ₁ (1)				446	417	447
59	R(25) F ₂ (6)		0 31	466	464	617	464
60	R(25) F ₁ (7)		0 31	467	465	617	
61	S(20) F ₁ (5)	E _g	0 65	474			
62	S(20) E(4)	E _g	2 01	474			473
63	Q(28) E(1)		116 75	475	476	103519	476
64	Q(28) E(2)		0 13	479			
65	Q(28) E(3)		0 15	479			

nr	transition	vib sym	S_S a u	ν_S [MHz]	ν_P [MHz]	S_P a u	ν_{exp} [MHz]
1	R(14) F ₂ (3)	E _g	0 54	9			1
2	P(10) F ₁ (1)	F _{2g}	0 16	140			164
3	R(17) E(2)	E _g	1 55	352			360
4	P(24) A ₂ (1)		0 10	430			*
5	R(16) A ₂ (1)	E _g	4 08	447			445
6	Q(31) F ₁ (7)		0 28	496	436	1235	*
7	Q(31) F ₂ (6)		0 28	497	436	1235	*

nr	transition	vib sym	S_S a u	ν_S [MHz]	ν_P [MHz]	S_P a u	ν_{exp} [MHz]
1	R(26) E(2)		0 12	170	-187	99	*
2	R(21) A ₂ (2)	E _g	0 12	102			*
3	R(22) A ₂ (1)	E _g			125	15	*
4	R(22) E(2)	E _g			476	16	*

nr	transition	vib sym	S_S a u	ν_S [MHz]	ν_P [MHz]	S_P a u	ν_{exp} [MHz]
1	P(7) F ₁ (2)	E _g	8 99	-319			*
2	P(7) E(1)	E _g	52 50	468			*

nr	transition	vib sym	S _G a u	ν_S [MHz]	ν_P [MHz]	S _P a u	ν_{exp} [MHz]
1	R(22) E(1)	E _g	8 84	-453	493	2485	-450
2	R(22) F ₁ (1)	E _g	2 84	-375	-415	1884	-374
3	R(22) F ₁ (3)	E _g	2 50	-375			
4	P(11) F ₂ (3)	F _{2g}	0 18	-374			
5	R(17) F ₂ (2)	E _g	5 94	-353	251	1362	-349
6	R(17) F ₂ (3)	E _g	0 13	-353	-351	31	
7	R(26) F ₂ (1)				-276	71	
8	R(26) E(1)				-274	91	-274
9	R(26) F ₁ (1)				273	54	
10	R(26) F ₁ (1)				-256	61	-255
11	R(26) E(1)		0 15	-240	-243	57	-242
12	P(20) F ₁ (3)	F _{2g}	2 01	-208	-206	499	-201
13	R(26) F ₂ (1)				-178	73	163
14	R(26) E(1)		0 12	-144	-161	66	-147
15	Q(36) F ₂ (7)				-137	1148	136
16	Q(36) F ₁ (7)				-136	1148	
17	P(29) A ₁ (2)				-48	341	
18•	R(18) F ₂ (2)	E _g	5 12	-46	48	1549	-41
19	Q(36) F ₁ (8)		34	-45			
20	P(29) F ₁ (7)		1 23	-44	-47	1024	
21•	P(29) E(5)		4 01	44	-46	1366	-45
22	Q(36) F ₂ (7)		0 14	-43			
23	Q(36) F ₂ (8)		0 34	-43			
24	Q(36) F ₁ (7)		0 14	-42			
25	R(26) A ₂ (1)		0 14	-8	-21	38	-6
26•	O(7) F ₁ (2)	F _{2g}	835 44	4	0	5564	6
27	O(7) F ₁ (1)	F _{2g}	99 73	4	0	702	
28	R(13) F ₂ (3)	E _g	7 87	142	164	654	161
29	O(9) F ₁ (2)	F _{2g}	5 36	152	152	133	
30	O(9) F ₁ (3)	F _{2g}	0 36	152			
31•	O(9) F ₁ (1)	F _{2g}	22 33	152	152	34	155
32	P(18) F ₂ (2)	F _{2g}	2 45	285	291	430	287
33	R(13) F ₁ (4)	E _g	7 87	320	342	653	354
34	R(18) E(1)	E _g	16 21	479	477	2022	480

nr	transition	vib sym	S _G a u	ν_S [MHz]	ν_P [MHz]	S _P a u	ν_{exp} [MHz]
1	P(37) E(4)		3 29	-482			483
2	P(37) E(3)		2 89	-479			
3	P(17) E(2)	F _{2g}	0 34	-460	-471	25	-468
4	P(18) E(1)	F _{2g}	0 43	-446	-456	46	-455
5	O(16) F ₂ (2)	F _{2g}	0 12	-419			
6	P(17) F ₂ (1)	F _{2g}	0 22	-331	-342	21	-345
7	O(16) F ₁ (1)	F _{2g}	0 12	-312			
8	O(16) F ₁ (4)	F _{2g}	0 11	-308			
9	O(16) F ₁ (2)	F _{2g}	0 15	-308			
10	P(35) F ₂ (3)		1 09	-250	-326	4646	*
11	R(20) F ₁ (3)	E _g			-171	32	-174
12	O(23) A ₂ (2)	F _{2g}	0 11	-96			
13	O(23) E(1)	F _{2g}	0 15	-95			-89
14	R(20) F ₂ (3)	E _g			-86	39	-64
15	P(17) A ₂ (1)	F _{2g}	5 60	-44	-56	52	-47
16	P(37) F ₂ (4)		0 88	197	107	4453	*
17	P(39) F ₂ (4)		0 67	235	152	3913	*
18	P(35) F ₁ (3)		1 03	265	199	4379	*
19	R(21) F ₁ (3)	E _g			360	23	356
20	O(11) A ₂ (1)	F _{2g}	4 99	399			*

Tabel 1^m 10P16-10P22 laser line combination

nr	transition	vib sym	S_S a u	ν_S [MHz]	ν_P [MHz]	S_P a u	ν_{exp} [MHz]
1	Q(37) F ₁ (9)				-411	409	*
2	Q(37) A ₁ (3)				-411	136	*
3	Q(37) E(6)		0 24	-409	-411	645	*
4	Q(25) A ₂ (2)		2 30	-264	-287	600	-263
5	Q(25) F ₂ (4)		0 30	-147	-169	356	*
6	Q(25) E(3)		0 96	-91	-112	475	*
7	Q(18) F ₁ (2)	E _g	0 18	-68	-88	65	-72
8•	P(6) F ₁ (1)	E _g	225 92	-5	26	708	-4
9	Q(22) E(2)	E _g	0 60	-4	-19	193	
10	Q(22) E(1)	E _g			-17	29	
11	Q(18) E(1)	E _g	0 68	108	88	109	99
12	Q(20) A ₂ (1)	E _g	0 33	198	180	34	*
13	Q(18) F ₂ (2)	E _g	0 29	311	291	108	301
14	P(6) F ₂ (2)	E _g	234 39	327	358	742	
15	P(6) F ₂ (1)	E _g	408 07	327	358	1231	298

Tabel 1ⁿ 10P16-10P24 laser line combination

nr	transition	vib sym	S_S a u	ν_S [MHz]	ν_P [MHz]	S_P a u	ν_{exp} [MHz]
1	Q(39) A ₂ (3)		0 10	376			*
2	O(9) F ₂ (2)	E _g	0 17	420	448	13	*
3	P(39) F ₁ (2)		0 70	430			*
4	P(39) E(1)		1 99	444			*
5	P(39) F ₂ (2)		0 67	457			*

Tabel 1^o 10P18-10P20 laser line combination

nr	transition	vib sym	S_S a u	ν_S [MHz]	ν_P [MHz]	S_P a u	ν_{exp} [MHz]
1•	P(6) A ₂ (1)	E _g	944 90	-435			-436
2	Q(29) F ₁ (6)				-423	14	
3	Q(29) F ₂ (6)				-421	14	-420
4	Q(29) F ₂ (1)		5 51	-403			-398
5	O(38) E(4)		0 27	-81			
6	O(38) E(3)		0 26	-79	-142	1098	*
7•	P(7) F ₁ (1)	E _g	247 82	-58			-59
8	O(15) A ₂ (2)	F _{2g}	0 17	-56			
9	O(15) A ₂ (1)	F _{2g}	0 10	-56			
10	Q(22) A ₂ (1)	E _g	0 12	-9			-6
11	O(38) F ₂ (4)				15	829	*
12	O(37) E(5)		0 43	100			
13	O(37) E(4)		0 40	103	24	1381	*
14	O(37) F ₁ (7)		0 13	120			
15	O(37) F ₁ (6)		0 13	120	40	1036	*
16	O(37) A ₁ (2)				75	346	*
17	P(29) F ₁ (2)				407	11	*

Tabel 1 ^P 10P18-10P22 laser line combination							
nr	transition	vib. sym.	S_S a.u.	ν_S [MHz]	ν_P [MHz]	S_P a.u.	ν_{exp} [MHz]
1	P(17) E(1)	E _g	0.23	-365			*
2	P(17) E(2)	E _g	0.29	-365			*
3	P(17) E(3)	E _g	0.17	-365			*
4	O(8) F ₁ (2)	E _g	2.06	-181			-188
5	P(14) F ₂ (1)	E _g	0.25	-134			-138
6	P(14) F ₂ (2)	E _g	0.45	-134			
7	Q(36) F ₂ (4)				-24	91	-13
8	O(8) E(2)	E _g	6.23	13			10
9	Q(37) F ₁ (5)				178	126	*

Tabel 1 ^Q 10P18-10P24 laser line combination							
nr	transition	vib. sym.	S_S a.u.	ν_S [MHz]	ν_P [MHz]	S_P a.u.	ν_{exp} [MHz]
1	O(33) F ₁ (1)		0.23	254			*
2	O(33) F ₁ (2)		1.39	254			*
3	O(33) F ₁ (3)		0.24	254			*
4	O(33) F ₁ (4)		15.71	254			*
5	O(33) F ₁ (5)		0.25	254			*

Tabel 1 ^R 10P20-10P22 laser line combination							
nr	transition	vib. sym.	S_S a.u.	ν_S [MHz]	ν_P [MHz]	S_P a.u.	ν_{exp} [MHz]
1	P(37) A ₂ (1)		0.10	180			*

Table 1: For each combination of laser lines, the predicted two colour, two photon transitions are listed in column 1, with their ro-vibrational symmetries. J -values up till 40 are included in the table; higher J -values are not observable in our spectra because of the poor population of these levels. In the third column, the vibrational symmetry is presented, this is only possible for transitions starting from low J -values because for higher J -values, the interaction between the different energy levels of the different symmetry branches causes the energy levels to shift. Due to this interaction the transitions can not be assigned to one vibrational symmetry anymore.

The calculated frequencies (ν_S and ν_P utilizing two different representations and different sets of lines in the fitting procedure) are listed in column 5 and 6; their strength factors are listed in column 4 and 7, respectively. In comparing the strength factors, S_S is approximately two orders of magnitude smaller than S_P ; only the relative strength of two different transitions can be compared with another. The experimental frequencies are listed in column 8. If it is not possible to assign a transition uniquely a * is plotted in column 8. Transitions utilized in the fitting procedure are marked with •.

tabel 2 3 and 4 photon transitions							
nr	CO ₂ lines	transition	S_S a u	ν_S [MHz]	ν_P [MHz]	S_P a u	ν_{exp} [MHz]
1	2P14+P22	R(6) F ₁ (1)	16	-239	-130	5 10 ⁴	-210
2	3P16	R(10) F ₂ (1)	2	-420			-338
3	3P16	N(5) E(1)	1900	990			852
4	2P16+P20	Q(11) F ₁ (2)	****	-32	-20	7 10 ⁶	2
5	2P16+P14	R(16) E(2)	22	-24			-10
6	2P16+P14	S(7) F ₂ (1)	3	-110	46	5 10 ³	-116
1	2P16+2P18	Q(5) F ₁ (2)	****	-308			-312
2	2P16+2P22	N(4) F ₁ (1)	****	326			278

Table 2: Predicted three and four photon transitions with experimental frequencies. In column 2 the combination of laser lines (needed to enter the spectral region in which the transitions listed in column 3 can be measured) is listed. The predicted frequencies and strength factors are listed in column 4 to 7; the measured frequencies are given in column 8. If a transition has a strength factor S_S ****, it is stronger than 100,000. For the four photon transitions no listing of ν_P is available at this moment. To get the calculated frequencies in better agreement with each other and with the experimental data, it is necessary to fit all two photon transitions and to include the three and four photon transitions in the fitting procedure.

References

- [1] M.O. Acef thesis at the Université de Paris-sud, centre d'Orsay (1989) 162
- [2] B. Bobin, C.J. Bordé, J. Bordé and C. Bréant, J. Molec. Spec. 121 (1987) 91
- [3] C.W. Patterson, F. Herlemont, M. Azizi and J. Lemaire, J. Molec. Spec. 108 (1984) 31
- [4] F. Herlemont, M. Lyszyk and J. Lemaire, Appl. Phys. 24 (1981) 369
- [5] A.F. Linskens, S. te Lintel Hekkert and J. Reuss, Infrared Phys. 32 (1991) 259
- [6] S. te Lintel Hekkert, A. Linskens, B.G. Sartakov, G. Pierre and J. Reuss, to be published
- [7] A.S. Pine and A.G. Robiette, J. Molec. Spec. 80 (1980) 388
- [8] C.W. Patterson, B.J. Krohn and A.S. Pine, J. Molec. Spec. 88 (1981) 133
- [9] C. Liedenbaum, S. Stolte and J. Reuss, Chem. Phys. 122 (1988) 443
- [10] M. Snels, R. Fantoni, M. Zen, S. Stolte and J. Reuss, Chem. Phys. Lett. 124 (1986) 1
- [11] W. Demtröder, Laser Spectroscopy, second printing, Springer Series in Chem. Phys. 5 (1982) 107
- [12] C. Freed, Metrologia 13 (1977) 151
- [13] A. Dax, Aufbau eines Lamb-dip-stabilisierten CO_2 -laser, diplomarbeit, Institut für angewandte Physik der Universität Bonn (1988)
- [14] P.K. Chakraborti, V.B. Kartha, R.K. Talukdar, P.N. Bajaj and A. Joshi, Chem. Phys. Lett. 101 (1983) 397
- [15] P.K. Chakraborti, R.K. Talukdar, P.N. Bajaj, A. Joshi and V.B. Kartha, Chem. Phys. 95 (1985) 145
- [16] V.M. Apatin, V.M. Krivtsum, Y.A. Kuritsyn, G.N. Makarov and J. Pak, Opt. Com. 47 (1983) 251
- [17] D.P. Hodgkinson and A.J. Taylor, Opt. Com. 50 (1984) 214
- [18] C. Liedenbaum, S. Stolte and J. Reuss, Phys. Rep. 178 (1989) 1
- [19] J. Oreg, F.T. Hioe and J.H. Eberly, Phys. Rev. A 29 (1984) 690
- [20] C.E. Carroll and F.T. Hioe, Phys. Rev. 36 (1987) 724

- [21] C.E. Carroll and F.T. Hioe, J. of Opt. Soc. of America B5 (1988) 1335
- [22] S. te Lintel Hekkert, A.F. Linskens, I. Holleman, B.G. Sartakov, G. Pierre and J. Reuss, to be published
- [23] C.J. Bordé, M. Ouhayoum, A. van Lerberghe, C. Salomon, S. Avrillier, C.D. Cantrell and J. Bordé, Laser Spectroscopy 4 (Edited by H. Walther and K.W. Rothe), Springer, New York (1979)

Chapter 6

Outlook

Measurements utilizing two counterpropagating CO₂ lasers interacting simultaneously with SF₆ molecules provided many new data which are used to investigate multiphoton transitions in SF₆ (chapter 4 and 5 of this thesis and [1, 2]) Utilizing this new technique together with the one laser measurements (chapter 2 and 3 of this thesis and [3]) two photon transitions starting from energy levels possessing F_{2g} vibrational symmetry are fit within 3 MHz

For the transitions ending on energy levels possessing E_g vibrational symmetry, the discrepancy between theoretically predicted and experimentally determined frequencies has been diminished one order of magnitude utilizing only the ¹²C¹⁶O₂ isotope as a laser medium These transitions are now predicted with an accuracy of ± 20 MHz Utilizing a laser tuned to the 10P14 ¹²C¹⁶O₂ transition in combination with a laser tuned to the 10R42 ¹³C¹⁶O₂ transition [4], the frequency region in which transitions possessing E_g vibrational symmetry and low J-values can be probed, in the future this will lead probably to a further improved Hamiltonian

For the two photon transitions possessing A_{1g} vibrational symmetry, a laser tuned to the 10P14 ¹²C¹⁶O₂ transition has to be combined with a laser tuned to the 10P34 ¹²C¹⁸O₂ transition in order to enter the frequency region in which transitions are expected Combinations of the CO₂ isotope lasers and the N₂O laser will probably provide enough data to come to a quantitative understanding also of these 2h ν_3 A_{1g} levels

Three lasers can be utilized in a similar way, interacting at the same time with the SF₆ molecules, many multiphoton transitions with energies of 3000 cm⁻¹ or more can be investigated in this way

Due to the interaction with dark states the energy levels of the transitions (starting from the ground state) might be shifted Comparing the theoretically predicted frequencies with the measured ones will provide information about these effects SF₆ is a very special molecule in which these dark state interactions appear to be practically absent for excitation energies ≤ 3000 cm⁻¹ Once the three photon transitions are fit, the four and five photon transitions can be predicted with the same set of parameters for the Hamiltonian The 5000 cm⁻¹ region is generally expected to be the start of the quasicontinuum/stochastisation [5] However, probably not all the frequency regions will be affected by this process In some frequency regions spectral blobs are expected to appear due to the start of the quasicontinuum In other regions, even with much higher energies we expect still isolated transitions giving rise to sharp spectral features An interesting subject of further investigation is, up to what

energy isolated transitions can be resolved and assigned.

Utilizing the high power Apollo laser [6] with its TEM₀₀ mode to further excite the molecules from a well known energy level will provide interesting information on the dependence of multiphoton excitation and multiphoton dissociation on the rotational and vibrational energy of the molecules.

Concerning the field of molecular quantum electronics we want to draw the attention to three interesting items of investigation; first of all, the Stark effects can be investigated utilizing two counterpropagating lasers. If one of the lasers is set on the P(4) E(0) one photon transition shifted 250 MHz with respect to the 10P16 CO₂ laser line with full power (i.e. 600 times the intensity needed to saturate this transition), the energy levels involved will be shifted. The ground state level shift of this transition can be probed by the second laser, utilizing the P(4) E(0) two photon transition shifted 174 MHz from the 10P16 CO₂ laser line. An interesting feature in these measurements is that the intermediate level of the two photon transition is also shifted giving rise to a change of transition probability. Theoretical predictions and preliminary measurements are at hand.

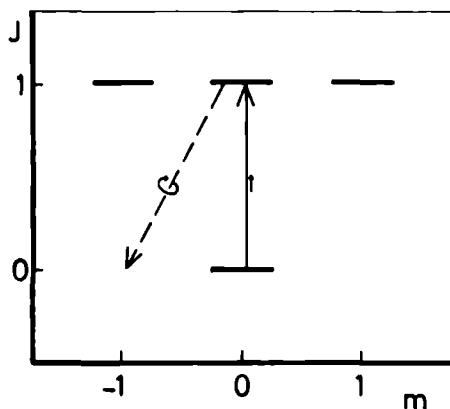


Figure 1: Effects of polarized light on R transitions starting from the $J=0$ level. The molecule is excited by linearly polarized light ($\Delta m=0$). Depopulation of the excited level utilizing circularly polarized light is not possible; only linearly polarized light can depopulate the excited level taking the molecule again to the ground state.

Secondly, exploring the two photon Ramsey fringes [7] it is possible to create a new frequency standard in the infrared region. In order to do so, the molecular beam is crossed

twice by the same laser radiation which is afterwards retro-reflected. In this way, the time of flight of the molecules between the two interaction regions of the standing wave laser radiation with the molecular beam determines the distance between the Ramsey fringes. With this method we expect to produce a frequency standard with an accuracy much higher than 1 Hz. Ultra stable lasers are evidently needed to perform these experiments.

A third interesting subject of future research concerns polarization effects [8], expected to be pronounced for the transitions starting from low J -values. One photon R transitions starting from $J=0$, pump the molecules up for 100% (under RAP conditions [9, 10]), with linearly polarized light, to the level with $J=1$ and $m=0$. Probing this level with a second laser tuned to the same frequency, produces a (negative) bolometer signal if this second deexcitation laser is linearly polarized parallel to the polarization of the excitation laser. If circularly polarized light is used, no bolometer signal will be observed (fig 1). For transitions starting from $J=1$ levels the signal will be decreased by 33% going from linearly to circularly polarized light. For transitions starting from $J=2$ this effect is 20%, and for transitions starting from levels with $J=3$ the effect will be only 11%, just at the limit of our experimental accuracy.

So far, the reasoning is based on simple straightforward selection rules. By applying a three step excitation to the SF_6 molecules, the possibility exists to produce spinning molecules with their rotation axis oriented to a high degree. In fig 2, the proposed experiment shows a) an excitation from $J''=4 \rightarrow J'=3$, a two photon excitation with $\Delta m=+2$, b) a de-excitation with the same laser frequency, but with a change of circular polarization so that again $\Delta m=+2$. For the third step we have two options:

c_1) employs an $1 h\nu$ excitation with $\Delta m=+1$ to a $J=3$ level, in this way SF_6 molecules are produced with $m=+1$, $+2$ and $+3$, all other sublevels are unoccupied.

c_2) is a $2h\nu$ transition to $J=3$, populated sublevels are those with $m=+1$ and $+2$.

Option c_1) needs two different laser frequencies, option c_2) works with a single laser frequency. Note that in all steps RAP processes are active so that the total population is transferred each time.

The molecules excited to well characterised energy levels can be used in a wide range of experiments. We collaborate with the group of Duren (Göttingen) to investigate the dependence of elastic, non-elastic and reactive collisions of SF_6 molecules with Na atoms on the internal energy of the SF_6 . Another way to employ the highly excited SF_6 molecules is chosen in collaboration with the group of S. Iannotta (Trento). In their machine a molecular beam can be scattered on a surface. The dependence of the surface scattering on the internal energy distribution is the subject of this investigation. The possibility of orienting excited SF_6 molecules as indicated in the previous paragraph, allows new scattering experiments (gas phase and surface collisions). Note that the oriented molecule SF_6 does not possess an electric dipole moment which normally is required for orientation. The asymmetrically corrugated surface mainly used by the Trento group, GaSe, in combination with the oriented

spinning SF_6 molecules is expected to show very interesting effects, e.g. strong out of plane scattering

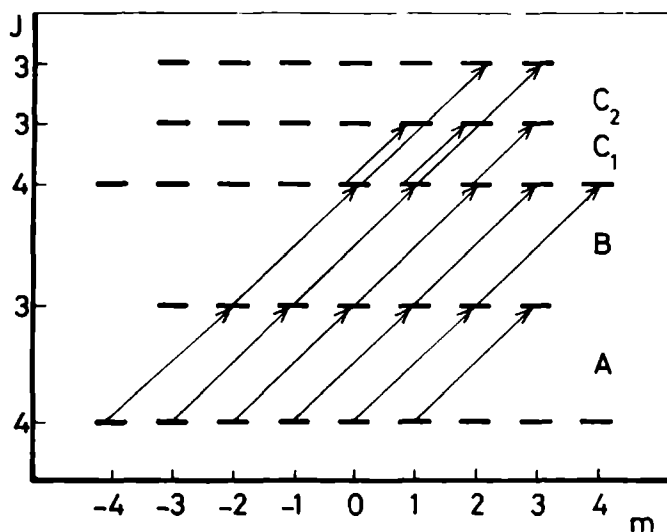


Figure 2 Excitation scheme to produce oriented spinning SF_6 molecules utilizing three step excitation with circularly polarized laser radiation a) $2 h\nu$ excitation $J''=4 \rightarrow J'=3$ b) $2 h\nu$ de-excitation with $J'=3 \rightarrow J''=4$ And finally either c1) $1 h\nu$ or c2) $2 h\nu$ excitation both to a level with $J=4$ Note that on the vertical axis sequential changes of J are shown by arrows, it does not necessarily mean that the energy increases

References

- [1] C W Patterson, F Herlemont, M Azizi and J Lemaire, J Molec Spec 121 (1987) 91
- [2] F Herlemont, M Lyszyk and J Lemaire, Appl Phys 24 (1981) 369
- [3] C J Bordé, M Ouhayoun, A van Lerberghe, C Salomon, S Avrillier, C D Cantrell and J Bordé, Laser Spectroscopy 4 (Edited by H Walther and K W Rothe), Springer, New York (1979)
- [4] L C Bradley, K L Soohoo and C Freed, IEEE J of Quantum electronics, QE-22 2 (1986) 234
- [5] V S Letokhov and A Makarov, Opt Comm 17 (1976) 250
- [6] Apollo laser, Laser Photonics, Carlsbad USA
- [7] W Demtroder in Laser Spectroscopy, Springer series in Chem Phys 5, Springer berlin (1982) 615
- [8] H Albrecht, H H Rutze, K P Francke, C Hartung and W Radloff, Chem Phys Lett 103 (1983) 161
- [9] C Liedebaum, S Stolte and J Reuss, Phys Rep 178 (1989) 1
- [10] U Gaubatz, P Rudecki, M Becker, S Schiemann, M Kulz and K Bergmann, Chem Phys Lett 149 (1988) 463

Samenvatting

Hoge resolutie multilaserexperimenten aan multifotonovergangen in SF₆

In dit proefschrift worden metingen aan SF₆ moleculen die met behulp van fotonen met een golflengte van $\pm 10 \mu\text{m}$ in trilling worden gebracht gepresenteerd. Hierbij worden de SF₆ moleculen eerst in een zo laag mogelijke energietoestand gebracht (de grondtoestand) door ze sterk te koelen. Dit gebeurt tijdens een expansie door een zeer kleine opening (de nozzle met een diameter van $50 \mu\text{m}$) in het vacuüm van de opstelling. Na deze expansie bewegen de moleculen zich allemaal met ongeveer dezelfde snelheid ($\pm 1200 \text{ m/s}$) in dezelfde richting.

De totale hoeveelheid energie die de moleculen nu nog bezitten (translationele, vibrationele en rotationele) wordt gemeten met een temperatuurgevoelig weerstandje (de bolometer), waar we de moleculen op laten vallen. Als we de SF₆ moleculen opwarmen met behulp van een CO₂ laser (waarmee we een specifieke trilling in het SF₆ aanslaan, in ons geval de ν_3 mode), zal de weerstand van de bolometer veranderen. Hoeveel de weerstand verandert is een maat voor de hoeveelheid energie opgenomen in het SF₆.

SF₆ is een interessant molecuul: het energiespectrum kan ruwweg verdeeld worden in drie stukken. Het eerste stuk bestaat uit een gebied waarin we te maken hebben met discrete energieniveaus (tot $\pm 5000 \text{ cm}^{-1}$), geleidelijk gaat dit over in een gebied waar de energieniveaus zo dicht bij elkaar komen te liggen, dat er altijd een resonante overgang aanwezig is binnen de bandbreedte van de lasers (het quasicontinuum). Bij nog hogere energieën verbreden de niveaus vanwege optredende dissociatie, zodat men niet meer kan spreken van geïsoleerde overgangen (het continuum).

In een poging te onderzoeken hoe het quasicontinuum tot stand komt, zal eerst goed onderzocht moeten worden wat er in het gebied met energieën lager dan 5000 cm^{-1} precies aan de hand is. Om de constanten in de Hamiltoniaan, die nodig is om de ν_3 mode van SF₆ te beschrijven en te bepalen, moeten veel meetgegevens verzameld worden. Een probleem hierbij is dat de CO₂ lasers of zeer slechte bundeleigenschappen hebben (gepulste lasers), of maar een klein deel van het te meten gebied bestrijken (continue lasers). In dit proefschrift worden twee manieren gepresenteerd om het te meten frequentiegebied uit te breiden. Ten eerste zijn acousto optic modulators (AOM's) gebruikt, in deze kristallen wordt de frequentie van de laserstraling $+100 \text{ MHz}$ of -100 MHz verschoven. De AOM kan voor een tweede keer gekruist worden, waardoor er een $+200 \text{ MHz}$ of -200 MHz shift ontstaat. Het frequentiegebied van de laser kan op deze manier verdubbeld worden. De metingen, verricht met deze

experimentele set-up, zijn beschreven in hoofdstuk 2 van dit proefschrift. De toekenning van de twee-fotonovergangen is gedaan in samenwerking met Sartakov (Moscow) en Pierre (Dijon), de resultaten zijn weergegeven in hoofdstuk 3.

Om het te bereiken frequentiegebied nog wat uit te breiden is een experimentele truc toegepast. Twee CO₂ waveguide-lasers worden precies op de moleculaire bundel gekruist. Twee-fotonovergangen, geproduceerd met twee fotonen ieder van een andere laser, kunnen nu gemeten worden. Door verschillende combinaties van laserlijnen te kiezen zijn 95 nieuwe twee-fotonovergangen gemeten en toegekend. De experimentele gegevens, alsmede enkele metingen, zijn besproken in hoofdstuk 4. In hoofdstuk 5 worden de meetresultaten gepresenteerd en besproken.

Niet alleen twee-fotonovergangen zijn gemeten, er is ook een begin gemaakt met de spectroscopie van de drie- en vier-fotonovergangen. Enkele toegekende lijnen zijn gegeven in hoofdstuk 5.

Naast de spectroscopie, die de hoofdmoot vormt van dit proefschrift, zijn nog enkele andere interessante effecten bestudeerd. Ten eerste het rapid adiabatic passage proces, waarmee het mogelijk is de moleculen voor 100% in de aangeslagen toestand te krijgen. Door middel van een juiste keuze van de lenzen die gebruikt worden om de CO₂ lasers te focuseren op de moleculaire bundel kan RAP verwezenlijkt worden. Dat we er ook in geslaagd zijn deze condities te verwezenlijken is bewezen in hoofdstuk 2, waar door middel van probing van het aangeslagen niveau, in een dubbelresonantie-experiment een negatief bolometersignaal waargenomen is. Dit is alleen mogelijk als er populatie-inversie veroorzaakt is bij de eerste laserinteractie. Een andere indicatie voor het feit dat we in onze experimenten onder RAP condities meten, is de afwezigheid van vermogensverbreding en Rabi-oscillaties. In conventionele spectroscopie worden lijnbreedtes van meer dan 100 MHz verwacht bij de vermogens die wij gebruiken (typisch in de orde van grootte van 10 Watt, dit is 1000 keer het vermogen nodig om een één-fotonovergang te verzadigen), wij meten een FWHM van 2 MHz.

Dat het ook mogelijk is onder niet-RAP condities te werken is bewezen in hetzelfde hoofdstuk. Voor het eerst is een twee-foton Rabi-oscillatie gemeten.

In een aanzet om het quasicontinuum te onderzoeken is gekeken naar welke energieniveaus er een rol spelen in het multifotonproces waarbij met een sterke laser in één keer vijf fotonen in het molecuul gestopt worden. Het blijkt dat vooral de moleculen die zich al in een aangeslagen toestand bevinden (hot bands) meedoen in dit proces. Moleculen die starten vanuit de grondtoestand spelen een ondergeschikte rol.

Een overzicht van onderzoeken die gedaan kunnen worden gebruik makende van de kennis vergaard in dit proefschrift is gegeven in hoofdstuk 6, de outlook.

Curriculum Vitae

Sacco te Lintel Hekkert

Geboren 11 maart 1963

Geboorteplaats Deventer

1975–1979 MAVO, Gemeentelijke Scholen Gemeenschap Doetinchem

1979–1981 HAVO, Gemeentelijke Scholen Gemeenschap Doetinchem

1981–1983 VWO, Gemeentelijke Scholen Gemeenschap Doetinchem

1983–1988 Studie natuurkunde aan de Katholieke Universiteit Nijmegen, afgestudeerd bij de experimentele afdeling Molecuul- en Laserfysica van prof dr J Reuss

1987–1988 Onderzoek naar de mogelijkheden om het frequentiebereik van een gepulste YAG-laser te vergroten met behulp van een Raman-shifter, een heatpipe en niet-lineaire kristallen, tevens metingen verricht aan het foto akoestische effect van kool-waterstofverbindingen opgelost in tetra (afstudeerproject)

1988 Bouw dubbele CO₂ intra-cavity laser in dienst van de afdeling Molecuul- en Laserfysica

1989 Bij het onderzoekscentrum ENEA, Frascati (Italië) onderzoek verricht naar het multifotonproces in SF₆ met behulp van een gepulste continu verstembare hogedruk CO₂ laser

1989–1993 Promotie-onderzoek op de afdeling Molecuul- en Laserfysica met prof dr J Reuss als promotor Resultaten van het onderzoek zijn weergegeven in dit proefschrift In het kader van de onderwijsbegeleiding werd een half jaar assistentie verleend bij het practicum voor scheikunde studenten en anderhalf jaar begeleiding gegeven aan studenten bij het basiscolloquium, een algemeen vormend colloquium

januari 1991 Op het Max-Planck instituut te Gottingen botsingen tussen Na-atomen en aangeslagen SF₆ moleculen onderzocht

juli 1992 Universiteit in Dijon bezocht om te helpen de in Nijmegen verkregen meetresultaten theoretisch te onderbouwen

